



*Barrier properties of spray-coated epoxy-graft-acrylic films on tin-plate in corrosive environments.*

SMITH, Stuart D.

Available from the Sheffield Hallam University Research Archive (SHURA) at:

<http://shura.shu.ac.uk/20375/>

## A Sheffield Hallam University thesis

This thesis is protected by copyright which belongs to the author.

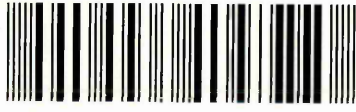
The content must not be changed in any way or sold commercially in any format or medium without the formal permission of the author.

When referring to this work, full bibliographic details including the author, title, awarding institution and date of the thesis must be given.

Please visit <http://shura.shu.ac.uk/20375/> and <http://shura.shu.ac.uk/information.html> for further details about copyright and re-use permissions.

LEARNING CENTRE  
CITY CAMPUS, POND STREET,  
SHEFFIELD S1 1WB.

101 667 487 2



**REFERENCE**

ProQuest Number: 10701021

All rights reserved

INFORMATION TO ALL USERS

The quality of this reproduction is dependent upon the quality of the copy submitted.

In the unlikely event that the author did not send a complete manuscript and there are missing pages, these will be noted. Also, if material had to be removed, a note will indicate the deletion.



ProQuest 10701021

Published by ProQuest LLC (2017). Copyright of the Dissertation is held by the Author.

All rights reserved.

This work is protected against unauthorized copying under Title 17, United States Code  
Microform Edition © ProQuest LLC.

ProQuest LLC.  
789 East Eisenhower Parkway  
P.O. Box 1346  
Ann Arbor, MI 48106 – 1346

**Barrier Properties of Spray-Coated Epoxy-graft-Acrylic  
films on Tin-Plate in Corrosive Environments.**

**Stuart Douglas Smith, C.Chem M.R.S.C.**

A thesis submitted in partial fulfilment of the requirements of  
Sheffield Hallam University for the degree of Doctor of Philosophy

**DECEMBER 1998**

Collaborating Establishment: I.C.I. Packaging Coatings

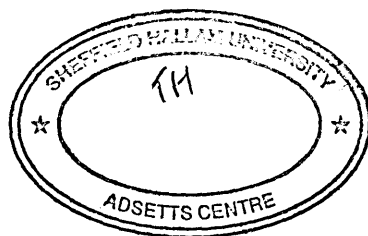
1. The first part of the report is a summary of the work done during the year.

2. The second part is a detailed account of the work done during the year.

3. The third part is a summary of the work done during the year.

4. The fourth part is a summary of the work done during the year.

5. The fifth part is a summary of the work done during the year.



### Barrier Properties of Spray-Coated Epoxy-graft-Acrylic films on TinPlate in Corrosive Environments.

This thesis describes an investigation of corrosion processes occurring under thin polymeric layers (3 -5  $\mu\text{m}$ ) and suggests ways by which the films suppress the onset of corrosion of the bulk metal in corrosive aqueous environments.

Synthetic solutions have been developed which replicate pH and conductivity conditions, likely to be found in beverage cans and which have been used to conduct corrosion studies of commercial lacquer systems. Studies carried out highlight the following points:

- i) The degree and nature of the film cross-linking has a role in the anti-corrosive action of the films.
- ii) The quantity of iron released into the beverage is much lower than expected when the corrosivity of the solution and the relative thinness of the film are considered. Work carried out indicates a possible means by which the iron might be complexed by the phenolic cross-linker component of the film with evidence having been obtained showing the ease with which phenolic cross-linker / iron complexes can be formed.
- iv) Optical Emission Glow discharge spectrometry has provided evidence that iron corrosion products are trapped within the polymer matrix. The work has also highlighted a means of accurately determining the film thickness.
- v) Water permeation across the cured films was followed using infra-red spectroscopy. The amount of water found to migrate across films of different cross-linking densities was observed to vary with phenolic cross-linker level present
- vi) Permeation of ions across cured films has been followed with the use of ion selective electrodes. The films have also been shown to be perm-selective towards the diffusion of sodium ions in preference to chloride ions, in aqueous sodium chloride solutions, thus exhibiting a duality in the nature of the coatings towards the constituents of corrosive environments.
- vi) Alternating Current Impedance spectroscopy, has been used to observe the electrolyte penetration and corrosion initiation processes, *in situ*. A knowledge of the electrochemical processes occurring for these water-based epoxy-acrylate films during electrolyte penetration, saturation of the film and development of corrosion underneath the film has been obtained.

## *Acknowledgments*

My acknowledgements go to Professor D.W.Allen, Dr P Sheridan, Mr R.J. Kitchingman for their help and guidance, for Dr M. Ives for carrying out the OEGDS work and to

I.C.I. Packaging Coatings for the time released to me to allow the studies to be carried out.

My gratitude should be expressed to my wife, Helen without who's forbearance this work would not have been possible.

## ***1.1 Table of Contents***

Section Number	Page Number	Description
1.1	2	Table of Contents
1.2	13	<b>Introduction</b>
1.2.1		The Packaging Industry -An Overview
1.3	15	The metal can as a container
1.4	17	Can Manufacture
1.4.1		Three peice cans
1.4.2		Drawn and wall-ironed beverage cans. ( Two piece cans)
1.5	19	<b>Corrosion of Cans</b>
1.5.1	19	Introduction to corrosion
1.5.2	22	Anaerobic conditions without complexing agents
1.5.3	22	Anaerobic conditions in the presence of complexing agents
1.5.4	22	Aerobic conditions without complexants
1.5.5	23	Aerobic conditions with complexants
1.6	23	Corrosion processes and the factors that affect them
1.6.1	23	Acidic Packs
1.6.2	24	Tin-plate characteristics
1.6.3	24	Surface Staining
1.6.4	25	Carbonated beverages
1.7	28	Protective and Decorative Coating Systems
1.8	29	Water-Borne Spray lacquers for application onto tin-plated steel
2	33	<b>The Study of Corrosion under Organic Coatings</b>
2.1	38	Scope of work
3	39	<b>Experimental methods and test programme</b>
3.1	39	Development of a synthetic corrosive solution
3.2	40	Corrosion study of tin-plated steel beverage cans
3.2.1	41	Can filling and incubation
3.2.2	41	Atomic absorption spectroscopy
3.2.3	42	Scanning Electron Microscopy/ Energy Dispersive Analysis ( EDX) studies of the metal surface of tin-plated steel coated with lacquer SS1.
3.2.4	43	Conclusions from SS1 study
3.3	45	Lacquer System SS2 Atomic Absorption Spectroscopy



3.3.1	46	Scanning Electron Microscopy / Energy Dispersive Analysis ( EDX ) of the metal surface of tin-plated steel coated with lacquer SS2
3.4	48	Assessment of main areas of corrosion from Rapid Pack Test Storage
3.4.1	48	Lacquer system SS1
3.4.2	49	Lacquer system SS2
3.5	51	Flexibility Measurements of lacquer films
3.6	53	Inferences from initial corrosion studies
3.7	55	Reaction of the bi-products of phenolic resin with Iron
3.7.1	55	Experimental
3.7.2	56	Amount of iron required to cause a colouration of phenolic <u>resin</u> ?
3.8	57	Characterisation of reaction product of iron and phenolic resin
3.8.1	57	Infra-red spectroscopy
3.9	59	Complexing of iron into films detached from the metal substrate
3.10	60	Studies of Iron impregnation into cured films
3.10.1	60	Experimental
3.10.2	61	Atomic Absorption Spectrometer Calibration
3.10.3	63	Inferences from Iron impregnation studies
4	64	<b>Experimental Design to Assess Barrier performance with changing Phenolic loading</b>
4.1	64	Experimental Design Matrix
4.2	65	Can filling and corrosion testing
4.3	66	Results
4.3.1	66	Iron contents determined by atomic absorption spectroscopy
4.4	69	Data fitting and interpretation
4.5	70	Trends observed within data
4.5.1	70	Iron content after 14 days exposure
4.6	71	Number of leaking cans observed
4.7	71	Flexibility of two coat application of film
4.8	72	Results and Conclusions from Experimental Design to Assess Barrier Performance with Changing Phenolic loading

5	73	<b>Optical Emission Glow Discharge Spectrometry (OEGDS) study of Epoxy-graft-acrylic films exposed to Rapid Pack Solution.</b>
5.1	77	Polymer unexposed to corrosive solution
5.2	77	Polymer exposed to corrosive solution
6	78	<b>Water permeation through lacquer films SS1 and SS2</b>
6.1	78	Experimental
6.2	79	Theory of water permeation
6.3	80	Fourier-Transform Infra-red -Multiple Internal Reflection Spectroscopy
6.4	83	Water Permeation Experimental Procedure
6.4.1	83	Water Uptake Experiments
6.4.2	84	FTIR-MIR in situ measurement of coated specimens
6.5	86	Results and Discussion from water permeation study by IR
6.6	88	Conclusions from observing water permeation by IR spectroscopy
7	89	<b>Ion Permeation Studies</b>
7.1	90	Experimental method
7.1.2	92	Detection of ions
7.2	94	Preparation of the polymer films
7.3	94	The Permeation Experiment
7.4	94	Data Analysis
7.5	95	Epoxy-Acrylate Coatings Permeation studies
7.5.1	95	Sodium ion permeability
7.5.2	97	Chloride ion permeability
7.6	98	Formation of idealised ion exchange resins
7.6.1	98	Cation resins
7.7	100	Epoxy-graft-acrylic films as " ion exchange " resins
7.8	103	Diffusion of sodium and chloride ions through epoxy-graft-acrylic films
8	105	<b>Alternating Current Impedance Spectroscopy</b>
8.1	105	Theory
8.2	109	Circuit elements and their AC Impedance Equations
8.3	110	Examination of Electrochemical systems in terms of their equivalent electrical circuits.
8.4	111	Warburg impedance and diffusion control

8.5	112	AC Impedance plots
8.5.1	114	Bode Plots
8.6	115	Equipment used to carry out AC Impedance studies
8.6.1	115	The Wheatstone Bridge
8.6.2	117	Sine Wave Correlation
8.6.3	118	Solatron 1250 Frequency Response Analyser
8.7	119	AC Impedance Experimental Detail
8.7.1	119	Running an AC impedance experiment
8.7.2	119	Data processing
8.8	120	AC Impedance spectroscopy of epoxy-acrylate films on tin-plated steel
8.8.1	120	Experimental Details
8.8.2	121	0.01M NaCl solution /SS1 film
8.8.3	123	0.1M NaCl solution /SS1 film
8.8.4	126	1M NaCl solution / SS1 film
8.9	129	Investigation of SS1 in aqueous phosphoric acid solutions
8.9.1	129	0.01M H <sub>3</sub> PO <sub>4</sub> / SS1 film
8.9.2	130	0.1M H <sub>3</sub> PO <sub>4</sub> / SS1 film
8.9.3	132	1M H <sub>3</sub> PO <sub>4</sub> / SS1 film
8.10	134	AC Impedance analysis of SS2 Polymer film
8.10.2	135	1M NaCl solution / SS2 film
8.11	137	1M H <sub>3</sub> PO <sub>4</sub> / SS2 film
8.12	139	Discussion of AC Impedance Analysis Data of SS1 and SS2 polymer films
8.12.1	139	Sodium chloride solutions
8.12.2	139	Phosphoric Acid solutions
8.13	140	Variation of Impedance Performance with composition of a coating system
8.13.1	140	Experimental Design Matrix
8.13.2	141	Specimen can preparation
8.13.3	141	Impedance Measurements
9	146	<b>Overall Conclusions and suggestions for further work</b>
9.2	149	Suggestions for further work
10	152	<b>Appendix 1: FRA programs</b>
11	157	<b>References</b>

### ***Table of Figures***

Figure No.	Page No.	Description
1	13	Different uses of packaging in the UK
2	14	Consumption of packaging materials
3	29	Epoxy resin production
4	30	Epoxy resin backbone acrylation
5	31	Neutralisation of 50% of acid functionality
6	32	Phenol-formaldehyde cross-linker production
7	41	Iron content versus exposure time for SS1 film
8-11	44	SEM/ EDX plots of metal surface after 0-30 days exposure SS1 film
12	45	Iron content versus exposure time for SS2 film
13-16	47	SEM/EDX plots of metal surface after 0-30 days exposure SS2 film
17	57	Infra-red spectrum of phenolic resin
18	57	Infra-red spectrum of reaction product of phenolic with iron
19	58	Infra-red spectrum 1230-1000cm <sup>-1</sup> of phenolic resin & phenolic-Fe
20	58	Structure of possible phenolic resin-Iron complex
21	61	Atomic absorption spectrometry : Iron calibration graph
22	66	Fe content after 4 days exposure to RPT solution 1 at 50°C
23	67	Fe content after 7 days exposure to RPT solution 1 at 50°C
24	67	Fe content after 9 days exposure to RPT solution 1 at 50°C
25	68	Fe content after 11 days exposure to RPT solution 1 at 50°C

**Figure No. Description**

26	68	Fe content after 14 days exposure to RPT1 solution
27	69	Contour plot representing Cumulative Leakers ( Colours ) v System number and days of exposure to RPT1 at 50 ° C
28	70	Adjusted Response curve for Iron content in solution after 14 days
29	71	Adjusted Response curves for number of leaking cans observed
30	71	Adjusted Response curves for Wedge Bend Flexibility trends
31	74	OEGDS profile from an uncorroded can
32	75	OEGDS profile from a can exposed to corrosive environment
33	76	OEGDS Crater profile plot
34	79	Fourier-Transform Infra-Red water permeation cell
35	84	Water uptake as a function of time
36	85	MIR spectra of epoxy-acrylate films exposed to water
37	86	Intensity change of $3478\text{cm}^{-1}$ absorbance band with exposure time
38	88	Water at interface versus time of exposure
39	91	Permeation cell schematic
40	92	Calibration curve for chloride ion selective electrode
41	93	Calibration curve for sodium ion selective electrode
42	95	Sodium ion permeability of films
43	96	Rate of change of sodium ion concentration for lacquers SS1 and SS2
44	97	Chloride ion permeability of films

**Figure Page No. Description**

**No.**

45	98	Cation exchange resin formation
46	99	Anion exchange resin formation
47	99	Formation of anion exchange resins
48	101	Transport of $\text{Na}^+$ across the membrane
49	102	Diffusion coefficient versus time for sodium ion
50	102	Diffusion coefficient versus time for chloride ion for all epoxy-g-acrylic films
51	106	AC Waveforms for an applied potential and a resulting current
52	107	Vector representations of Impedance
53	110	Equivalent Circuit 1 A non -porous conducting film
54	110	Equivalent Circuit 2 A porous conducting film
55	111	Equivalent Circuit showing a porous film exhibiting electrochemical reactions
56	112	The Nyquist Plot ( Cole-Cole plot )
57	113	Changes in Nyquist plot as electrolyte permeates through the coating
58	114	The Bode plot
59	115	Wheatstone Bridge
60	117	Sine Wave Correlation
61	118	Solartron 1250 FRA Schematic

<i>Figure No</i>	<i>Page No</i>	<i>Description</i>
62	121	Bode Plot: SS1 film exposed to 0.01M Sodium chloride solution
63	123	Nyquist Plot: SS1 film exposed to 0.1M Sodium chloride solution
64	124	Nyquist plots 0.1M NaCl / SS1 film Day 49 Expanded
65	125	Polarisation resistance v exposure time for 0.1M NaCl/ SS1 film
66	126	Bode Plot: SS1 film exposed to 1M NaCl solution
67	127	Nyquist Plot: SS1 film exposed to 1M NaCl solution
68	128	Variation of Polarisation resistance of SS1 film in 1M NaCl
69	129	Bode Plot: SS1 film exposed to 0.01M Phosphoric acid solution
70	130	Bode Plot: SS1 film exposed to 0.1M Phosphoric Acid solution
71	132	Bode plots SS1 film exposed to 1M Phosphoric Acid solution
72	133	Variation of Polarisation resistance of SS1 film in 1M Phosphoric Acid solution
73	135	Bode Plot SS2 film exposed to 1M NaCl solution
74	136	Polarisation resistance v exposure time for 1M NaCl / SS2 film
75	137	Bode plots SS2 film exposed to 1M phosphoric acid solution
76	138	Variation of $R_p$ for SS2 film exposed to 1M phosphoric acid solution
77	143	Adjusted Impedance plots for Impedance
78	144	Contour plot: Impedance at epoxy=80, temp= 118° C
79	145	Contour plot : Impedance at epoxy=85: temp=125° C

### ***List of Tables***

Table No.	Page No.	Description
1	24	Composition of tin plated steel
2	24	Steel types used for Packaging
3	28	Protective and Decorative coating systems
4	39	Rapid Pack test media
5	48	Enamelrater readings for SS1
6	49	Enamelrater readings for SS1- 28 day hold outs
7	49	Enamelrater readings for SS2
8	50	Enamelrater readings for SS1- 28 day hold outs
9	52	Wedge bend flexibility of SS1 and SS2
10	54	Phenolic resin / iron experiments
11	56	Phenolic monomers- iron colouration studies
12	56	Amount of iron required to colour resin
13	60	Film impregnation studies
14	60	Changes in film appearance with time
15	62	Iron contents in solutions and films
16	63	Variation in the amount of iron trapped by changing the phenolic loading of the film
17	64	Experimental Design Matrix for phenolic loading experiments
18	95	Films used for permeability studies



Table No.	Page No.	Description
19	109	Circuit elements and their impedance representation
20	120	Preliminary electrolytes used in AC Impedance Studies
21	122	Analysis of Bode Data for SS1 exposed to 0.01M NaCl solution
22	128	Analysis of Bode data for SS1 exposed to 1M NaCl solution
23	130	Analysis of Bode data 0.01M phosphoric acid / SS1 polymer film
24	131	Analysis of Bode data for SS1 in 0.1M Phosphoric acid
25	132	Analysis of Bode data for SS1 in 1M Phosphoric acid
26	135	Analysis of Bode data for SS2 in 1M NaCl solution
27	137	Analysis of Bode data for SS2 in 1M Phosphoric acid solution
28	140	Composition of Coatings for Impedance measurements

Section 1

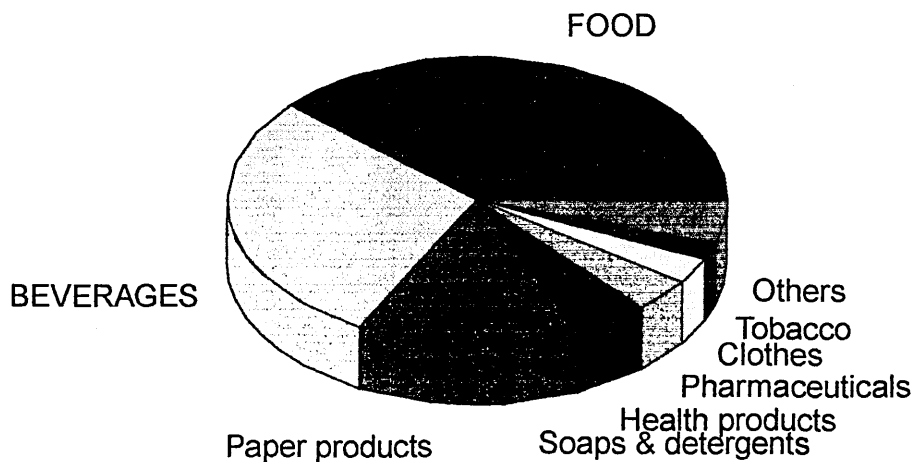
# **Introduction**

## **1.2 INTRODUCTION**

### **1.2.1 The Packaging Industry - An overview**

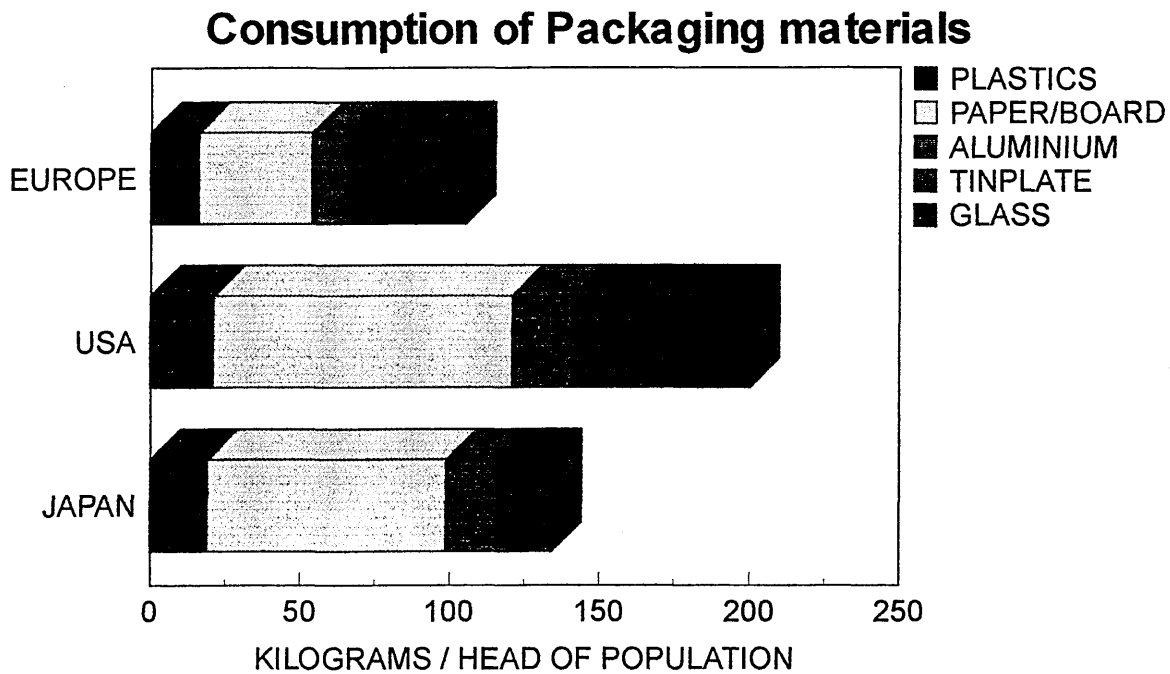
The main purposes of packaging food are to preserve the foodstuff, contain the food, to facilitate distribution, to describe the contents so that customers know what the product is, what its contents are, its weight, how they can use it and any special instructions, e.g. cooking times that may have to be followed. The packaging of a product also helps people to choose when purchasing, reduces food spoilage, promotes and advertises the product, and also helps to prevent tampering of the goods. The packaging industry is a major industry both in the United Kingdom and worldwide. In one year, 1986, in the U.K. alone, £5.3 billion was spent by manufacturers on packaging. Figure 1, below, shows the usage of different packaging materials in the U.K.

### **Different usages of Packaging in the U.K.**



*Figure 1 Different uses of Packaging in the UK*





*Figure 2 Consumption of Packaging Materials*

The above bar chart shows the distribution of the consumption of packaging materials per capita in the different parts of the World. The predominant materials used on a global scale are plastics, paper and board then glass and metal, in roughly equal proportion.

The present study is concerned with the use of tin-plated steel as a packaging material.

1. The first part of the document is a list of the names of the persons who were present at the meeting.

2. The second part of the document is a list of the names of the persons who were absent from the meeting.

3. The third part of the document is a list of the names of the persons who were present at the meeting.

4. The fourth part of the document is a list of the names of the persons who were absent from the meeting.

5. The fifth part of the document is a list of the names of the persons who were present at the meeting.

6. The sixth part of the document is a list of the names of the persons who were absent from the meeting.

7. The seventh part of the document is a list of the names of the persons who were present at the meeting.

8. The eighth part of the document is a list of the names of the persons who were absent from the meeting.

9. The ninth part of the document is a list of the names of the persons who were present at the meeting.

10. The tenth part of the document is a list of the names of the persons who were present at the meeting.

11. The eleventh part of the document is a list of the names of the persons who were present at the meeting.

12. The twelfth part of the document is a list of the names of the persons who were present at the meeting.

### *1.3. The metal can as a container*

Can preserved foods and drinks are aspects of modern life that are generally taken for granted. A wide variety of food is packaged into cans , ranging from baked beans to fruit salad, alcoholic drinks to evaporated skimmed milk , and yet the consumer of the foods often pays little attention to the can in which the food is delivered to his plate. The concept of preserving food in a metal container is almost two hundred years old, so it is not surprising that it is accepted as part of culinary life. The original stimulus for the development of the can for packaging food and drinks is believed to have originated with Napoleon. During the Napoleonic Wars , the French Government offered a prize for an improved method of preserving food. The prize was awarded, in 1810, to the Frenchman Nicolas Appert, a chef, who had found that food could be preserved against spoilage by sealing it in an airtight glass jar and heating. Shortly afterwards, an English inventor, Bryan Donkin, used metal ( iron ) plates which were dipped into tin , to protect them against rusting and soldered them together to form a container. Thus the tin-plated canister, or "can", was substituted for the glass jar, as being more durable and the first food can was born. When the more robust iron canisters were introduced, the reason why the food was preserved was not understood but the innovation meant that food could be kept in a condition suitable for eating over much longer periods of time . The immediate consequence of this was that it was possible for military personnel involved in campaigns to be supplied with food which was suitable for consumption months after the food was prepared. The first recorded usage of food cans for military use was in 1854 during the Crimean War. In 1910, Captain Scott took cans of food on his expedition to the Antarctic and in 1939 a can of roast veal and gravy dating from Captain Sir Edward Parry's third voyage in search of the North West Passage in 1824 was found and examined. The contents were found to be still wholesome and laboratory tests

showed that had the meat been of good quality originally it would have retained its nourishing qualities to a high degree for over a century.

The canisters were at first very heavy requiring a hammer and chisel to open them, but their convenience was soon realised and they then began to appear for general packaging use.

Each of the early cans was handmade individually with a skilled craftsman typically producing six cans a hour. Nowadays, the modern can is produced at a rate of up to six hundred a minute, with research being carried out to find out the optimum amount of material from which to make the cans, constantly improving strength and safety while still reducing weight and cost.

The modern container is thin and light, but very strong. Strong enough in fact to be safe from tampering, to stack smartly on the supermarket shelf and to be safely stored for some time in the kitchen cupboard.

Whilst modern technology has pushed the evolution of the can to the sophisticated pack that is used today, the basic idea is quite simple. Having been used for almost two centuries, the can has proved itself effective. Fresh food or drink, in peak condition is put into the can. The lid is put on and in the case of food, the food is cooked, just as though the can were a little pressure cooker. It is this cooking process, carried out while the food is in its protective container, that preserves the food ready for consumption. No chemical processes or preservatives are generally needed and all the natural vitamins and minerals are safely captured within the can. When the consumer is ready to eat or drink the contents, the lid is taken off to reveal the food as fresh as the day it was canned.



## ***1.4. Can Manufacture***

Two distinct processes are in use for the manufacture of cans

### ***1.4.1 Three piece cans***

Tin- plate , produced by steel companies, is delivered to the canmakers as sheets or in the form of a huge coil. Three sections are needed for each three piece can: a "blank" for the can body, and top and bottom ends. The body blank is rectangular and is curled into a cylinder and the two edges either wire welded or soldered together at high speed. The bottom end is then seamed on and the empty can sent to the canner to be filled. Often the inside of the can is lacquered especially if it is to hold an acidic foodstuff such as tomatoes or rhubarb. The lids are sent separately to be fitted after the cans have been filled.

### ***1.4. 2 Drawn and wall-ironed beverage cans. ( Two piece cans)***

Drawn and wall ironed ( D & WI ) cans are formed by a sequence of processes. Coils of aluminium or tin plate are first cut into circular blanks which are then formed into cylindrical cups by the action of a punch followed by drawing through a circular die. The cups are then normally redrawn, to form a cylinder of smaller diameter. The cylinders are forced by a punch through a series of progressively smaller diameter dies. This has the effect of elongating the cans by an ironing process. The base of the can is formed by a press, and the cans trimmed to a uniform height and washed in preparation for the application of internal and external coatings.

A coater then coats the outside wall of the can with a protective coating and a base colour. The coated cans are then stoved in a gas fired hot air oven to cure the external coat. The design of the can is then applied in up to six colours by a decorator. Varnish is then applied to the can base by a bottom rim coater. The next stage in the can manufacture is the

application of an internal coating or protective lacquer to maintain product quality. This is followed by a final stoving stage in an oven to cure the internal coating.

The can is then transported to the neck flanging machine which shapes the can end so that the lid will fit onto it.

After quality testing and palletising, the cans are passed onto the warehouse from where they are distributed to the can fillers.

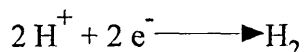
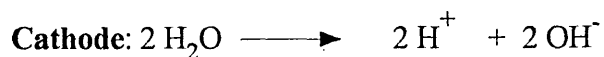
When canning foods, the empty cans are delivered to the canneries, which are situated in the heart of the growing area. The fruit and vegetables to be canned are picked at their prime and quickly dispatched to the canning site. They are washed under high pressure water jets to ensure they are ultra clean and then peeled, trimmed, cored and sliced automatically. The prepared fruit or vegetables are scooped into the cans at high speed with the cans being filled to the correct weight. The brine, syrup, fruit juice or appropriate liquor is poured over the can contents and then the can lid is sealed onto the can body. The can is then conveyed to the most important stage of the process; the cooking stage. The sealed cans are stacked in large retorts which cook their contents under pressure for times and at temperatures that have been carefully worked out by a combination of laboratory tests and consumer research to ensure the food retains both its nutritional content and its taste. When the vegetables or fruit have been cooked, the cans are ready to be labelled, shrink wrapped and sent to the distribution centre and from there to the retailer and consumer.

## 1.5 . Corrosion of cans

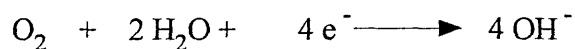
### 1.5.1 Introduction to corrosion

Electrochemical corrosion is a very complex phenomenon but in steel the tendency to corrode electrochemically results from the non-uniform structure of the surface , resulting in some areas being anodic in relation to other areas that are cathodic. When steel is immersed in water having some degree of conductivity, iron dissolves ( corrodes ) at the anodic sites.

The electrochemical reactions that occur initially at the anode and cathode areas in the absence of oxygen are as follows :-



If these were the only reactions occurring, corrosion would rapidly halt because of polarisation, one type of which ,cathodic polarisation, results from depletion of  $\text{H}^{+}$  ions near the cathodic areas. If oxygen is present ( dissolved in the water ) a secondary reaction occurs at the cathode;



Thus the overall reaction occurring during corrosion is;



In the presence of adequate oxygen, the cathodic reaction no longer depends upon the concentration of  $H^+$  ions, and cathodic polarisation is eliminated. It is said that "depolarisation" has occurred. As the concentration of oxygen dissolved in water increases, the rate of corrosion increases <sup>[1]</sup>. Since the corrosion rate depends upon oxygen concentration in the water, exposure of a piece of steel to different local oxygen concentrations can lead to electrochemical cells and thus accelerated corrosion. Evans <sup>[2]</sup> gives further discussion of "differential aeration" effects.

Polarisation of the anode can occur with an accompanying decrease in the corrosion rate as a result of an accumulation of  $Fe^{2+}$  ions near the anodic sites. Anodic polarisation can be decreased or eliminated by removing the  $Fe^{2+}$  ions.

Low carbon steel is susceptible to damage by corrosion in a wide range of aqueous environments and the effects of small amounts of sulphur dioxide,  $H_2S$ , and organic and inorganic acids can be to increase the corrosion rate by several orders of magnitude. The speed and extent of corrosion depends upon the establishment of areas of different electrical potentials, anodic and cathodic areas between which current can flow. Conventionally, these are described as galvanic cells with the most damaging situation arising when there is a large potential developed between a large cathode and a small anode. Anodic polarisation will accelerate the conversion of a metal into its ions, which if soluble, are removed from the vicinity of the anode, thus thinning a section of the metal until it is perforated by solution or weakened until it is fractured by stress or pressure. The concentration of the soluble ions in the electrolyte will continue to increase as corrosion persists.

Tin-plate is highly resistant to atmospheric and aqueous corrosion but, nevertheless, major problems are still encountered. Pinholes in the tin coating are especially damaging; the tin in tin-plated steel is the cathode and the exposed iron becomes the reactive anode. Under severe conditions, very heavy localised corrosion can occur at pinholes or other surface imperfections.

In food packaging containers, the permitted extent of corrosion is minimal, in terms of pick up by the contents, as this may cause changes in the flavour and appearance of the product ( e.g. loss of colour in fruit and haze in beer) and discoloration of internal can surfaces.

The internal corrosion processes are complicated by several factors :

- 1) The normal polarity of the tin-iron galvanic couple can, under certain conditions, be reversed, the tin becoming the anode and thus being sacrificial to the iron. In this case, the tin will be dissolved, exposing large areas of iron which are then rapidly corroded.
- 2) The corrosion rate is greatly affected by the extent of the porosity of the tin layer giving access to the underlying steel base metal. The structure of the intermediate  $\text{FeSn}_2$  alloy and the passivated oxide layer on the plate surface also have an effect on the corrosion rate.
- 3) The rate of corrosion of iron metal will vary considerably with the composition of the metal ( especially copper, phosphorus and sulphur content) , the metallurgical structure and the pickling and annealing practices.
- 4) The corrosivity of the packed product can vary considerably according to the type of product, and also from batch to batch of the same product.
- 5) The environment will also be affected by complexing agents ( e.g. organic fruit acids ) and the presence of accelerators or inhibitors. Residual oxygen in the packed can will also affect the corrosion rate.

Gabe <sup>[3]</sup> discussed the conditions under which polarity reversal occurs and indicated a method of calculating the conditions for reversal , stannous ions can be complexed by food products containing tartrates, citrates etc. Relative polarities also depend on the hydrogen overpotential, with tin developing high values whilst iron does not. Studies of these effects have been described by Kamm <sup>[4]</sup> , Willey <sup>[5]</sup> and Britton <sup>[6]</sup> . Scully <sup>[7]</sup> has discussed the complexing of tin ions by organic acids. Patrick <sup>[8]</sup> gives a useful review of the internal environment obtained in unlacquered cans packed with acid fruits and shows that more complexing agents are present than the usual fruit acids ( oxalic, citric, malic and tartaric ) with the same effects. Other substances shown to complex tin are chloride and hydroxyl ions [9,10]

The possible corroding conditions may be described under the following categories;

#### ***1.5.2 Anaerobic conditions without complexing agents***

Tin is normally cathodic but may become anodic if depolarisers are present. The rate of tin dissolution is slow, but the amount may become objectionable. Beer cans are internally lacquered to ensure a very low level of metal exposure.

#### ***1.5.3 Anaerobic conditions in the presence of complexing agents***

Tin is anodic and will protect the iron until completely removed. This is the normal condition for citrus fruit and similar packs.

A typical citrus fruit pack would for example have the following electrochemical parameters

pH	2.5
Conductivity ( $\mu\text{S cm}^{-1}$ )	15,000
O <sub>2</sub> concentration (ppm)	100 - 200

#### ***1.5.4 Aerobic conditions without complexants.***

The tin is cathodic and exposed iron rusts rapidly. Normal atmospheric corrosion.

### ***1.5.5 Aerobic conditions with complexants***

Corrosion rates are high in the presence of oxidising (depolarising) foodstuffs; these include green vegetables and alkaline detergents in aerosol packs.

## ***1.6 Corrosion processes and factors that affect them***

### ***1.6.1 Acidic packs***

The general pattern of corrosion in a lacquered can is different from the pattern when no lacquer is present because the only exposure of the metal is at scratches in the lacquer coat and at cracks at the neck flange area. The protection from the anodic behaviour of tin is minimal and thus the principal mechanism is the dissolution of the metal by the acids. The corrodibility of the base steel then assumes great importance. In an unlacquered can, the controlling reaction will be the dissolution of the tin ; this metal gives initial protection to the iron substrate but it is removed at a rate controlled by the cathodic reaction on the exposed steel. When the dissolution of the tin has exposed a large area, the rate of attack on the substrate will depend on the extent to which the intermetallic alloy layer is present as a secondary protective layer .

In both cases ,the metal will be taken into solution and hydrogen gas will be evolved with the ultimate shelf life of the can depending upon whether the gas pressure builds up to such an extent so as to cause the can to bulge.

### 1.6.2. Tin-plate characteristics

The steel base of tinplate is a low carbon mild steel with the following broad composition limits: <sup>[11]</sup>

	% w/w
Carbon	0.04 - 0.15
Silicon	<0.08
Sulphur	0.015-0.05
Phosphorus	0.01 - 0.14
Copper	0.02 - 0.20
Manganese	0.20 - 0.70
Nitrogen	0.001 - 0.025

*Table 1: Composition of tin-plated steel*

Hoare et al <sup>[12]</sup> stated that for the best corrosion resistance , the phosphorus and sulphur content of tin-plate should be kept as low as possible and that the presence of more than 0.5% of copper increases the rate of corrosion. On the basis on many experiments , both in laboratories and in industrial application, three types of steel have been specified for packing food products according to their corrosivity:

Steel Type	% P	% Cu	Suitability
L	<0.015	<0.06	Most corrosive foodstuffs
MR	<0.02	<0.20	mildly corrosive products
MC	0.03 - 0.15	<0.20	less corrosive products where strength of container is important

*Table 2: Steel types used for packaging*

### 1.6.3 Surface Staining

Many food products can cause staining of the tin coating. This can range from general to localised and vary in colour from deep blue to almost black. Although not harmful, the appearance of staining is often objectionable. Iron sulphide deposits can also be formed at



sites of damage to the metallic substrate when sulphur containing volatiles from protein compounds react with the tin-plate surface. This sulphur staining is associated with the following factors:

- i) high temperatures which may be responsible for the formation of  $H_2S$ ;
- ii) the hydrogen sulphide may come from sulphur containing amino-acids, e.g. cysteines, tripeptides, glucathions, mercaptans;
- iii) the pH of the pack is of significance;
- iv) the formation of hydrogen sulphide is catalysed by metal ions.

#### ***1.6.4. Carbonated beverages***

As with many acid fruits and other foods, the corrosivity of carbonated beverages packed into tin-plate cans varies widely from relatively inert to highly corrosive. Carbonated soft drinks are formulated mixtures of flavoured syrups and carbonated water containing flavours, acidulants, colours and sometimes other ingredients. Daly <sup>[13]</sup> in his general paper dealing with most aspects of internal and external can corrosion, reported that the behaviour of soft drinks depended on the presence of azo dyes, nitrates, copper and the amount of oxygen remaining in the filled can. It was recommended that formulations should be test packed before commercial marketing; this involves small scale filling and storage of cans for at least six months, with examination of trace metal pick up, organoleptic features and the appearance of the can's internal surface. Beese et al <sup>[14]</sup> have described their studies of the corrosion mechanism in a range of carbonated soft drinks, including the test methods developed for these purposes. They classified canned soft drinks as described below:

- Group 1      Beverages containing dyes or oxidants which once permeated through any coating tend to attack the tin directly; as they vary considerably, the group is further subdivided into those in which tin is anodic to steel, and the type where steel is anodic to tin.
- Group 2      Beverages which do not cause appreciable corrosion of the tin, either by direct attack or by coupling to the iron. Here, the tin tends to serve as an inert barrier, resulting in a relatively low iron pick up . The Colas fall into this group.
- Group 3      This includes the products in which tin is anodic and protects the steel electrochemically; gradual detinning takes place at exposed areas, and rates of iron pick-up range from low to moderate.

Beers in general are less corrosive than the majority of soft drinks but similar product testing is essential to ensure very low levels of metal from the can metal do not leach into the beer.

As a result of these findings and general experience, it is usual practice for can manufacturers and packers to agree a code of practice covering the following points:-

1. The formulation must be established prior to commercial packing
2. Specified carbonation levels must be adhered to which are related to can size, coupled with specified headspace levels and residual oxygen contents.
3. Sulphite levels must be kept to agreed low levels
4. Adequate treatment of water is vital, including filtration to remove colloidal matter.
5. Trace metal ( e.g. copper) contents in water.

The application of organic coatings to metal containers for protective and decorative purposes has been practised for a number of years. Growth in the range of products to be

packed in metal containers and the need for longer storage periods has led to the development of more effective internal protective systems. Most of the protective systems were originally applied to flat sheets of metal before being formed into containers but modern techniques such as drawn and wall ironing to produce two piece cans have demanded the use of more sophisticated materials ; these demands have also been reinforced by the introduction of severe regulations covering health and safety. The Food and Drug Authority (F.D.A.) , in the United States and European Community (E.C.) Directives , and similar safety rules in most countries impose strict rules calling for sophisticated formulations and formulations followed by careful product testing. A basic coating systems will consist of:

- 1) One or two coats of lacquer on the surface intended for the can interior
- 2) Externally: a coat of a sizing agent and, when the can making and filling processes are demanding, a base coat or a base white ink, followed by several ink passes to form a print design, and finally a varnish coat. Normally each coat will be stoved after application (except when specially formulated varnishes are applied “wet on wet” over inks)

The types of resins used for application onto tin-plated steel , their properties and suitability are described in Table 3 ( overleaf )

## 1.7. Protective and Decorative Coating systems

### Steel Can Coatings

Coating & products	Can Type	Comments
<p><i>Acrylic</i></p> <p>Applied as liner for cherries, pears, pie fillings, single serve puddings, some soups and vegetables</p> <p>Acceptable to aseptic packs</p>	<p>For all exteriors, and interiors where a clean, white look is desired.</p> <p>As a high solids side seam stripe for roller and spray application to wire welded cans</p> <p>Water-borne spray liner for 3-piece beverage cans</p>	<p>Expensive, but takes heat processing well and is suited to water-borne and high solids coatings. Employed primarily on can exteriors because of flavour problems with some products</p>
<p><i>Epoxy-amine</i></p> <p>Beer &amp; soft drinks</p> <p>Dairy products</p> <p>Non-foods such as furniture polish, hair spray and paint</p>	<p>D &amp; WI as beer and beverage base coat</p> <p>Draw / Redraw</p> <p>Can Ends</p> <p>Over varnish on aerosol cans and domes</p>	<p>Costly, but has excellent flexibility, adhesion, colour and no flavour problems. Used in interior or as varnish and as size coat. Employed as water-borne with polyamide as a side stripe</p>
<p><i>Epoxy-phenolic</i></p> <p>Beer &amp; soft drinks</p>	<p>All steel cans</p>	<p>Big volume for can interiors. Used in Europe as a universal coating. Main attributes are steam processing resistance, adhesion flexibility and no flavour problems</p>
<p><i>Epoxy-phenolic with Zinc oxide/ carbonate</i></p> <p>For sulphur containing foods: fish, meats, soups and vegetables</p>	<p>3- piece tinplate can ends</p> <p>2-piece single draw cans</p>	<p>Used primarily to prevent tin sulphide staining, flexibility and clean appearance are main attributes</p>
<p><i>Phenolic</i></p> <p>Acid fruits, fish, meats, pet food, soups and vegetables</p> <p>Non foods</p>	<p>All steel cans where coating can be flat applied</p>	<p>Low-cost, exceptional acid resistance and good sulphur resistance</p>
<p><i>Vinyl</i></p> <p>Beer &amp; soft drinks</p> <p>Fruit juices</p> <p>Tomato juice</p> <p>Non-foods</p>	<p>Draw/Redraw, even in triple draw cans-coating is very formable</p>	<p>Flexible and off-flavour free. Resistant to acid and alkaline products. Not suitable for high temperature processed meats and foods. Big use as clear exterior coating</p>

Table 3: Protective & Decorative Coatings 28

### 1.8. Water-Borne Spray lacquers for application onto tin-plated steel

The coatings used to protect the inner surfaces of beer and beverage cans are based on epoxy acrylate co-grafted polymers with either phenolic or amino functional cross-linking agents, ( Figures 3 and 4). The polymer is acid functional with half of the acid functionality neutralised with dimethyl amino ethanol (DMAE) to enable the system to be water dispersible . The finished lacquer contains solvents and low level additions of lubricants to aid film formation and flow properties.

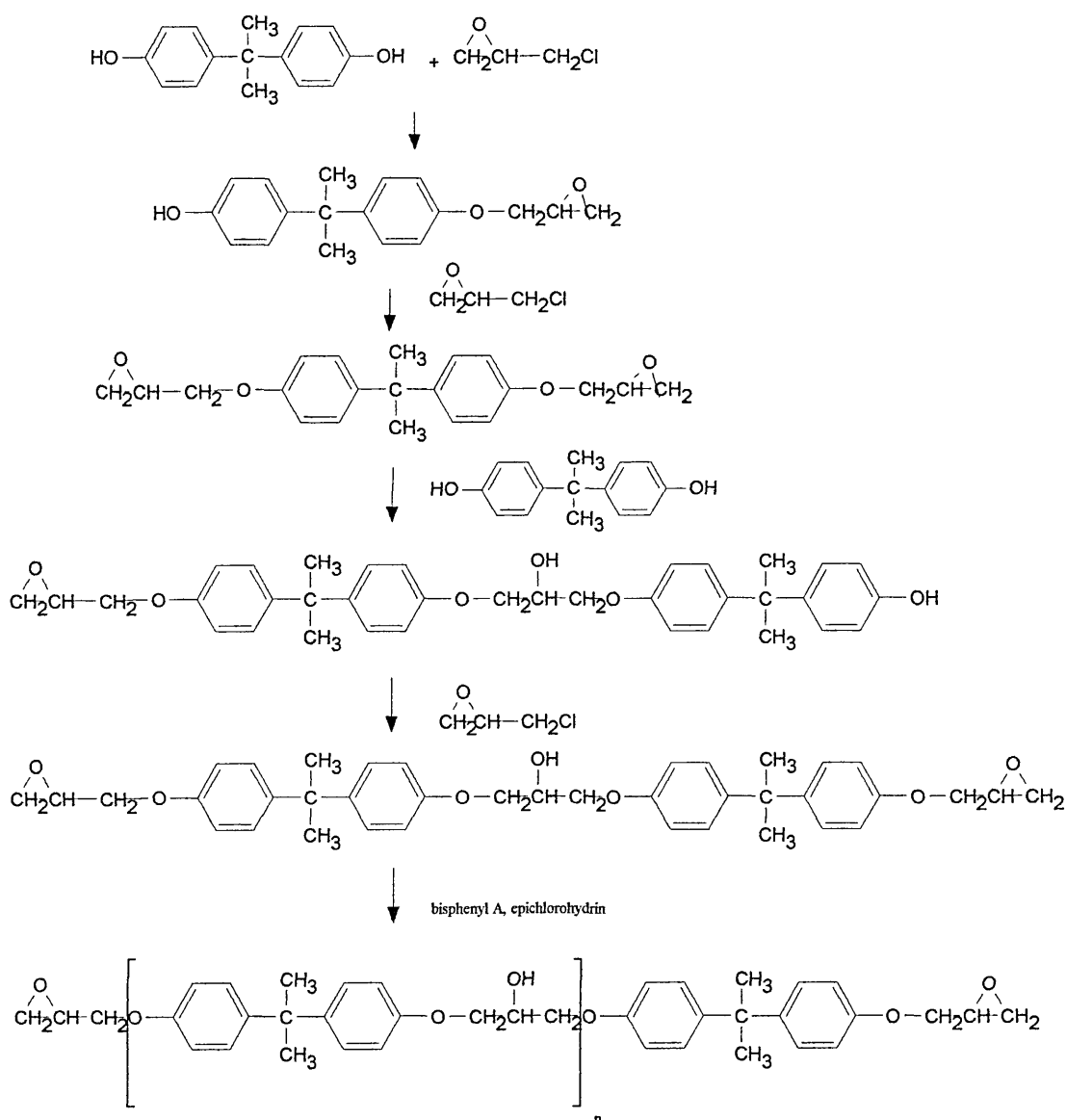
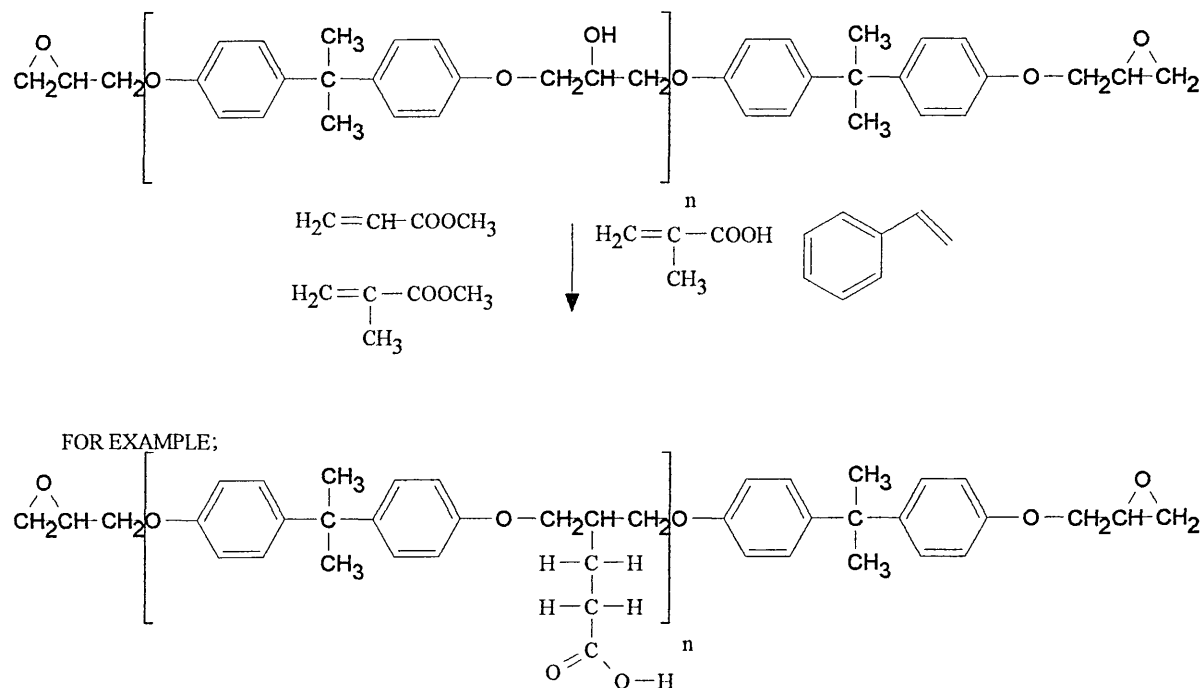
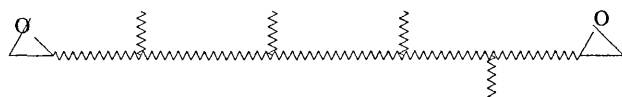


Figure 3 : Epoxy Resin production

The epoxy resin is next acrylated along the polymer backbone using a free radical ( p-tertiary butyl peroxide ) initiated mechanism;



NOW LET THE POLYMER BACK BONE BE REPRESENTED THUS;



THE EPOXY BACK BONE IS ACRYLATED ( TYPICALLY 80% EPOXY: 20% ACRYLATE )

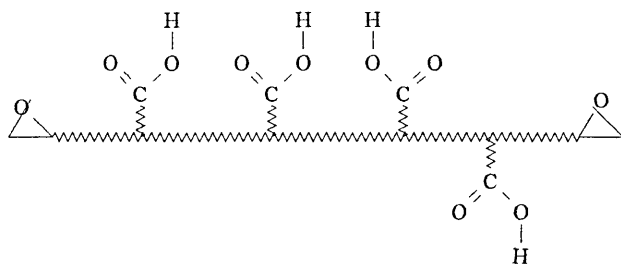


Figure 4 : Epoxy resin backbone acrylation.

In this state, the polymer is insoluble in water and therefore the acid functionality must be reduced, this is achieved by the addition of dimethylamino ethanol (DMAE)

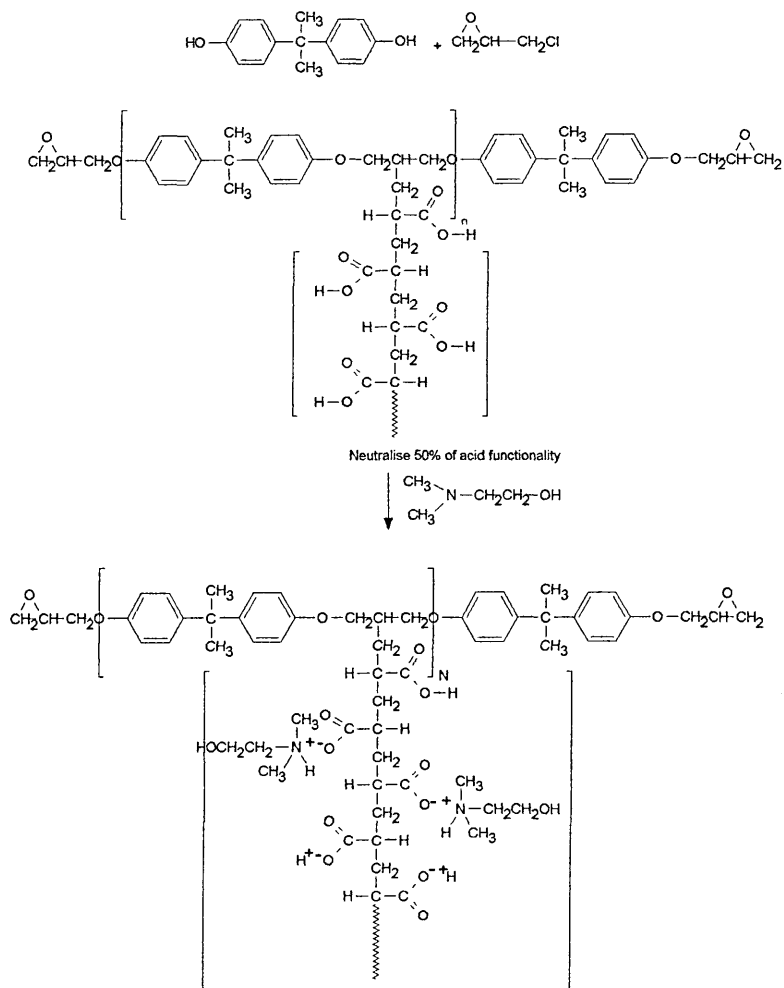
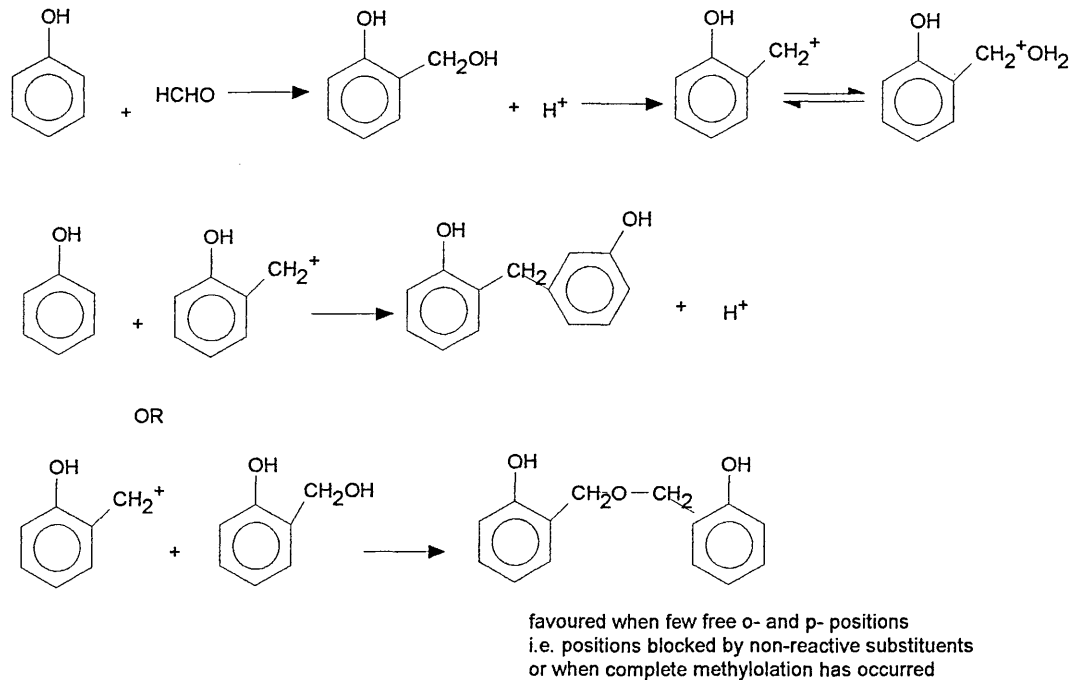


Figure 5 Neutralisation of 50% of acid functionality

Thus at this stage of synthesis the polymer system is dispersible in water but the degree of cross-linking required for the application would not be achieved by this system alone. It is therefore necessary to add a cross-linking agent. The cross-linker in main use for

water-borne polymers for spray application onto metal sheet is based on the reaction of phenol with formaldehyde thus;



Possible Cross-linked phenolic structure

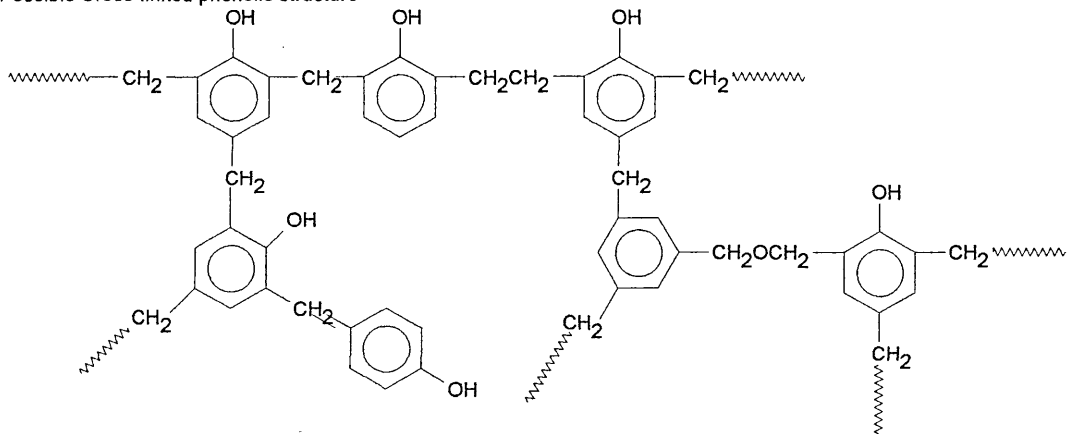


Figure 6: Phenol-formaldehyde cross-linker production

Thus, the polymer system, dispersed in water, comprises an epoxy -acrylic ( typically 80:20 epoxy : acrylic ), 50% neutralised with DMAE, with a cross-linking agent typically at 10%w/w with co-solvents ( n-butanol and 2-butoxy ethanol ) to aid in film formation.



## Section 2

# **The Study of Corrosion under Organic Coatings**

## *2 The Study of Corrosion under Organic Coatings*

The mechanism by which an organic coating protects a metallic material from an aqueous environment is a complex process that is not well understood. Many properties of polymers ( processability, electrical properties, chemical, mechanical and thermal stability ) affect their suitability as protective coatings <sup>[15]</sup> . Among these properties, the nature of the water / coating interactions are important in determining the change in polymer properties during use. A survey of the literature reveals that the protection offered by an organic coating can be accredited to one of the following mechanisms (i) suppression of anodic or cathodic processes, (ii) introduction of a high electrical resistance into the circuit of the corrosion cell; this is the situation found in most decorative types of coating application where the barrier coating is laid down to a thickness of approximately 25-30  $\mu\text{m}$  and (iii) as a barrier to aggressive species <sup>[15 - 20]</sup> . It is currently accepted that the sorption and transport of charged ions and uncharged species such as water and oxygen affect the corrosion behaviour of the polymer / metal system <sup>[15 - 19]</sup> .

Funke <sup>[20]</sup> described the major types of defects in paint layers related to metal corrosion as loss of adhesion and blistering caused by osmosis ; osmotic pressures of the order of 2500-3000kPa may be built up under a film acting as a barrier coating whereas the mechanical resistance of coatings to deformation , as described by Bullett <sup>[21]</sup> , is much lower, of the order of 6 to 40kPa . Blister formation mechanisms have been described ; Meyer and Schwenck <sup>[22]</sup> described alkaline blistering which occurs in the presence of salts like sodium chloride as being due to migration of cations to cathodic areas of corrosion under the film and the subsequent formation of sodium hydroxide giving rise to highly alkaline regions under the film. Neutral blistering which occurs in the absence of cations involved in the

corrosion process was suggested by Evans <sup>[23]</sup> as being an additional possible blister formation mechanism. Under-deposit rusting, which starts when blistering has reached its maximum potential, was described by Ruggeri and Beck <sup>[24]</sup> and proceeds from anodic corrosion sites via differential aeration. Water and ion transport through organic coatings is the subject of many papers as it is thought to be fundamental to the onset of corrosion. For example, Murray <sup>[25]</sup> gives insight into ionic permeability studies of coatings and relates changes in the permeation rate to subtle changes in the polymer structure. Couves <sup>[26]</sup> relates an experimental method for measuring the permeability of organic coatings to ions by the use of ion selective electrodes. Mayne and co-workers <sup>[27]</sup> studied the ionic conduction of detached coatings and found that polymer films are heterogeneous but contain localised areas of high conductivity. The high conductivity areas were considered, in the case of cross-linked films, to be related to the degree of cross-linking.

Many papers have addressed the physical nature of organic coatings as a barrier to aggressive permeants<sup>[27-33]</sup> but the concept of an organic coating being an impermeable membrane has largely been discredited by permeability data reported especially by Funke<sup>[28]</sup>. In many systems investigated, it was found that rate of the water permeability through the coating substrate was high enough to sustain the corrosion rate of the bare metal substrate indicating that, in these cases that the transport of water and / or oxygen to the metal surface was not the rate determining step<sup>[28]</sup>. Water transport through organic coatings has been studied using Fourier Transform infra-red analysis by Yarwood<sup>[29]</sup> whilst Belluci and Nicodemi<sup>[30]</sup> utilised electrochemical impedance spectroscopy to follow the change in film capacitance as water permeated the organic polymer layer and compared this method with the classical gravimetric method. Good agreement was observed for polyethyleneterephthalate (PET) and

polyimide free standing films with the electrochemical method being preferred because of its non-destructive nature.

As corrosion mechanisms are predominately electrochemical reactions, the use of electrochemical methods plays an important role in the evaluation of the corrosion performance and in providing a better understanding of how a coating protects a metal substrate. Leidheiser <sup>[31]</sup>, in a useful review of electrochemical methods for appraising the performance of corrosion protective coatings describes various means of assessing coating performance on a metal substrate; corrosion potential measurements ( the voltage potential at which cathodic and anodic reactions are at equilibrium ) of polymer / metal systems can be obtained but the difficulties of the technique are highlighted in that meaningful results are not achieved unless the metal substrate is in contact with the electrolyte through the coating. Acrylic ,alkyd, epoxy and polyurethane coatings develop a corrosion potential within a short time of immersion in an electrolyte whereas vinyls and vinyl esters may require a month to develop a corrosion potential . DC resistance measurements of coatings , first developed by Bacon, Smith and Rugg, <sup>[32]</sup> have been the basis of much current research. It appears to be firmly established that a coating provides a superb barrier protection when the DC resistance is greater than  $10^9$  ohms  $\text{cm}^{-2}$  of measured area and coatings of the order of fifty microns in thickness have been reported to have DC resistances of  $10^{10}$  ohm  $\text{cm}^{-2}$  when first immersed in electrolyte <sup>[33,34,35]</sup> and this resistance decreases with time of exposure to the electrolyte. As corrosion occurs and additional water penetrates into the coating, the single pore( or multiple pore) size increases in diameter and the resistance of the coating falls.

Although the DC resistance of a coating upon exposure to a corrosive environment is an excellent measure of the absence or presence of corrosion, it is not infallible as the DC voltage passed can cause polarisation of the coating leading to measurement inaccuracies.

Electrochemical studies using impedance measurements over a frequency sweep range of  $10^{-3}$  to  $10^5$  Hz have become very common with the availability of commercial equipment.

AC impedance measurements have an advantage over DC measurements in that more useful information can be obtained and since the AC impedance value at  $10^{-3}$  Hz is approximately the same, for the majority of coatings, as the resistance of a coating using a DC measurement, it substitutes for DC measurements. Useful review papers by Cole<sup>[36]</sup>, Mansfeld and Tsai<sup>[37]</sup> and Hollaender et al<sup>[38]</sup> provide the basic theory of the technique for assessing the protective properties of coatings on metal substrates and give an insight into the way in which electrical equivalent circuits and modelling help to give resistive and capacitance changes of the films in the changing electrolytic environment.

Data representation has not yet been standardised, but two major ways of representing impedance data are at the forefront; the Bode plot (log frequency v log impedance) is more commonly used for coatings than the Nyquist plot (real v imaginary impedance) with both plot forms being transposed from traditional alternating current theory for use in the interpretation of electrochemical cell data.

Thompson and Campbell<sup>[39]</sup> related AC impedance plots for coated metal substrates and developed a protocol for the interpretation of the data in order to distinguish which responses are due to differing corrosion reactions. They observed that two clearly defined Nyquist responses due to the coating and corrosion cell rarely occur in neutral solution.

Coating defects which develop after immersion were observed to produce two Nyquist responses and as the defects become blocked with corrosion reaction products, the coating response begins to dominate the spectrum producing only single response. Leidhesier and Kendig<sup>[40]</sup> attributed changes in the impedance spectra of coatings to the penetration of the electrolyte and found that it was the polymer properties such as glass transition temperature, cross-linking density and modulus of elasticity that determined the site of corrosion initiation. Work carried out by Geenen et al<sup>[41]</sup> studied the effect on the impedance spectrum of model epoxy coatings on a steel substrate when the corrosion is artificially enhanced by introducing a point defect into the 70-200 $\mu\text{m}$  thick film. They proposed equivalent circuits of the different systems studied and found that capacitance and resistance values could be easily related to whether the coating was permeated by electrolyte or if the metal under the coating was beginning to corrode. Tait, Handrich and Maier<sup>[42]</sup> have developed an approach which attempts to predict the corrosion behaviour of steel containers by the impedance technique with reference to the change in the charge transfer resistance of a coating after a set period of time. Their work seems to concur with the earlier work of Bacon, Smith and Rugg<sup>[32]</sup> and concludes that a container service lifetime of significantly less than one year would be observed if the charge transfer resistance of the film falls to below  $10^7 \text{ ohms cm}^{-2}$  within one hundred days of the coating being exposed to the electrolyte but would be greater than two years if the resistance was above  $10^9 \text{ ohm cm}^{-2}$  with a film capacitance of less than  $1 \text{ nFcm}^{-2}$ . Rammelt and Reinhard<sup>[43]</sup> showed that the capacitance of films firstly increases linearly due to water uptake, then plateaus over a long period of time before there is a rapid change in film capacitance when the coating fails and underfilm corrosion starts. Al-Hashenn and Habib<sup>[44]</sup> followed the changes in impedance spectra of polyhydroxy ethers with retained solvent content. They demonstrated that at higher drying

temperatures, polymer films have a smaller pore volume which gives rise to a slower change in coating resistance with exposure time to electrolyte and hence corrosion was retarded for a longer period.

The corrosion of tin-plated steel contacted by various food packaging materials has been discussed in several articles where the food pack has ranged from green beans to dog food<sup>[45-49]</sup> and new views on the corrosion mechanisms of tin-plated steel given by Servais et al<sup>[50]</sup> emphasise the differences in the metallurgical structures of blackplate batch and continuous annealing produced tin-plate and the effects that the resulting surface features might have on the distinct corrosion properties of the corresponding tinplates.

Most of the work outlined above relates to films with thicknesses above 20 $\mu\text{m}$ .

### ***2.1. Scope of work***

The aim of the study described in this thesis is to develop knowledge of the corrosion processes occurring at the polymer / metal interface of industrial coating systems which are spray applied onto tin - plated steel to a coating depth of approximately 3-5  $\mu\text{m}$ .

This presents interesting possibilities for investigation in that permeation of a thin film will be effected much faster than that of a thick film and thus an environment in which corrosion could occur could be established much more rapidly than in the case of thicker protective films.

An assessment is made of coating performance versus composition of the coating. In practice, the polymer systems of interest prevent corrosion of the metallic substrate and subsequent ingress of the metallic ions into the pack material for longer periods of time than would be expected by consideration of the film thickness. The reason why this is so has been investigated and conclusions drawn as to the way in which such polymer coatings exert their anti - corrosive properties.

Section 3

# **Experimental Methods and Test Programme**



### **3 EXPERIMENTAL METHODS AND TEST PROGRAMME**

#### **3.1 Development of a synthetic corrosive solution**

To assess the ability of a lacquer system to retard the onset of corrosion in commercial tin-plated steel cans it was necessary for a synthetic pack solution to be developed. This solution would replicate the conditions in terms of solution pH and conductivity likely to be found when packing beverages into cans. Extension of work carried out by James <sup>[46]</sup> evaluated rapid pack test solutions for tin plated steel cans. The composition of the rapid pack test solution deemed to be most appropriate was: -

<b>Pack No</b>	<b>Contents</b>	<b>pH</b>	<b>Conductivity (<math>\mu\text{S cm}^{-1}</math>)</b>	<b>Sealed pack pressure (p.s.i.)</b>
RPT1	981mg/L sodium acetylsalicylate 2924mg/L sodium citrate 4921mg/L sodium bicarbonate 1000mL Water	6	4,000	30

*Table 4: Rapid Pack Test Medium*

### ***3.2 Corrosion study of tin-plated steel beverage cans***

A series of beverage cans were studied after exposure to a pack test solution.( RPT1)

Experiments, in duplicate, were carried out after 0, 1, 2, 3, 4, 7, 14 and 21 days exposure to the corrosive environment. Analytical determinations were carried out to determine any changes in;

- a) the chemical composition of the aqueous pack test solution with time.
- b) the atoms present in the region of the polymer / metal interface,( studied by elemental surface analysis by energy dispersive X-ray analysis and observation of physical changes at the metal surface by scanning electron microscopy )

Two lacquer systems were selected to enable a variation in coating performance; these were

SS1 ( 10% phenolic cross-linking agent )

SS2 ( 5% phenolic cross-linking agent )

### 3.2.1 Can filling and incubation

A set of tin-plated steel cans was weighed and spray coated with SS1 and SS2 to give coating densities above, below and at the optimum coating weight. The coatings were fully heat cured and a second layer of coating applied followed by a second stoving. The integrity of the coating was checked by Enamelrater current readings. The cans were filled to the neck flange with RPT1 and easy open ends were sealed onto the can body. The filled cans were placed in an incubation oven held at 50°C for the duration of the corrosion test.

### 3.2.2 Atomic absorption spectroscopy

The solutions removed from the cans after exposure to RPT1 test solution were analysed using atomic absorption spectroscopy . The results are as follows;

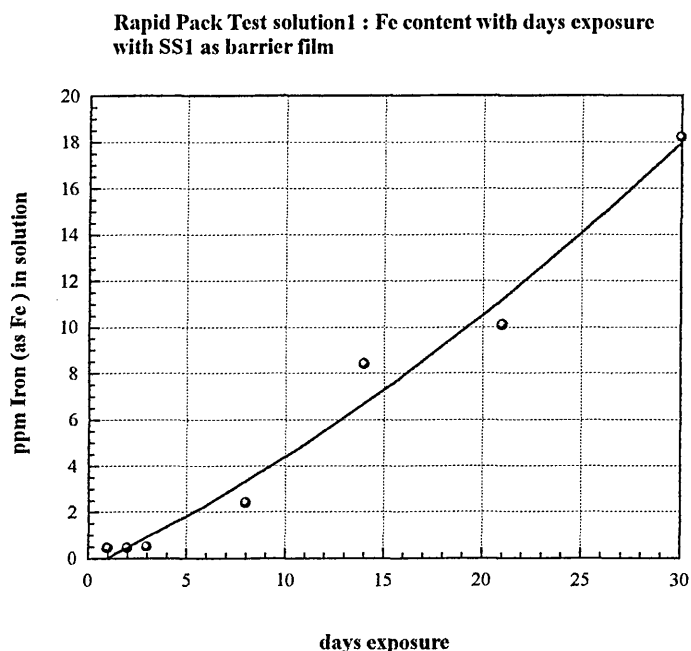


Figure 7: Fe content v exposure time for SS1 film

The graph shows a slow initial period for the iron content in solution but once corrosion is established the iron content in solution rises dramatically.

### ***3.2.3 Scanning Electron Microscopy / Energy Dispersive Analysis ( EDX) studies of the metal surface of tin-plated steel coated with lacquer SS1.***

#### **Results**

##### **Day 0 ( Blank ) ( Figure 8 )**

High levels of  $\text{Fe}^{2+}$  and  $\text{Fe}^{3+}$  .Low levels of tin in three oxidation states with a trace amount of chlorine. Steel-Tin intermetallic layer intact below the polymer surface.

##### **Day 8 ( Figure 9)**

Area 1 ( Small pin prick of corrosion )

$\text{Fe}^{2+}$  /  $\text{Fe}^{3+}$  signals much reduced compared to Day 0 .The steel-tin intermetallic layer below the polymer surface appears to be intact but the appearance of a fourth oxidation state of tin suggests that the tin in the tin-plate layer is oxidising preferentially to the iron. The reduction in  $\text{Fe}^{2+}$  and  $\text{Fe}^{3+}$  may be explained by the fact that these ions are dissolved in the corrosive solution above the polymer. The high chlorine level may be due to  $\text{SnCl}_2$  from the electroplating process being exposed as corrosion occurs in the tin-iron area.

##### **Day 21 ( Figure 10)**

The levels of  $\text{Fe(II)}$  and  $\text{Fe(III)}$  are very low with the different tin oxidation states being observed , indicating nearly complete oxidation of the tin-iron layer. A high response is observed from Cl ( may be from  $\text{SnCl}_2$  ) and at this stage the appearance of a sodium peak may be an indication of breakthrough of the polymer by the rapid pack test solution. This may indicate either the saturation of the polymer by the solution or the onset of corrosion at the metal-polymer interface.

##### **Day 30 ( Figures 11)**

The EDX spectrum is similar to that on Day 21 but with a higher level of  $\text{Na}^+$  being found, presumably due to increased saturation of the polymer with RPT solution.

### *3.2.4 Conclusions from SS1 study*

As the exposure to the rapid pack test solution continues, the levels of iron (II) and iron (III) rapidly decrease at the metal surface. There is an increase in the number of oxidation states of tin observed after approximately eight days and chlorine begins to appear, presumably due to exposure of residual  $\text{SnCl}_2$  from the electrocoating process. The appearance of sodium ions in the EDX spectra, with increasing concentration after 21 days is thought to be due to either;

- 1) Migration of  $\text{Na}^+$  ions across the polymer
- 2) Saturation of the polymer by rapid pack test solution.
- 3) Breakdown of the polymer leading to localised high  $\text{Na}^+$  areas due to the RPT solution collecting under the polymer.

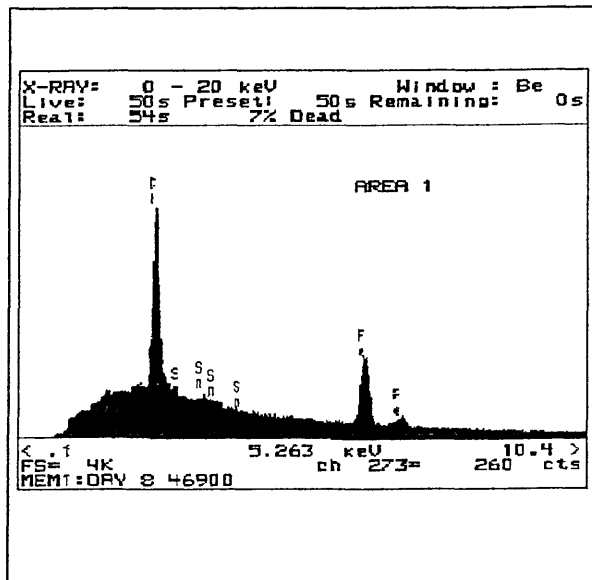
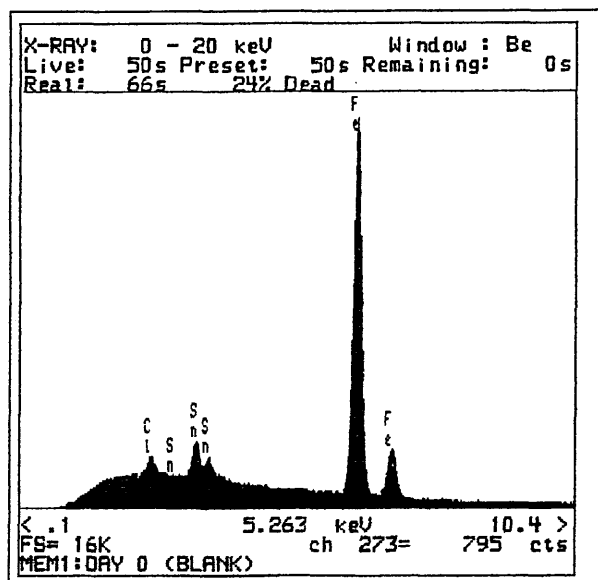


Figure 8: zero days exposure to RPT1/SS1

Figure 9 : 8 days exposure to RPT1 /SS1

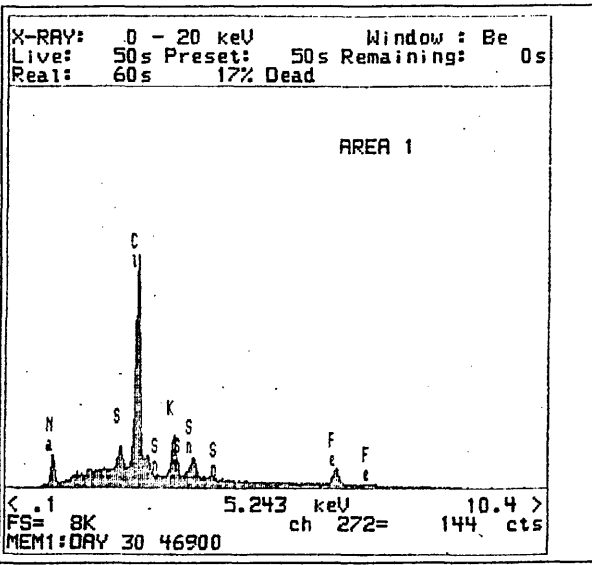
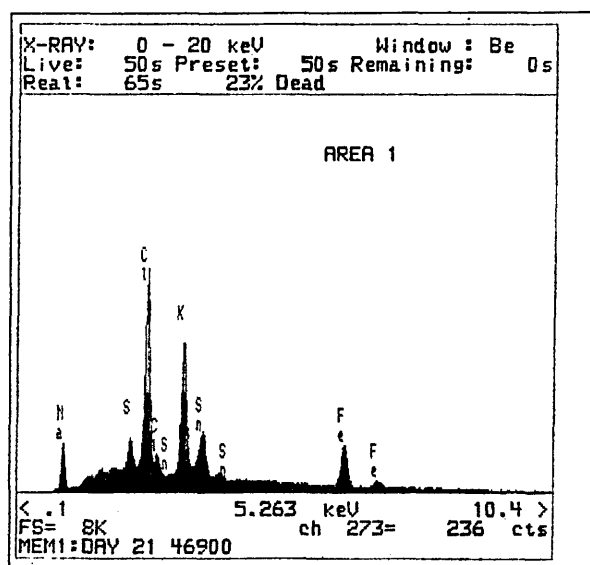


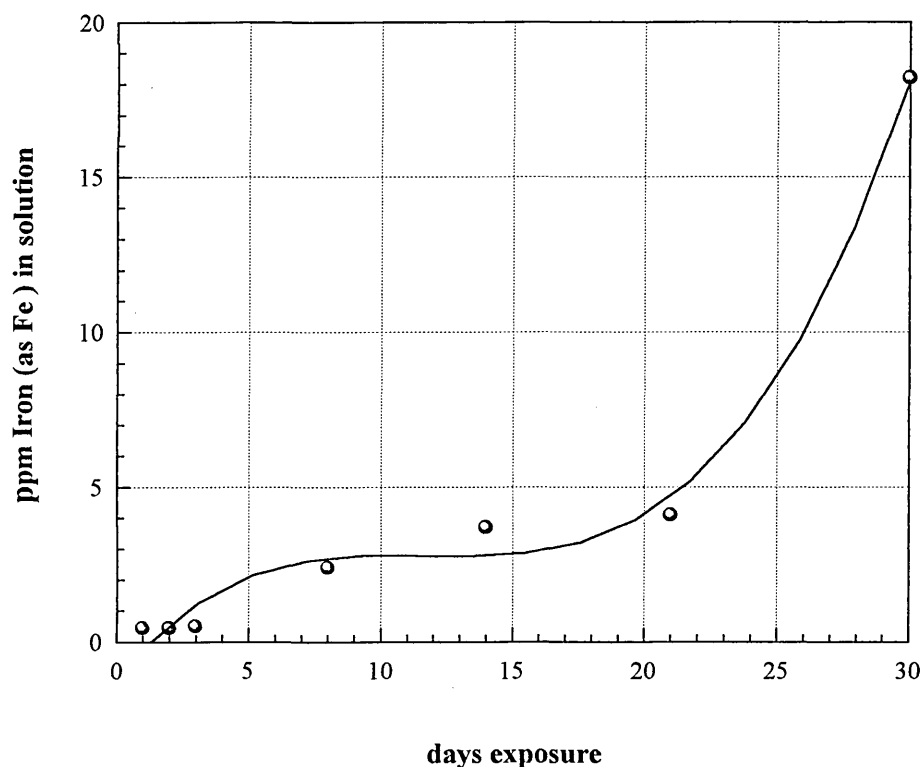
Figure 10: 21 days exposure to RPT1 /SS1

Figure 11: 30 days exposure to RPT1 /SS1

### 3.3 Lacquer System SS2 Atomic Absorption Spectroscopy

The solutions removed from the cans coated with SS2 , exposed to pack test solution 1 at 50°C for 28 days were analysed by atomic absorption spectroscopy. The results are as follows;

**Rapid Pack Test solution1 : Fe content with days exposure with SS2 as barrier film**



*Figure 12: Iron content versus exposure time for SS2 film on steel in RPT1 solution*

SS2 ( 5% phenolic cross-linking agent ) and SS1 ( 10% phenolic cross-linking agent ) appear to provide approximately the same barrier to the passage of ions from the metal surface to the solution . Although the total iron detected in solution after 30 days exposure is the same, the shape of the iron versus exposure time curve is different for the two coating systems with SS2 showing less permeation of iron during the early stages of the test, compared with SS1 .

### ***3.3.1 Scanning Electron Microscopy / Energy Dispersive Analysis ( EDX ) of the metal surface of tin-plated steel coated with lacquer SS2***

Day 0 ( Blank ) (Figure 13)

Very little contamination of the polymer / metal interface. Response from  $\text{Fe}^{3+}$  and  $\text{Fe}^{2+}$  as well as Cl only suggests the metal layer to be intact.

Day 8 ( Figure 14)

Appearance of other ionic species suggests that SS2 is very quickly permeated by the pack test solution (  $\text{Na}^+$  ions shown at this stage - not observed until day 21 with SS1 ).

Day 21 ( Figure 15 )

Different oxidation states of tin observed indicating that corrosion is occurring in the bulk metal underneath the polymer layer.

Day 30 ( Figure 16 )

A large amount of corrosion has occurred causing staining of the polymer film by  $\text{Fe}_2\text{O}_3$  trapped between the disbonding polymer and the metal surface. The EDX spectrum supports this conclusion in that a very high  $\text{Fe}^{3+}$  signal is observed in comparison to the  $\text{Fe}^{2+}$  signal.



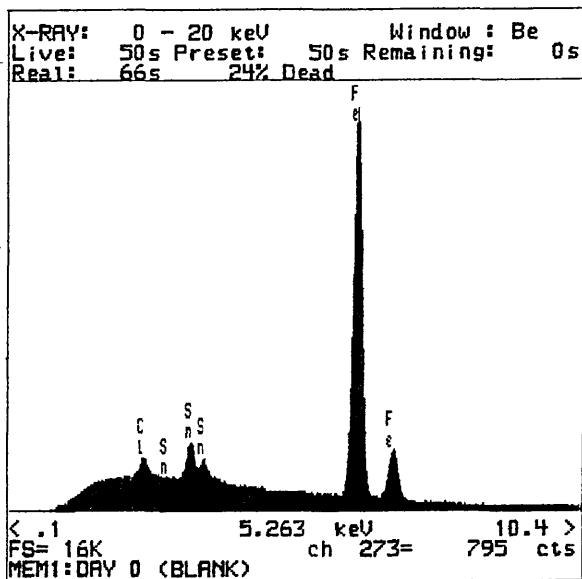


Figure 13 : 0 days exposure to RPT1 /SS2

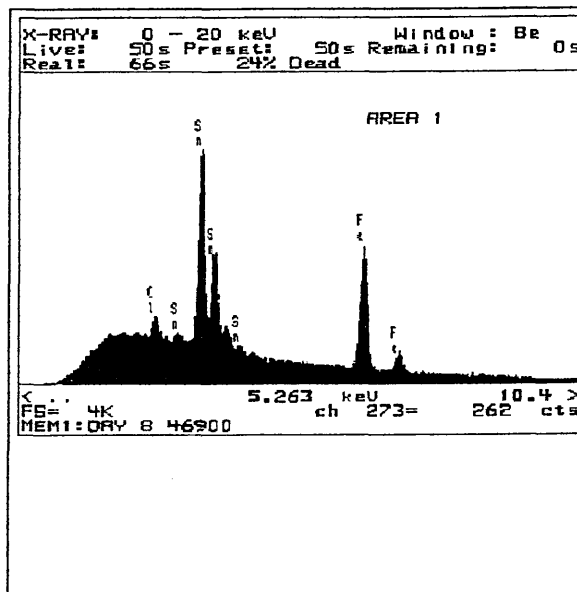


Figure 14: 8 days exposure to RPT1/ SS2

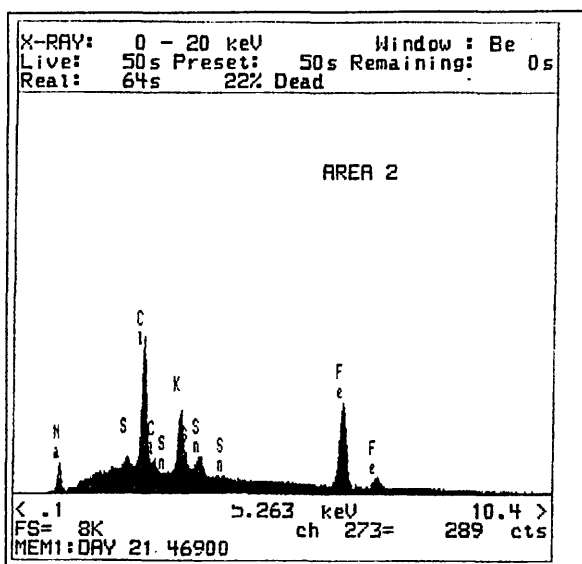


Figure 15: 21 days exposure to RPT1/SS2

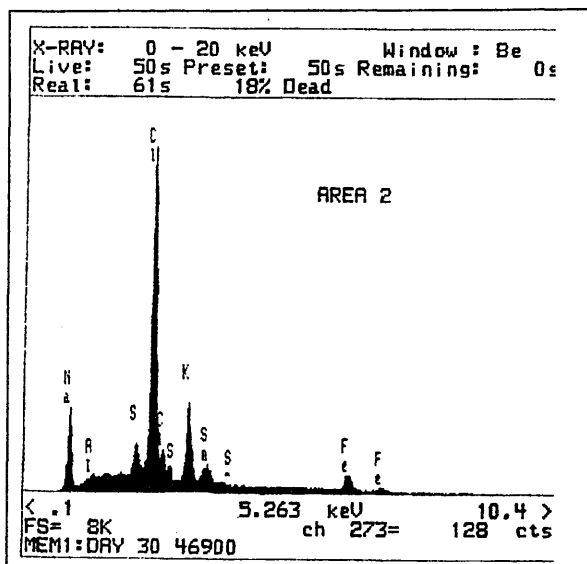


Figure 16: 30 days exposure to RPT1/ SS2

### 3.4 Assessment of main areas of corrosion from Rapid Pack Test Storage

A well established test method used in the canning industry to check the integrity of the polymer coating is Enamelrater™ measurements.

The technique applies a direct voltage ( 6.3V ) across a can under examination and measures the current flowing as a result of electrolyte within defects in the film causing a short circuit to the metal.

The cans removed from the rapid pack test storage were Enamelrated to detect the presence of defects in the coating. The corrosion on the can side walls and dome area was assessed by filling the can with 200mL of electrolyte (1% NaCl ), attaching the anode to the side of the can, inserting steel counter electrode , passing the DC voltage and then measuring the current flow.

The corrosion in the neck area of the can was assessed similarly but involved filling the can completely so there was no overspill of electrolyte when the steel counter electrode was inserted.

The results of these tests are tabulated below (Tables 5 -8 ):

#### 3.4.1. Lacquer system SS1

Days exposed to RPT1	Enamelrater Readings (mA) ( Dome and Side wall )			Enamelrater Readings (mA ) NECK region		
	Can 1	Can2	Can3	Can 1	Can 2	Can 3
1	0.0	0.0	0.0	0.0	0.0	0.0
2	0.0	0.1	0.0	0.1	0.1	0.1
3	0.0	0.0	0.0	0.1	0.1	0.1
4	0.0	0.0	0.0	0.1	0.2	0.2
7	0.0	0.0	0.0	0.4	0.5	0.6
10	0.0	0.0	0.0	0.5	0.5	0.7
14	0.0	0.1	0.1	0.8	0.8	0.9
21	0.0	0.1	0.2	20.4	25.7	30.5

Table 5: Enamelrater readings for SS1 film

Eight cans were available for study up to until 28 days exposure with RPT solution at 50°C. The Enamelrater readings were recorded and a visual assesment of the amount of corrosion in the neck area was made;

Can No	mA	% neck corrosion	% Dome and Side wall corrosion
1	100.5	75	<5
2	120.2	85	<5
3	102	75	<5
4	108.6	80	<5
5	109.2	80	<5
6	135.8	90	<5
7	147	85	<5
8	110.3	75	<5
Average	116.6	80.6	<5

*Table 6: Enamelrater readings SS1-28 day exposure*

#### **3.4.2. Lacquer system SS2**

Day	Enamelrater Readings (mA) ( Dome and Side wall )			Enamelrater Readings (mA ) NECK region		
	Can 1	Can2	Can3	Can 1	Can 2	Can 3
1	0.0	0.0	0.0	0.0	0.0	0.0
2	0.1	0.2	0.1	0.1	0.1	0.1
3	0.0	0.0	0.0	0.2	0.2	0.3
4	0.0	0.0	0.0	0.4	0.4	0.4
7	0.0	0.0	0.0	0.7	0.7	0.5
10	0.0	0.0	0.0	0.7	1.1	1.2
14	0.0	0.0	0.0	5.2	5.2	10.8
21	0.0	0.5	0.2	25.3	27.1	28.4

*Table 7: Enamelrater readings SS2 film*

Eight cans were available for study up to 28 days exposure with Rapid Pack Test Solution 1  
The Enamelrater readings were recorded and a visual assesment of the amount of corrosion  
across the internal surface of the cans was made;

Can No	mA	% neck corrosion	% Dome and Side wall corrosion
1	188.8	15	<5
2	39.2	20	<5
3	61.9	15	<5
4	200	20	<5
5	5.9	25	<5
6	195.1	25	<5
7	110.1	20	<5
8	104.4	20	<5
Average	113.2	20	<5

*Table 8: Enamelrator readings of cans coated with SS2 film after 28 day exposure to RPT1*

Comparison of the results of pack testing lacquer systems SS1 and SS2 is interesting as the data appear to present differences in the percentage of corrosion visible in the neck region of the cans which can only be accounted for by the difference in phenolic crosslinker level present in the variables.

Thus the following inferences could be drawn from the initial pack test studies;

- 1) No significant corrosion is observed in the can wall and dome regions
- 2) The solutions taken from a series of cans coated with the variant containing 10% phenolic SS1 show approximately the same amount of iron in solution after 30 days exposure to RPT 1 as the solutions from SS2 ( 5% phenolic ).

3) The degree of overall can side wall and dome corrosion assessed by Enamelrator current readings in both coating systems is approximately equal.

4) Interestingly, the amount of visual corrosion in the cans coated with SS2 is less in the neck region than in the cans coated with SS1.

### ***3.5. Flexibility Measurements of lacquer films***

The fact that SS2 contains less phenolic cross-linker than SS1 but gives rise to less visible corrosion in the neck region seems to suggest that it is not the degree of cross-linking that has an influence upon the anti-corrosive abilities of the films but the cross-linking density.

A film with higher cross-linked density should therefore show less flexibility and be more susceptible to break down during the formation of the neck flange and be prone to fracture during the process of seaming an easy open end.

To investigate this proposal, samples of SS1 and SS2 were flood spun (flood spinning involves depositing a quantity of the liquid lacquer onto the metal, rotating the metal and liquid lacquer at high speed for short time periods to leave a thin layer of the lacquer on the metal surface) onto tin-plated steel to give a coating density of 150 - 160 mg /m<sup>2</sup> . The films were cured in a box oven giving a peak metal temperature of 1 minute at 188°C .

A commonly used measure of the degree of flexibility in the metal coating industry is the use of Wedge bend flexibility measurements.

The method involves bending a coated metal specimen over a bar to form the specimen into a U shape. The specimen is placed on a tilted platform and then subjected to a drop of a 1Kg mass from a height of 1 metre. The degree of fracturing of the coating is then assessed by ratioing the length of the coating fracture to the length of the specimen panel under test.

The flexibility of the coating under test is then expressed as the Wedge Bend Flexibility with high figures representing coating that are less susceptible to impact fractures in areas of high stress.

	Wedge Bend Flexibility (%)										
	1	2	3	4	5	6	7	8	9	10	Avg
SS1	85	84	83	86	85	84	81	85	84	83	84
SS2	87	88	85	86	87	87	86	87	88	88	86.9
SS1 Data 1 standard deviation= 1.3, SS2 Data 1 standard deviation = 0.9											

Table 9: Wedge bend flexibility measurements of SS1 and SS2

Although not vastly different, the film formed from lacquer system SS2 does appear to exhibit more flexibility on flat sheet than SS1.

Comparison of the overall corrosion after 28 days in RPT solution shows a similar degree of overall film porosity for both lacquer systems ( 116 mA for SS1 compared with 113mA for SS2 ) but the corrosion occurs in different regions of the can body. The corrosion exhibited in the high cross-link density film is predominately in the neck flange area where the reduced film flexibility causes film breakage upon end seaming. SS2 is more flexible in this region and thus shows less visible corrosion.

### *3.6 Inferences from initial corrosion studies*

Inferences made from the above series of studies are that the fully cured polymer films are totally permeated in approximately 21 days of being exposed to the pack solution. This is indicated by the appearance of sodium ions at the metal surface after this time (detected by energy dispersive analysis by SEM). When permeation of the film has been achieved, a rapid increase in the amount of iron is found in the pack test solution, typically rising to 20 ppm after 28 days exposure to the corrosive environment for a poorly protective film ( see Figures 7 and 12 ). The levels of iron detected in the solutions are still low at this stage and this may suggest that the transport of iron ions is being impeded across the polymeric membrane and that the iron is being physically trapped below or chemically entrained into the polymer matrix. Visual investigation of polymer films exposed to corrosive solutions over long periods of time shows evidence of colouration of the film. The colours range from red / brown to purple. The red / brown colouration can easily be explained by reference to the aqueous chemistry of iron ( III ) and is indicative of hydrated ferric oxides but the appearance of purple colourations is more problematic.

Previous observations in commercial usage of these lacquer systems had shown on rare occasions the lacquer to be a pink / purple colour just prior to spray application. A possible connection was envisioned by the author between the colouration observed in the bulk lacquer and the purple spots observed in cured films in cans exposed to corrosive environments.

A classical test for the presence of phenolic compounds is the addition of a few drops of neutral ferric chloride to the phenol dissolved in water or methylated spirit. A positive reaction results in a violet, blue or green colour depending on the nature of the phenol involved in the reaction. . The colouration is due to a complex being formed between  $d$

orbitals on the ferric ions and *p* - orbitals on the oxygen atom of the phenolic hydroxyl group. The water based lacquers under investigation can be formulated with either phenolic or amino functional cross-linking agents but it was observed through experiment that only the phenolic- containing resin systems produced a pink-purple colouration when heated in the presence of finely divided iron powder.

To investigate the formation of resin-iron complexes the experiments detailed below were performed. The experimental procedure was as follows :-

30 mL aliquots of SS1 lacquer ( 10% phenolic ) were placed into contact with different substrates at the temperatures and times as detailed below ( Table 10 ):

TEMPERATURE ( °C )	SUBSTRATE	COLOUR AFTER 1/2 HR	COLOUR AFTER 1 HR	COLOUR AFTER 6HR
21	NONE	NO	NO	NO
50	NONE	NO	NO	NO
80	NONE	NO	NO	NO
21	Tin Plated steel (T.P.S.)	NO	NO	NO
50	T.P.S.	NO	NO	NO
80	T.P.S.	NO	NO	NO
21	Tin free steel (T.F.S)	NO	NO	NO
50	T.F.S.	NO	NO	NO
80	T.F.S.	NO	NO	NO
21	IRON FILINGS	NO	NO	SLIGHT
30	IRON FILINGS	NO	NO	YES
40	IRON FILINGS	NO	SLIGHT	YES
50	IRON FILINGS	SLIGHT	YES	YES
80	IRON FILINGS	YES	YES	VERY DARK

*Table 10: Phenolic resin-iron reaction experiments*



Investigation showed that at 50°C, in the presence of iron filings , SS1 developed a dark pink colouration after only one hour of holding at this temperature.

It is suggested that the colouration observed with phenolic resin containing spray lacquers could be due to some complexing occurring between the phenolic resin and the iron, present as either  $\text{Fe}^{2+}$  or  $\text{Fe}^{3+}$

The phenolic resin used in the SS1 spray lacquers is based on a phenol-formaldehyde reaction as described in Section 1.8

Chain extension in the phenolic resin is effected by the formation of ether or methylol linkages, depending upon reaction bi-products Thus the possible bi-products from the reaction are phenol, formaldehyde, water, 2-hydroxybenzyl alcohol ( 2-HBA), 3-hydroxybenzyl alcohol ( 3-HBA) as well as small quantities of the para substituted 4-hydroxybenzyl alcohol (4-HBA) and di and trisubstituted low molecular weight oligomers.

### ***3.7 Reaction of the bi-products of phenolic resins with iron filings***

#### ***3.7.1.Experimental***

The phenol (0.1 mole ) (AR grade ex BDH) was weighed into a 50mL round bottomed flask. De-ionised water ( 10 mL ) was added to the flask and the mixture heated gently to dissolve the phenol. To this aqueous phenol mixture, iron filings (0.1 mole) was added. A reflux condenser was fitted to the flask and the mixture gently heated under reflux over a period of one hour.

The results are tabulated below ( Table 11 ):

PHENOL	COLOUR AFTER 0 HRS	COLOUR AFTER 0.5 HR	COLOUR AFTER 1 HR
PHENOL	NO	SLIGHT PINK	SLIGHT PINK
2- HBA	NO	NO	SLIGHT PINK
3- HBA	NO	NO	NO
4-HBA	YES (RED)	YES (RED )	YES (DARK RED)
PHENOLIC RESIN	YES (DARK RED)	YES (DARK RED)	YES (DARK RED )

Table 11: Phenolic Monomers-Iron colouration studies

### 3.7.2 Amount of iron required to cause a colouration of 1g of phenolic resin

Portions of resin (1 g) were weighed into 50mL round bottomed flasks. 10mL of 2-butoxyethanol, 50 % aqueous solution, was added. The mixture was swirled to dissolve the solids. Various amounts of iron filings were added. A reflux condenser was fitted to the flask and the mixture gently heated to reflux. Heating was continued for a period of one hour. Observations were made at the start of the reflux period, after 30 minutes and at the end of the one hour period.

The results are presented below (Table 12 ):

AMOUNT IRON ADDED / g Resin	COLOUR AFTER 0 HRS	COLOUR AFTER 1/4 HR	COLOUR AFTER 1/2 HR	COLOUR AFTER 3/4 HR	COLOUR AFTER 1 HR
0.0001g	NO	NO	NO	NO	NO
0.0005g	NO	NO	NO	NO	NO
0.001 g	NO	NO	NO	NO	NO
0.002 g	NO	NO	NO	NO	NO
0.005 g	NO	NO	NO	NO	NO
0.010 g	NO	NO	NO	NO	NO
0.020 g	NO	NO	NO	SLIGHT	YES
0.030 g	NO	NO	NO	YES	YES
0.050 g	NO	NO	SLIGHT	YES	YES
0.100 g	YES	YES	YES	YES	YES (DARK)
0.500 g	YES (DARK)	YES (DARK)	YES (DARK)	YES (DARK)	YES (DARK)

Table 12: Amount of Iron required to colour resin

### 3.8. Characterisation of reaction product of iron and phenolic resin.

#### 3.8.1 Infra-red spectroscopy

The infra-red spectrum of the phenol -formaldehyde resin was recorded using a Nicolet DX4 Fourier Transform Infra-Red spectrometer. A vacuum oven was used to remove the solvent present prior to acquisition of the spectrum.

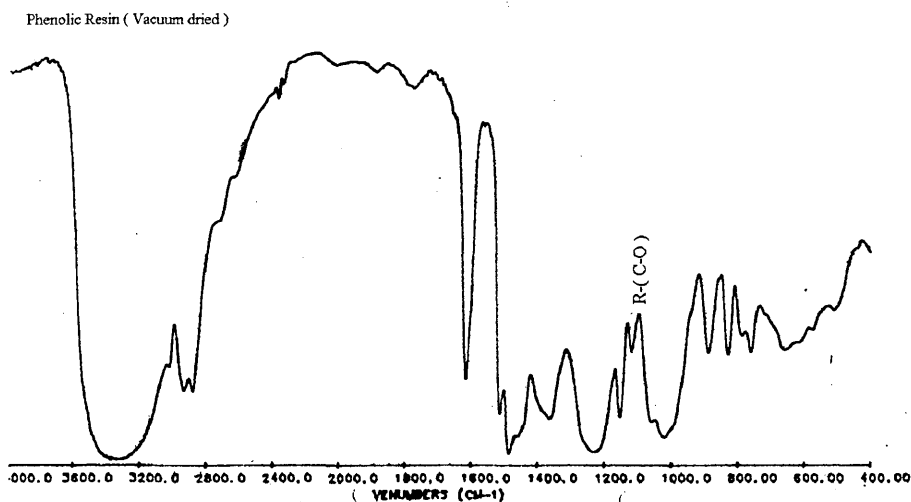


Figure 17: Infra-red spectrum of phenolic resin

The dark red coloured resin -iron product from section 3.12.2 was vacuum dried and the infra-red spectrum recorded;

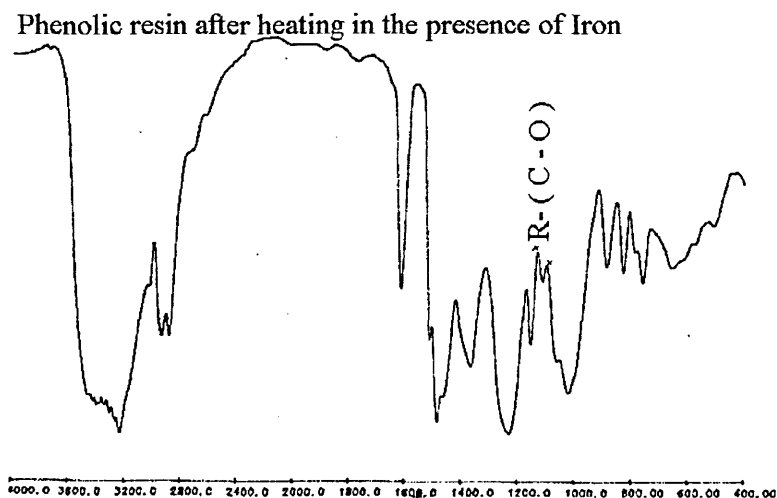


Figure 18 : Infra-red spectrum of reaction product of phenolic resin with Iron

The region of the spectra in which differences are observed is expanded below;

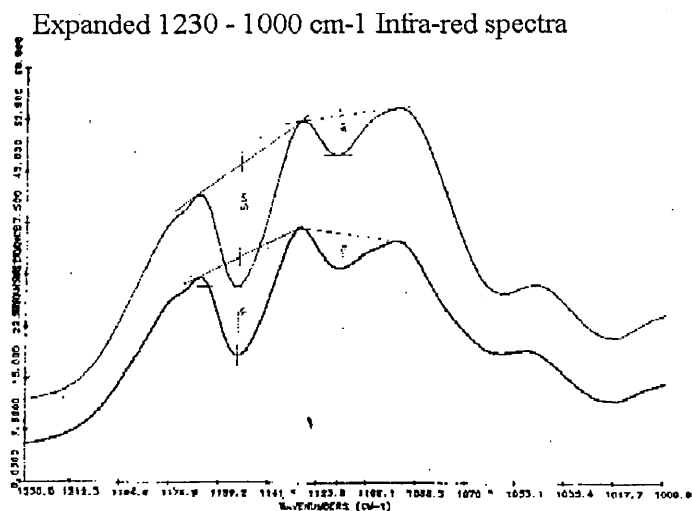
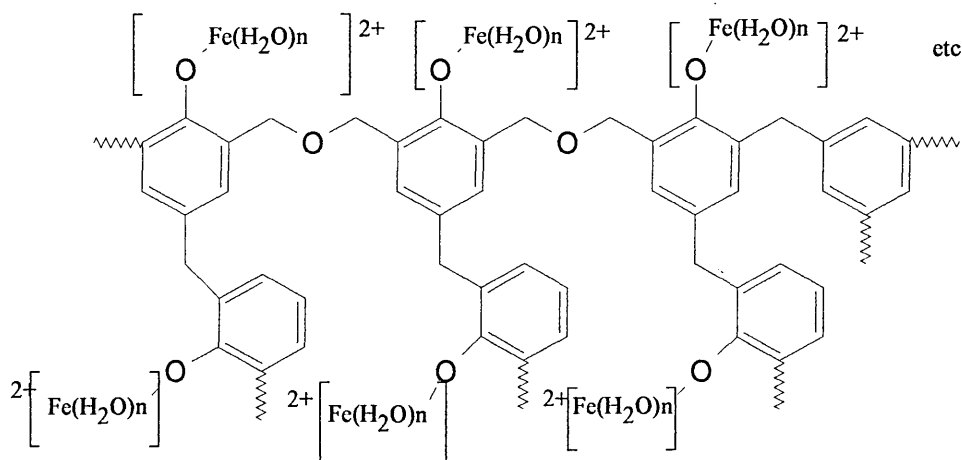


Figure 19: Infra-red spectrum 1230-1000 $\text{cm}^{-1}$  of phenolic resin and phenolic-iron complex

The significant difference observed in the spectra of the phenolic resin and phenolic resin treated with iron is the reversal of the relative intensities of the absorption bands at 1158 and 1115  $\text{cm}^{-1}$ . Both of these absorption bands are in the region of absorption due to R - (O-C) stretching modes and it is postulated that introduction of iron atoms into the polymer matrix causes slight differences in the structure of the polymer around the phenolic oxygen.

The iron- phenolic complex is thought to have the following type of structure;



*Figure 20: Possible structure of Phenolic-Iron complex*

It is thought that this complex may be the possible cause of the pink colouration observed in the commercial use of SS1 when heated and stored in metallic containers. A similar type of complexing reaction may occur in a can, causing the iron removed from the metal surface at the onset of corrosion to be complexed into the polymer matrix, hence accounting for the surprisingly low iron contents in the pack solution even when visible corrosion has commenced.

### ***3.9 Complexing of iron into films detached from the metal substrate***

To further investigate the complexing phenomenon, a procedure needed to be devised to allow the study of the effects of localised high concentrations of iron in the cured film.

Obtaining films that were detached from the metal substrate proved to be problematic and considerable experimental effort was expounded before a reliable means of obtaining cured film free from the metal substrate was settled upon.

The method of choice was

- (a) spray coat the liquid lacquer onto aluminium can bodies at 150 mg/ can.
- (b) Cure the film in a conveyor oven set to obtain 188 ° C for 1 minute at peak metal temperature.
- (c) After cooling, remove the film from the aluminium can body by dissolving away the metal by immersion in 5M sodium hydroxide solution.
- (d) Wash the film until the wash residues are pH neutral.
- (e) Dry the film by firstly blotting away surface water with an absorbent tissue and then allow to air dry for 48 hours.

### 3.10 Studies of Iron impregnation into cured films.

#### 3.10.1 Experimental

2.5 cm<sup>3</sup> cured film was placed into baths containing various solution.s.

TEST NUMBER	TEMPERATURE	ELECTROLYTE
1	21	D.I.WATER (BLANK)
2	21	1000ppm Fe <sup>3+</sup>

Table 13: Film impregnation studies

Observation of any changes in the appearance of the film are detailed below;

DAYS	Observations
1	No visible change in appearance of film
14	No visible change in appearance of film
21	Slight haziness of film
28	No change from day 21
35	No change from day 28
42	Very slight darkening of film
49	Film is beginning to darken
56	Film has a overall brown colouration
63	Film has brown colouration

Table 14: Changes in film appearance versus exposure time to 1000ppm Fe(NO<sub>3</sub>)<sub>3</sub>

The change in SS1 film colouration after 50-60 days exposure to iron nitrate solution suggests some change to be occurring either at the film surface or within the polymer matrix.

To investigate if the colouration was due to a physical or chemical change , a sample of brown coloured SS1 lacquer film ( 0.0164g) , exposed to 1000ppm Fe(NO<sub>3</sub>)<sub>3</sub>, was weighed into a High Pressure Parr Bomb reaction vessel.

Concentrated nitric acid ( Analar grade s.g. 1.43) (2.5mL) was added and the bomb assembly completed. The reaction bomb was placed into a thermostatically controlled oven held at 150°C for 2 hours. After this time, the bomb assembly was allowed to cool to ambient

temperature and the dissolved contents transferred to a 10.0mL volumetric flask . The same procedure was followed for the colourless film exposed to deionised water for 60 days. The solutions, diluted to 10.0mL with de-ionised water, were analysed by atomic absorption spectroscopy. The results are as follows;

### 3.10.2 Atomic Absorption Spectrometer Calibration

A series of standards was prepared from A.A. grade  $\text{Fe}(\text{NO}_3)_3$  to cover the range 0.1 to 100 ppm iron, as Fe. The solutions were analysed using the following conditions;

<u>Condition</u>	<u>Setting</u>
Wavelength	248.3 nm
Slitwidth	0.2nm
Flame Conditions	Air-Acetylene flame ( lean blue )

The calibration graph is plotted below;

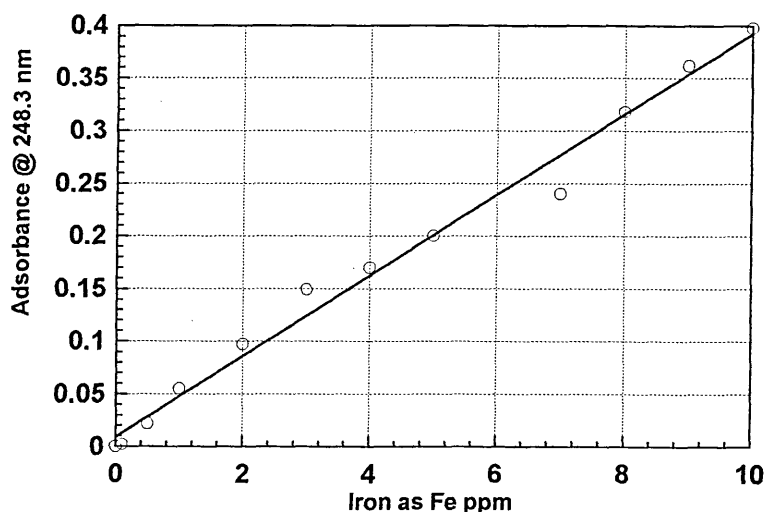


Figure 21 Atomic absorption spectroscopy-Iron calibration graph

The solutions of SS1 polymer were analysed by atomic absorption spectroscopy and the absorbances converted to parts per million iron by use of the above graph.

	Iron ppm in solution	Iron as Fe as %w/w of total film
SS1 exposed to D.I. water	0.34	0.03
SS1 exposed to 1000ppm Fe solution	3.94	0.24

*Table15: Iron contents in solution and film*

Thus , iron appears to be entrapped into SS1 polymer film upon prolonged exposure to high concentrations of ferrous or ferric ions which may be found in localised corrosion spots on a D & WI can wall.

Since evidence has been obtained that the phenolic resin used in the lacquer system can chemically react with iron , thus trapping it in the polymeric network, it was decided to investigate whether changing the amount of phenolic component in the lacquer affected the ability of the final film to entrap ferric ions in the matrix.

Three variants of SS1 were prepared with 10% phenolic, 5% phenolic and 3% phenolic component, (SS4 SS5 and SS6, respectively). All three lacquers were spray coated onto 330mL tin-plated steel cans at the standard coating density and were fully cured. The cans were then filled with RPT1 solution and were incubated for 17 days at 35°C.

The film was removed from the can by dissolution of the metal substrate with concentrated hydrochloric acid.. The films were washed with copious amounts of deionised water to ensure that subsequent analysis would only detect iron entrained in the polymer. The films were taken into solution using the high pressure acid digestion bomb procedure described



previously in section 3.10.1. Analysis by atomic absorption spectroscopy gave the following results;

Iron , Fe (ppm )	10% phenolic	5% phenolic	3% phenolic
In solution	3.4	4.8	11.8
In Film	599	399	175

*Table 16: Variation in the amount of iron trapped as a function of the % phenolic loading of film*

### **3.10.3 Inferences from iron impregnation studies**

The data suggest that;

1) The best resistance to ion permeation is offered by highly crosslinked films

A 10% phenolic film retards the progress of ferrous/ferric ions through the film better than a 5% phenolic film which in turn provides more of a barrier than a 3% phenolic film- this is manifested by the iron content of the pack test solution

2) A film containing a higher level of phenolic component will entrap more iron in the film than a film containing a lower level of phenolic component.

## Section 4

# **Experimental Design to Assess Barrier performance with Changing Phenolic Loading**

#### ***4. Experimental Design to Assess Barrier Performance with changing Phenolic loading***

The purpose of the experiment was to:

- a) investigate the effect of changing the cross-linker level in the coating on barrier performance in terms of iron leakage through the coating into the solution
- b) investigate the effect of utilising a combination of coatings approach in order to determine if changing cured film flexibility has any influence upon the barrier properties of the coating
- c) to explore the influence of curing temperature upon the ability of the film to prevent the corrosion of the underlying metal .

##### ***4.1 Experimental Design Matrix***

The computer generated statistical experimental design was undertaken by the use of Domain RS1 ( BBN Ltd )<sup>[52]</sup>.

The variables are tabulated below ( Table 17 ):

Experiment no	1 st coat phenolic % of total film	1st coat stoving	Top coat phenolic % of total film	Top coat stoving
1	0	Low	10	Std
2	0	Std	15	Std
3	2	Low	10	Std
4	2	Std	5	Std
5	0	Std	10	Std
6	2	Low	5	Std
7	2	Low	15	Std
8	0	Low	15	Std
9	2	Std	5	Std
10	0	Low	5	Std
11	0	Low	15	Std
12	2	Std	10	Std
13	0	Std	5	Std

*Table 17 : Experimental Design Matrix*

All prepared lacquers were spray coated onto 33cL tinplate cans as two coat systems as dictated by the design matrix above. The film weight for each lacquer layer was 160 - 170 mg per 33cL can.

The standard curing condition was as used previously achieving a peak metal temperature of 188°C for 60 seconds on the can dome. The conditions utilised to give a low stove on the first coat film gave a peak metal temperature of 188°C for 12 seconds on the can dome.

#### ***4.2 Can filling and corrosion testing***

10 cans of each variable were filled to just below the neck line with RPT1 solution. The cans were sealed by seaming easy open ends and then placed into an incubator for 28 days at 50°C. Randomly chosen cans ( 2 per set ) were removed after 4 , 7, 10 ,12 and 14 days exposure to RPT1 at 50°C , the contents decanted into glass jars and then analysed for iron content by atomic absorption spectroscopy using the approach described in 3.14.2

The total number of cans that leaked during the test period was recorded as well as the position of the point of leakage.

The integrity of the coating was checked by Enamelrater current readings. Only cans produced giving Enamelrater current readings of  $<0.1$  mA were filled to the neck flange with RPT1 and easy-open ends were sealed onto the can body. The filled cans were placed in an incubation oven held at  $50^{\circ}\text{C}$  for the duration of the corrosion test.

Solutions from the cans were removed after 4,7,9,11 and 14 days incubation for iron content determination and the remainder left in the incubator until 28 days of exposure to assess the effectiveness of the coating system to retard pitting corrosion.

### 4.3 Results

#### 4.3.1 Iron contents determined by atomic absorption spectroscopy

Instrument conditions were as described previously ( see section 3.2.2 )

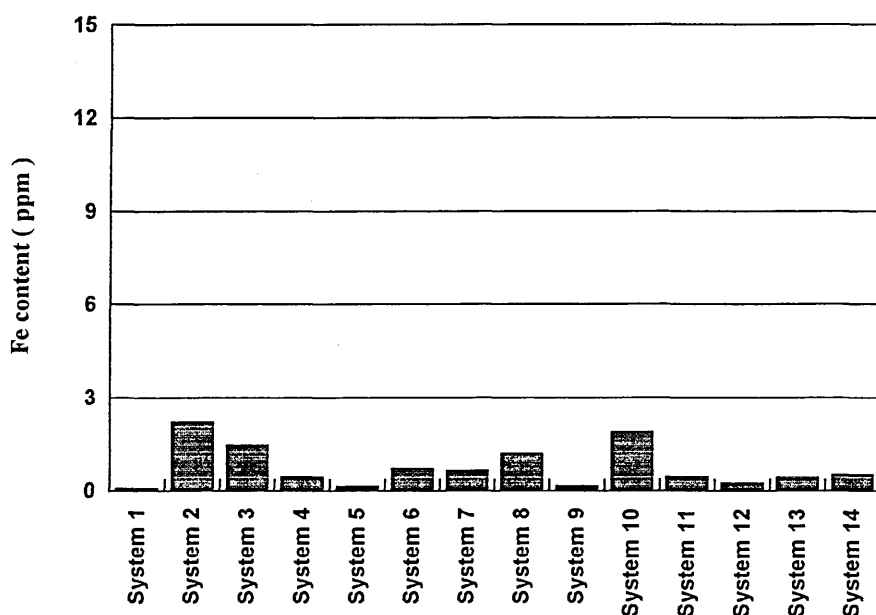


Figure 22: Fe content after 4 days of exposure to Rapid Pack Test Solution 1 at  $50^{\circ}\text{C}$

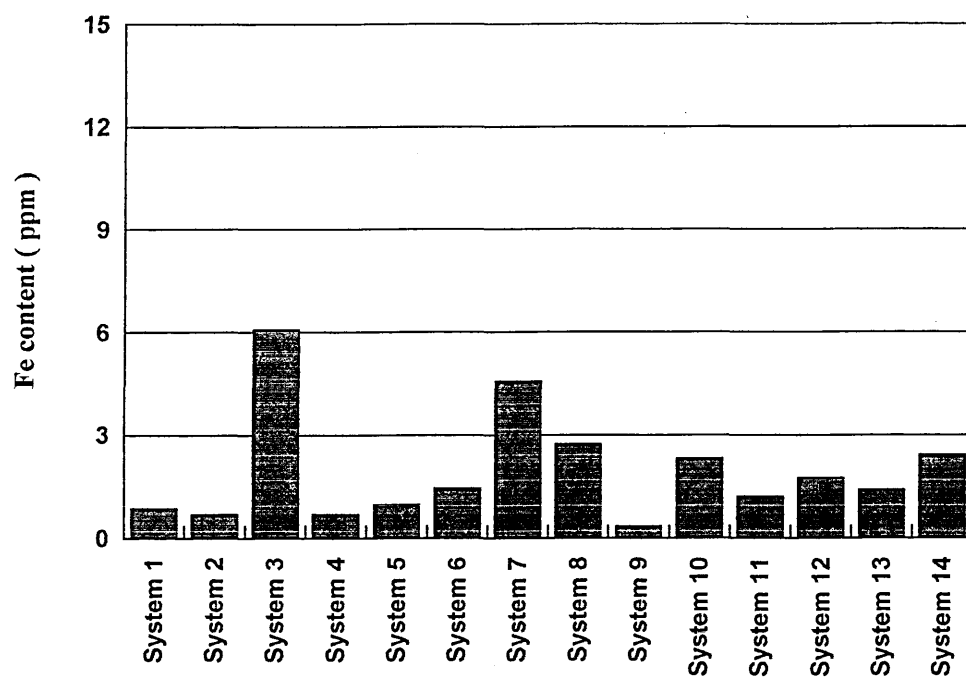


Figure 23: Fe content after 7 days of exposure to Rapid Pack Test Solution 1 at 50°C

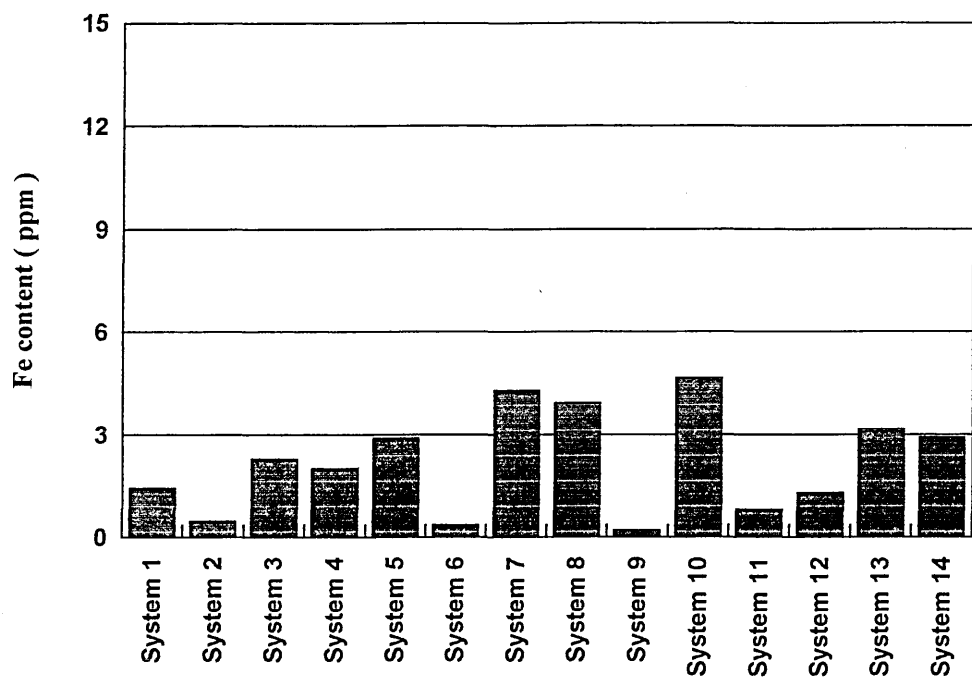


Figure 24: Fe content after 9 days of exposure to Rapid Pack Test Solution 1 at 50°C

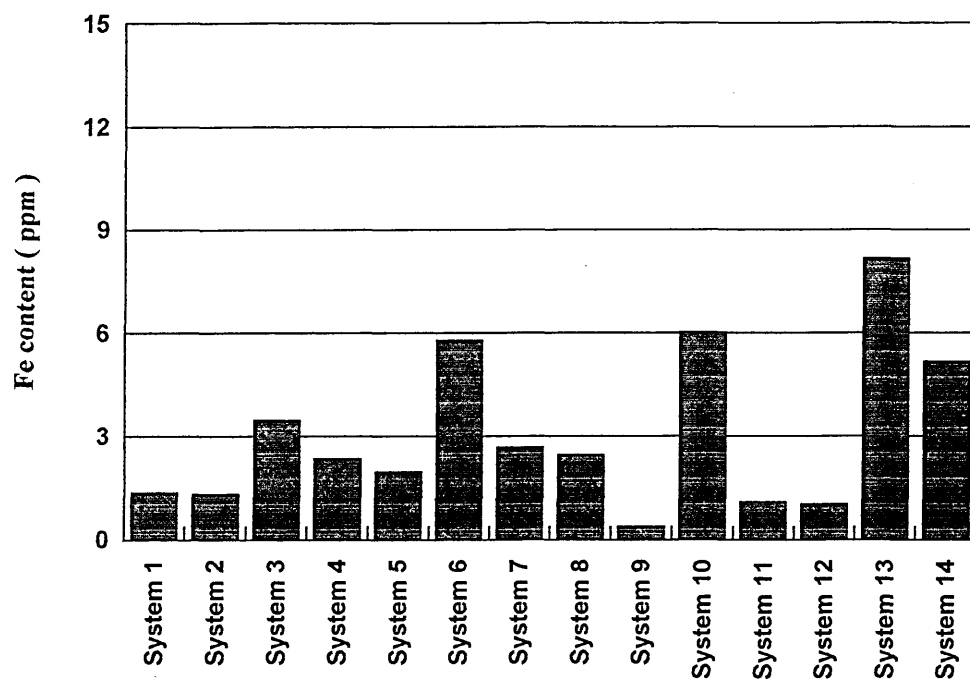


Figure 25: Fe content after 11 days of exposure to Rapid Pack Test Solution 1 at 50°C

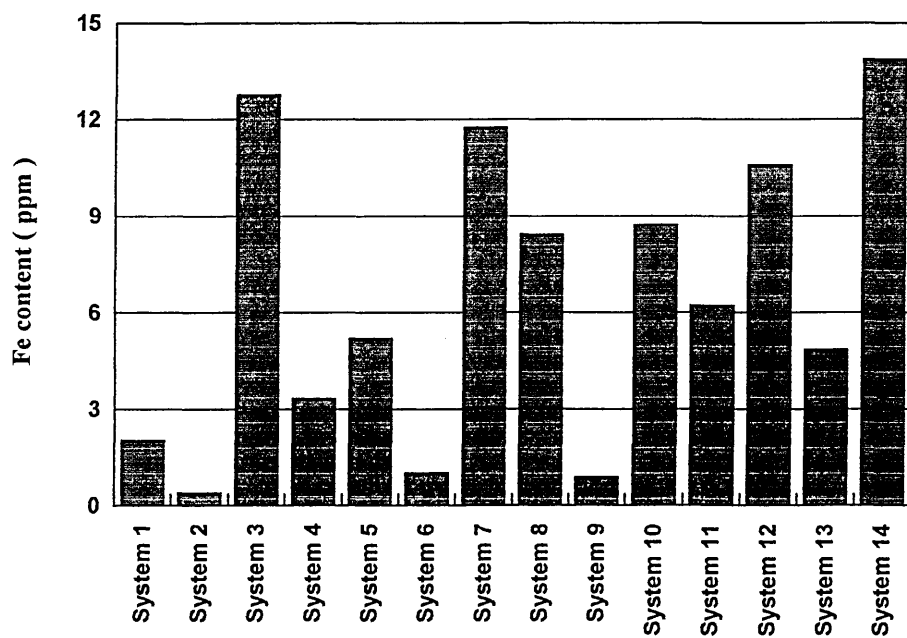


Figure 26: Fe content after 14 days of exposure to Rapid Pack Test Solution 1 at 50°C

The number of leakers versus time is represented by the contour graph below (Figure 27):

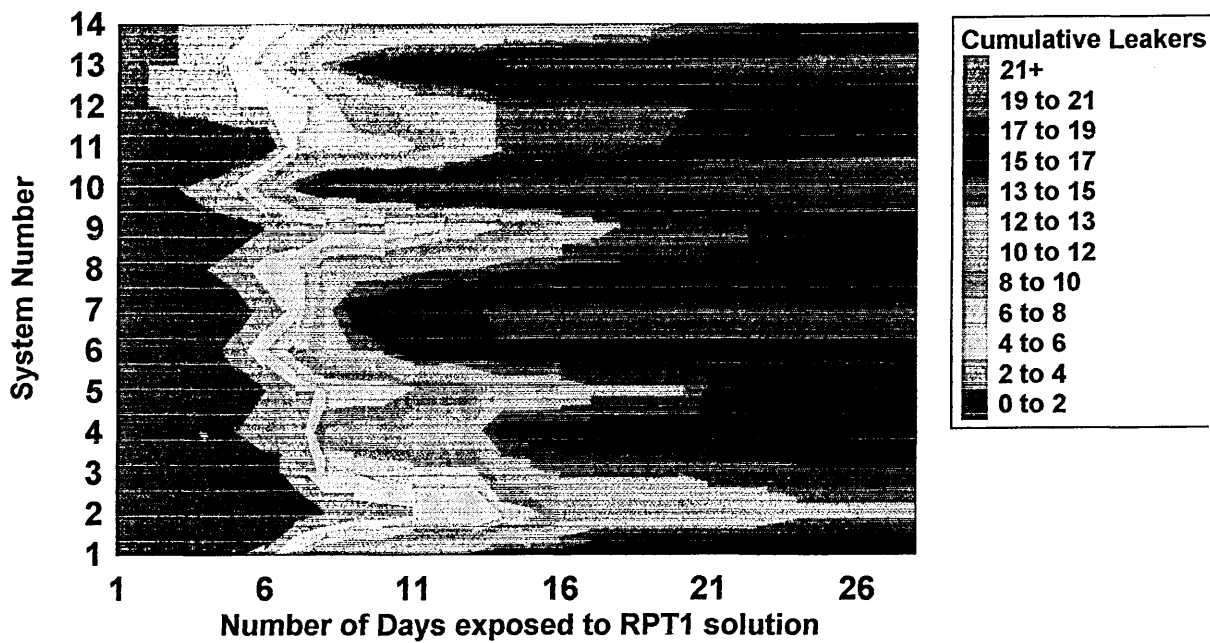


Figure 27: Contour plot representing Cumulative Leakers ( Colours ) v System number and days of exposure to RPT1 at 50 °C .

#### 4.4. Data Fitting and Interpretation

The iron content of each system after 14 days of exposure to RPT1 solution and the total number of leaking cans over the 28 day period of the test were inputted into the computerised chemometrics package. ( Figure 28)



#### 4.5. Trends observed within data

##### 4.5.1 Iron content after 14 days exposure

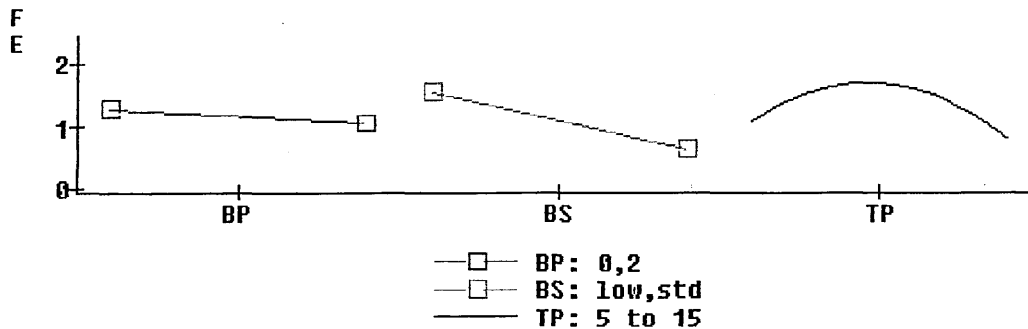


Figure 28 Adjusted Response Curve for Iron content in solution

##### 4.5.2 Graph Interpretation

The adjusted response curve highlights **trends** within the data set from analysis of the factorial effects. The graphs show that the amount of iron leaching through the coating (Y-axis in Figure 28) to be detected in the solution is lower after 14 days when :

- the level of phenolic resin in the bottom coat ( BP on the x-axis of Figure 28) is at 2% w/w,
- the bottom coat lacquer stoving ( BS on the x-axis of Figure 28) having achieved a peak metal temperature of 188°C for 60 seconds and
- preferentially when the top coat of lacquer contains the higher level of phenol formaldehyde cross-linker ( TP on Figure 28 x-axis )

#### 4.6. Number of Leaking cans observed

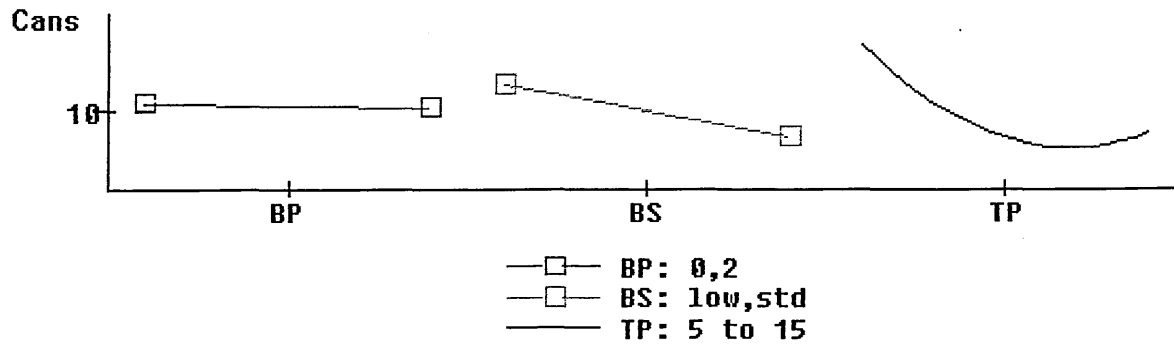


Figure 29: Adjusted Response Curves for number of leaking cans

The trends shown in Figure 29, above, suggest that to reduce the total number of cans that show perforation within the period of the test, it is necessary for the bottom coat lacquer to receive the standard cure schedule and for the top coat lacquer to contain a higher level of phenol-formaldehyde cross-linking agent.

The total number of perforated cans does not appear to be influenced by the level of phenolic present in the first coating application.

#### 4.7 Wedge Bend Flexibility of Two coat application of SS1 Lacquer film

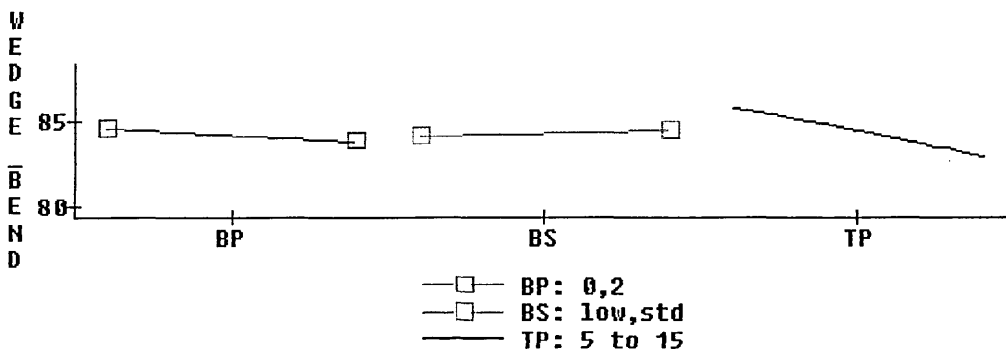


Figure 30: Adjusted Wedge Bend Flexibility

The primary factor influencing the Wedge Bend Flexibility of the coating system ( Figure 30) appears to be the level of phenolic resin present in the second lacquer application. The most flexible systems are present when the top coat phenolic content is at the lower concentration level ( 5 % ) .

The phenolic loading of the first application lacquer and the stoving of this first layer appear to have little effect upon the overall flexibility of the coating system.

#### ***4.8. Results and Conclusions from Experimental Design to Assess Barrier Performance with Changing Phenolic loading***

The level of iron determined in solution after storage at 50°C in RPT1 solution for tin-plated steel cans coated with lacquers of variable phenolic loading is at a minimum when the overall phenolic loading of the cured film is high and this level of total phenol-formaldehyde cross-linker is desirable for the prevention of pitting corrosion ( and thus perforation ) of the metal.

The higher level of phenol-formaldehyde cross-linking resin present, however, makes the film more susceptible to cracking ( see also section 3.10 ) especially during the process of seaming an easy-open end, which could lead to corrosion in the neck area of the can.

## Section 5

# **Optical Emission Glow Discharge Spectrometry (OEGDS) studies of Epoxy-graft-Acrylic films exposed to Rapid Pack Test Solution**

***5. Optical Emission Glow Discharge Spectrometry (OEGDS) study of Epoxy-graft-acrylic films exposed to Rapid Pack Solution.***

In order to determine whether the iron is trapped within the cross-linked film , or if the iron is at the polymer surface, a technique was required which would enable a cross-sectional elemental profile of the polymer to be obtained.

Optical Emission Glow Discharge Spectrometry ( OEGDS ) is traditionally used in the metal and metal alloy industry as a tool for checking the elemental composition of production material

OEGDS allows the rapid sputter removal of successive atomic layers by bombardment of the sample with high energy argon ions in a low pressure glow discharge plasma.

The removed surface atoms are excited in the plasma and subsequently emit light of characteristic wavelengths.

Dispersion and detection of these wavelengths of light in a polychromator allows the identification of the sample atoms. The intensity of the light at each wavelength relates to the ion concentration and the time of sputtering to the depth from within the sample from which the atoms were removed.

OEGDS using a Leco GDS 750 spectrometer fitted with a radio-frequency source was used to depth profile through the polymer coating on a steel can both before and after accelerated corrosion testing.

Depth profiling took 6000 seconds at 8W constant power to reach a depth of approximately 30  $\mu\text{m}$

The OEGDS profiles are given below ( Figures 31 - 33 ):

MATERIALS RESEARCH INST. SHEFFIELD HALLAM UNIV.		DATE	CLOCK
Tel. N. Ives 0114 2533500		00-00-00	00:00
E:\LEO\SPRAY\DATA\AMHBLK.DAT		MTL. NAME	PRESSURE
		TAKED	Endlevel
		EXITATION	
		800 V Flow :	203
		EI. Zoom.	Position
		FE 1.0	0.00
		SN 1.0	0.00
		C 1.0	0.00
		H 1.0	0.00
		3	3
		9	9
		15	15

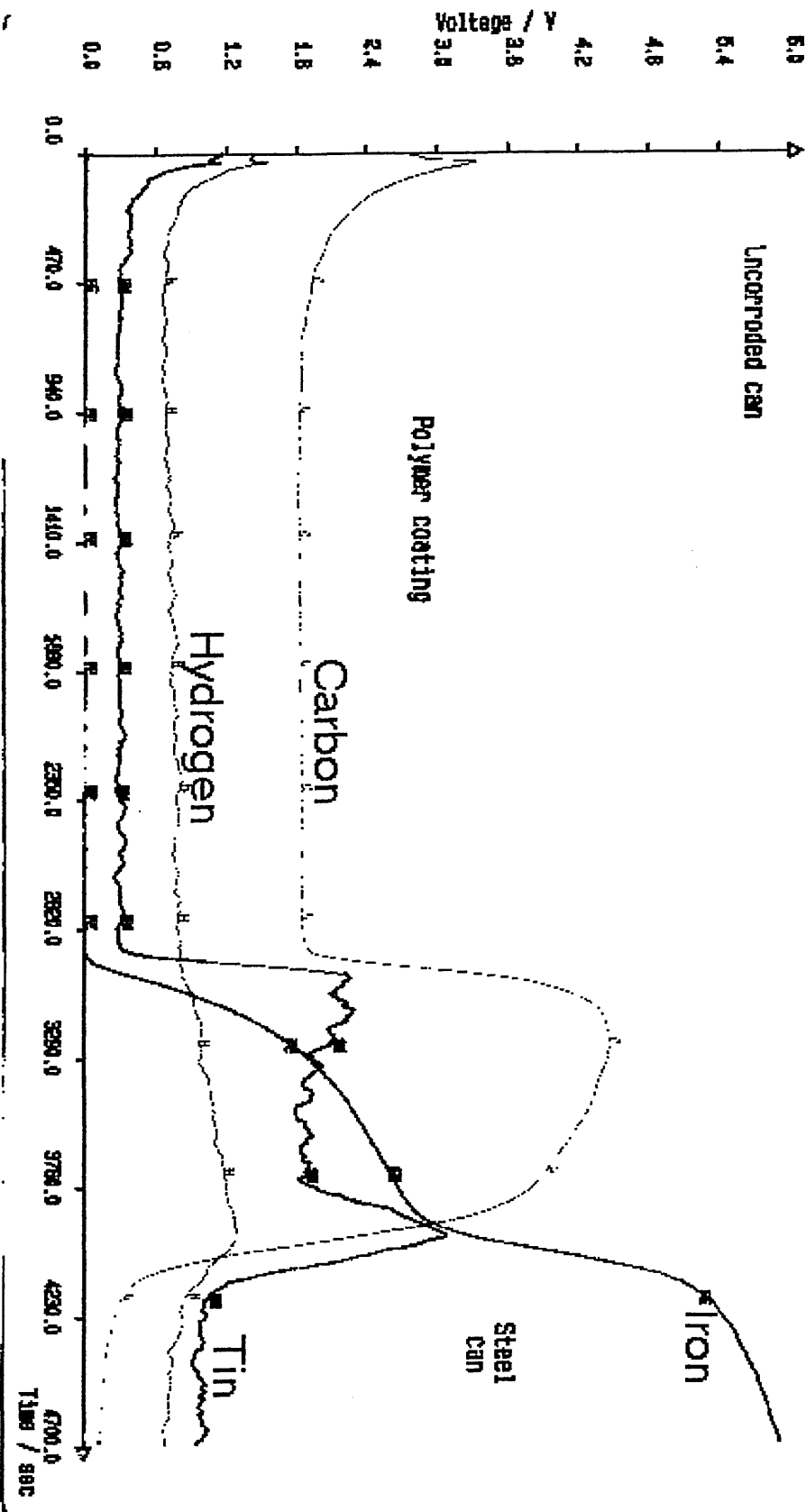


Figure 31 OEGDS profile from an uncorroded can

MATERIALS RESEARCH INST.  
 SHEFFIELD HALLAM UNIV.  
 Tel. M.Ives 0114 2533500  
 C:\ECON\SPP\DATA\VALU2.DHH

DATE 00-00-00 00:00  
 WTH.NAME PRESSURE  
 TANG0 Endlevel  
 EXITATION  
 800 V Flow : 203

El. Zoom. Position Smooth HS  
 FE 1.0 0.00 3 9  
 SN 1.0 0.00 3 15  
 C 1.0 0.00 3 9  
 H 2.0 0.00 3 15

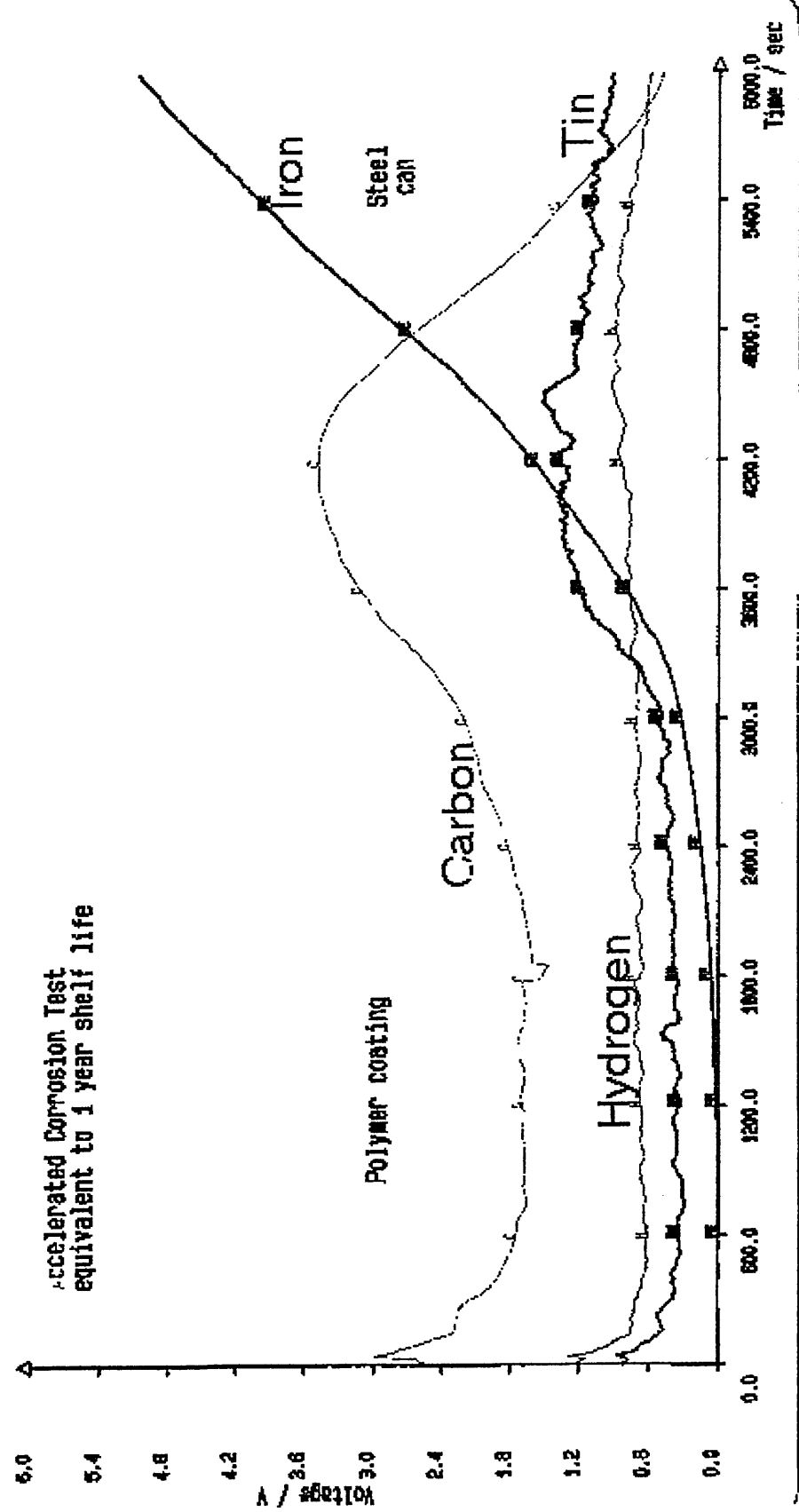


Figure 32: OEGDS profile from a can exposed to a corrosive environment

Uni Sheffield

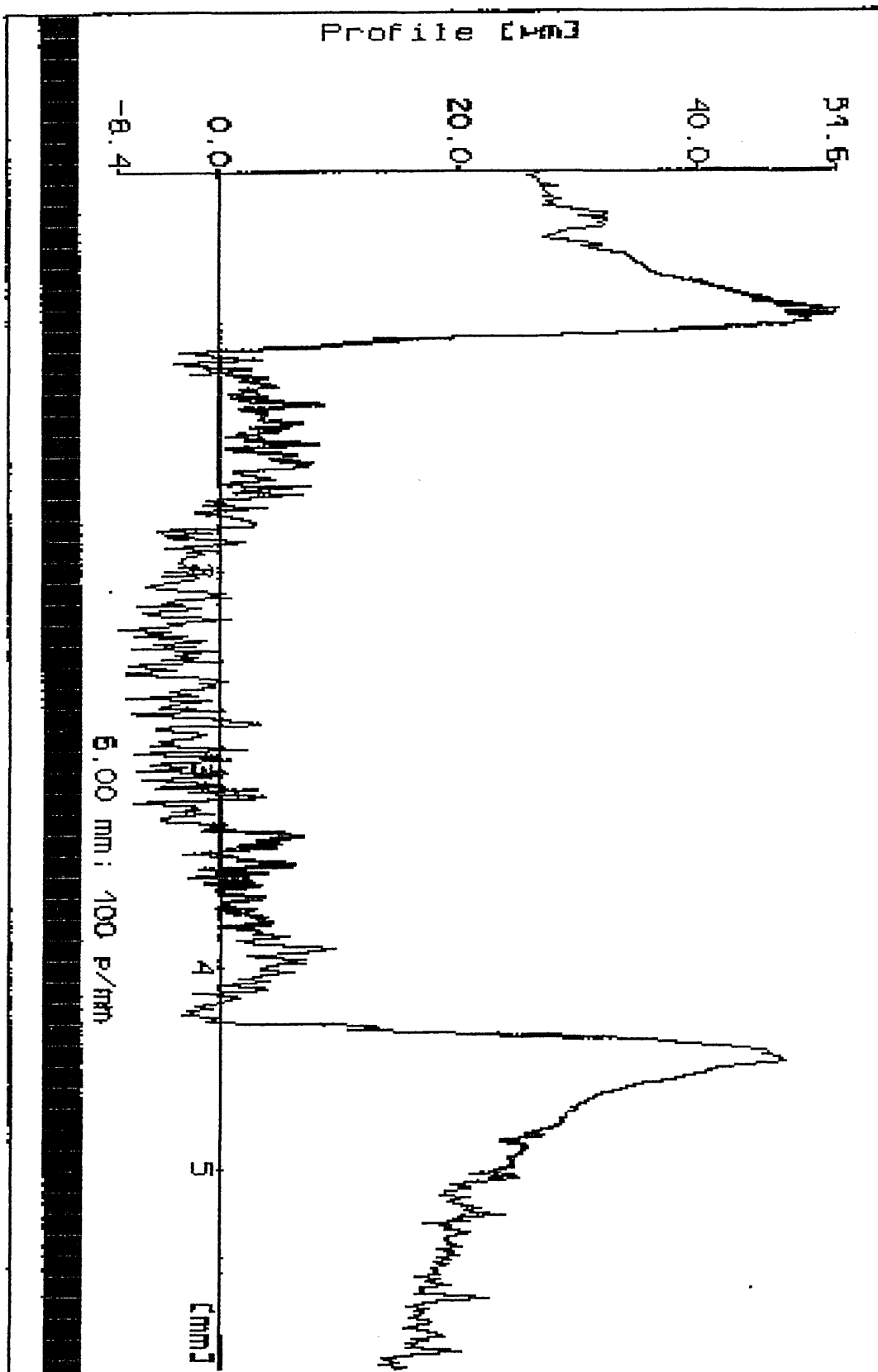
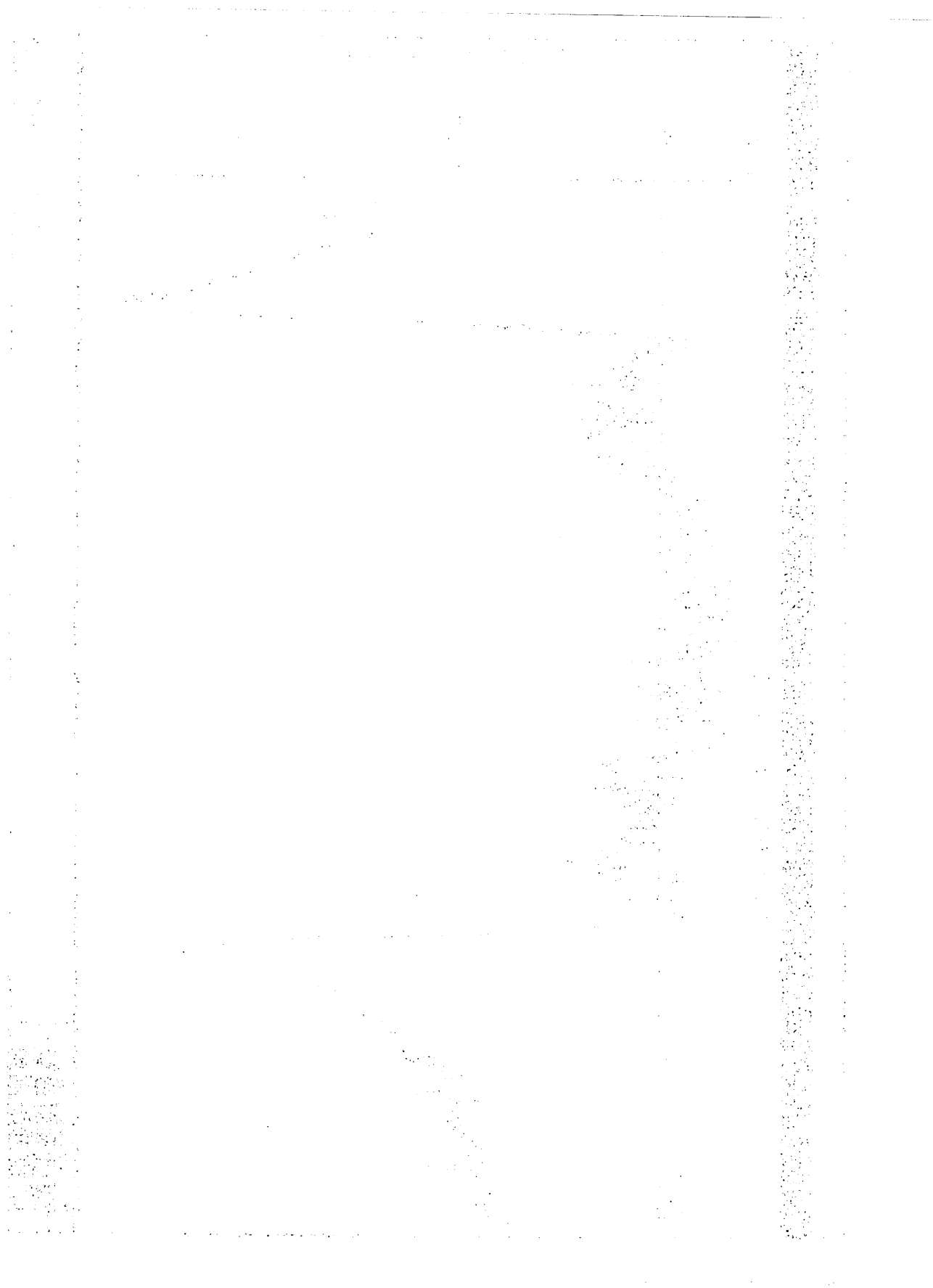


Figure 33 OEGDS Crater profile plot





Figures 31 and 32 show the glow discharge optical emission depth profiles of SS1 lacquer before and after exposure to RPT1 solution.

The plots show the following;

#### ***5.1. Polymer unexposed to corrosive solution***

a) An unexposed polymer / metal interface is very sharply defined after 2820 seconds of profiling.

The appearance of a high proportion of iron and tin in the plasma indicate this sputtering depth to be representative of the polymer / metal interface.

b) The time of sputtering before the appearance of iron gives an accurate measure of the depth of the coating - this was observed to be 9.4  $\mu\text{m}$ .

c) The relative intensities of elements observed after the onset of sputtering of the metal is disrupted from normal behaviour because there is a change in the composition of the plasma from non-conducting (polymer) to conducting (metal ).

#### ***5.2. Polymer exposed to corrosive solution***

The exposed polymer shows a totally different elemental depth profile to a polymer that has not been exposed to a corrosive environment.

Iron is detected after only 1300 seconds of profiling representing a depth of 4.3  $\mu\text{m}$  from the polymer surface ( 5.1  $\mu\text{m}$  from the polymer / metal interface )

This suggests that once corrosion has started at the polymer / metal interface, iron atoms are free to migrate through the cross-linked matrix but are impeded by the polymer itself from completely permeating across the cured film within the normal shelf life of the packed beverage.

## Section 6

# **Water Permeation Through lacquer films SS1 and SS2- FT-IR Spectroscopic Studies**

## ***6 Water permeation through lacquer films SS1 and SS2***

As shown in previous sections, rapid pack testing followed by S.E.M. of the metal surface and optical emission glow discharge spectrometry have shown that the level of iron present in the pack test medium, polymer and at the polymer/metal interface varies considerably with time of exposure. The migration of iron through the coating and subsequently detected in solution, indicates corrosion to be occurring at the metal surface.

To give more mechanistic information on the processes involved in the onset of corrosion, it was decided to investigate water ingress into epoxy-graft-acrylic systems containing different levels of phenolic cross-linking agents.

Water permeation across the polymeric membrane is thought to be an important rate determining step in the onset of corrosion at the metal / polymer interface. A polymer which resists water permeation for a long period of time will retard the onset of corrosion to a greater extent than one that rapidly takes up water ( and hence electrolyte for corrosion ).

Fourier Transform Infra-red ( FT-IR ) spectroscopy has been used to follow the ingress of water into a fully cured epoxy-acrylate resin system. Attenuated total reflectance (ATR) was utilised to ensure that good interfacial contact was maintained between the polymeric substrate and the permeating water.

### ***6.1.EXPERIMENTAL***

All FT-IR spectra were obtained with a Perkin-Elmer Paragon 1000 spectrometer equipped with a Specac ATR accessory with a KRS-5 crystal in a liquid cell ( illustrated below, Figure 34 ) All spectra were obtained at  $4\text{cm}^{-1}$  resolution and are the average of 64 scans. The polymer was bar coated onto the crystal and cured for 3 minutes at  $180^{\circ}\text{C}$ . The coating density for each polymer was found to be approximately  $150\text{ mg /m}^2$ .

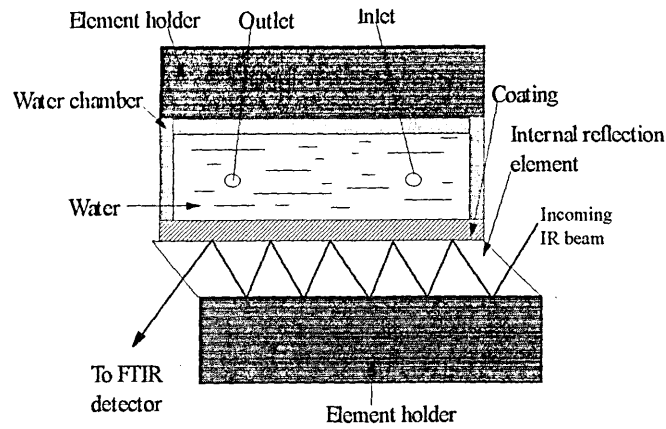


Figure 34: FT-IR Water Permeation cell

### 6.1.2 Theory of water permeation

From the instant water is admitted to the coating side of the coated substrate and before the attainment of a steady flow, both the rate of flow and the concentration of water within the coating layer vary with time. If the diffusion coefficient is constant and the initial concentration of water within the film and at the coating / substrate interface are negligible, the amount of water which passes through the coating layer in time  $t$  is given by the non-steady state equation; <sup>[53]</sup>

$$\frac{Q_w}{l_c C_l} = \frac{Dt}{l_c^2} - \frac{1}{6} - \frac{2}{\pi^2} \sum \frac{(-1)^n}{n^2} \exp\left(\frac{-Dn^2\pi^2 t}{l_c^2}\right) \dots\dots\dots(1)$$

where  $Q_w$  is the total mass of the water passing by diffusion through the coating in time  $t$ ,  $l_c$  is the thickness of the coating,  $C_l$  is the concentration of water on the outside of the coated substrate,  $D$  is the apparent diffusion coefficient, and  $n$  is an integer. The mass -time plot of Equation ( 1) has an initial build period but a linear relationship develops as  $t \rightarrow \infty$  .

For this study, only the finite time before the steady state is achieved is of interest ,and under these conditions, equation (1) reduces to:-

$$Q_w = \frac{DC_l}{l_c} \left( t - \frac{l_c^2}{6D} \right) \dots\dots\dots(2)$$

and the mass-time plot has an intercept on the ,  $t_{in}$  on the time axis given by;

$$t_{in} = \frac{l_c^2}{6D} \dots\dots\dots(3)$$

where  $t_{in}$  is known as the time lag.  $t_{in}$  is the time required for water to diffuse through the coating and reach the coating / substrate interface. Equation (3) provides the basis for the determination of the diffusion coefficient by the time lag approach.

### 6.3 Fourier-Transform Infra-red -Multiple Internal Reflection (FT-MIR) Spectroscopy

The theoretical basis of the method for determining the amount of water at the coating / substrate interface is derived from the penetration-depth concept of internal reflection spectroscopy derived by Harrick, <sup>[53]</sup> for thin and thick films. The validity of this concept for the study of polymeric systems has been shown by various workers <sup>[54,55]</sup>.

The absorbance,  $A$ , of a band of an IR internal reflection spectrum of the surface of a film of thickness ,  $L$ , on a substrate is given by <sup>[53]</sup>,

$$A = \frac{n_2 \alpha L_o^2}{n_1 \cos \theta} \frac{L}{o} \int e^{\left( \frac{-2z}{dp} \right)} dz \dots\dots\dots(4)$$

where  $\alpha$  is the absorption coefficient per unit thickness for the band of interest,  $\theta$ , is the incidence angle,  $n_2$  and  $n_1$  are the refractive indices of the sample and substrate,  $z$  is the depth

from the interface,  $E_o$  is the amplitude of the evanescent wave at the surface, and  $d_p$  is the depth at which the evanescent wave has decreased to  $1/e$  of its value at the surface where  $e = \log_{10} 2.303$

The term  $d_p$  is commonly referred to as the depth of penetration of the evanescent wave, which is given by;

$$d_p = \frac{\gamma}{2\pi n_1 \left[ \sin^2 \theta - \left( \frac{n_2}{n_1} \right)^2 \right]^{\frac{1}{2}}} \dots \dots \dots (5)$$

where  $\gamma$  is the wavelength of the infrared radiation in a vacuum.

More than 85% of the total absorption intensity of a band is within one  $d_p$ <sup>[53]</sup> but the probing depth of internal reflection spectroscopy is limited to three times  $d_p$ . Equation (5) thus indicates that the penetration depth of the evanescent wave in the sample is a function of the angle of incidence, the wavelength of the radiation and the refractive indices of the sample and substrate .

Nguyen et al<sup>[56]</sup> have shown that the effect of absorption on  $d_p$  is negligible at the O-H stretching ( $3400\text{cm}^{-1}$ ) of water and epoxy and that , at this frequency, Equation ( 5) is valid for calculating  $d_p$  in these materials.

When an organic coated specimen is exposed to an aqueous environment, water will enter the coating substrate interface and interact with the evanescent wave and be detected. The total amount of water detected is the sum of the amount of water at the coating / substrate interface and the water taken up in the coating being probed by the evanescent wave. This statement may be written;<sup>[56]</sup>

$$A(t) = \frac{n_2 \alpha_2 E_o^2}{n_1 \cos \theta} \int e^{\left( \frac{-2z}{d_{pw}} \right)} dz + \frac{c_w(t) n_3 \alpha_3 E_o^2}{n_1 \cos \theta} e^{\frac{(-2l_{wt})}{d_{pw}}} \int e^{\left( \frac{-2z}{d_{pw}} \right)} dz \dots \dots \dots (6)$$

where  $A(t)$  is the FTIR-MIR absorbance of the water band ,  $n_2$  and  $\alpha_2$  are the refractive index and absorption coefficient of water at the coating / substrate interface,  $n_3$  and  $\alpha_3$  are the refractive index and absorption coefficient of sorbed water in the coating ,  $l_{wt}$  is the thickness of the water layer at the coating / substrate interface,  $d_{pw}$  and  $d_{pc}$  are the penetration depths of the evanescent wave into the water and the coating respectively, and  $c_w(t)$  is the mass fraction of water sorbed into the coating.

$A(t)$ ,  $l_w(t)$  and  $c_w(t)$  all vary with time of exposure.

A reasonable assumption is that the refractive index and absorption coefficients of water at the coating / substrate interface and sorbed into the coating are the same, thus integrating equation (6) and rearranging yield an expression for calculating the thickness of the water layer at the coating / substrate interface as a function of time  $l_w(t)$ ;

$$l_w(t) = \frac{d_{pw}}{2} \left[ -\ln \frac{1 - \frac{A(t)}{A_\infty}}{1 - c_w(t) \frac{d_{pc}}{d_w}} \right] \dots\dots\dots (7)$$

where ;

$$A_\infty = \frac{n_2 \alpha_2 E_o^2 d_{pw}}{2 n_1 \cos \theta} \dots\dots\dots (8)$$

$A_\infty$  is the infra-red absorption when the water layer at the coating / substrate interface is very thick.

Assuming water is uniformly distributed over the entire surface area of the specimen, the amount of water at the coating / substrate interface,  $Q_{wi}(t)$  will be given by;

$$Q_{wi}(t) = l_w(t) a \rho \dots\dots\dots (9)$$



where  $a$  is the area in contact with the water and  $\rho$  is the density of the water at the coating / substrate interface

To obtain  $Q_{wi}(t)$ , the total mass of water passing through the film in time  $t$ , and data on  $A(t)$ ,  $A_{\infty}$ ,  $c_w(t)$ ,  $d_{pc}$  and  $d_{pw}$  in equation (7) must be known.

$A(t)$ , the absorbance corresponding to the total amount of water detected at a given exposure time is derived from FT-IR MIR experiments *in situ*;  $A_{\infty}$ , the FTIR-MIR absorbance of water of indefinite thickness is determined from the FTIR-MIR spectrum of water in contact with the substrate free of coating and from  $c_w(t)$  the mass fraction of water sorbed into the coating within the probing depth at a given exposure time is extrapolated from water uptake experiments in free films and finally,  $d_{pc}$  and  $d_{pw}$  are calculated from equation (5).

#### **6.4. Water Permeation Experimental Procedure**

Three separate experiments were carried out

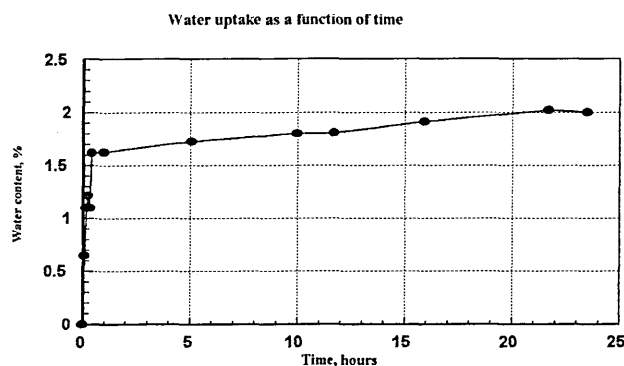
- (1) FTIR-MIR *in situ* measurements of organic coated specimens exposed to water,
- (2) FTIR-MIR analysis of water in contact with the coating free substrate and
- (3) water uptake experiments.

These experiments provide data for  $A(t)$ ,  $A_{\infty}$  and  $c_w(t)$  respectively.

##### **6.4.1 Water-uptake experiments**

The water uptake in films was determined using a gravimetric method. Films were prepared by applying the coating to a clean dry glass microscope slide, and drawing down the lacquer to ensure an even coating of the film on the surface of the glass slide. The glass slide with film was heated in an oven for 3 minutes at 188°C to effect curing of the epoxy-acrylate polymer.

After curing, the film samples ( in triplicate ) were weighed and immersed in distilled water. After known periods of time, the samples were removed from the water, blotted to remove any excess water, and reweighed. Water uptake was expressed as a percentage of the mass of the initial dry specimen and the figure presented ( Figure 35 ) represents the average of three determinations.



*Figure 35: Water uptake as a function of time*

#### **6.4.2 FTIR-MIR in situ measurement of coated specimens**

Multiple Internal Reflection Infra-red measurements of SS1 and SS2 were obtained by using a thallium bromide iodide (KRS-5) internal reflection element using a 45° incident angle; this provides 17 reflections inside the element. The Internal Reflection Element (IRE) used for the study was a previously used element which had lost some infra-red throughput but was found to be adequate for the experiment.

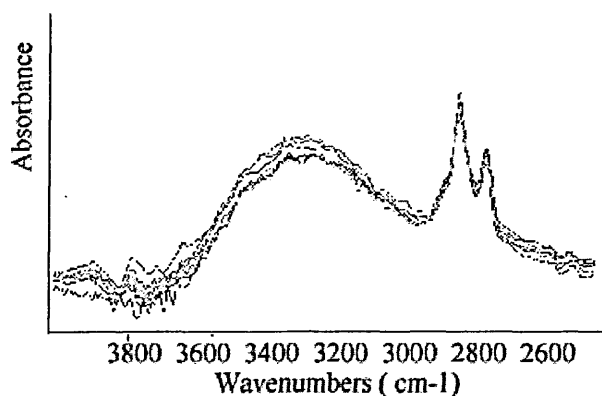
The application of the lacquer to the Internal Reflection Element was by flooding one end of the substrate and then drawing the coating down the crystal using a rounded glass rod. Any excess lacquer found on the crystal was removed by careful wiping with methyl ethyl ketone. The quality of the coating was good and no visible pinholes or air bubbles were observed.

( by the naked eye ) on the specimen surface . The lacquer was then cured in an convection oven for 3 minutes at 188°C.

The coating thickness was determined ,using a micrometer, on the dried free film removed from the substrate after the experiment. The IRE coated with lacquer was then placed into the water cell as described earlier.

The Infra-red spectrum of the surface of the coating was taken automatically every 30 minutes until the experiment was complete. Difference spectra were acquired by subtracting the spectrum of the unexposed lacquer from that of the water exposed lacquer at each time interval. All spectra were recorded at  $4\text{cm}^{-1}$  resolution using 64 scans using unpolarised radiation at a  $45^\circ$  incidence angle.

The spectra are presented below in Figure36.



*Figure 36: MIR-spectra of epoxy-acrylate applied to a KRS-5 substrate exposed to water for different times.*

The “peak height” method, which measures the absorbance at the absorption maximum of the band of interest was used for quantitative purposes.

### 6.5. Results and Discussion from water permeation study by IR

The amount of water at the applied film / substrate interface was determined using equations (7) and (9) and the results provided by the three experiments described previously.

The intensity of infra-red absorption bands in the region  $3000 - 3600 \text{ cm}^{-1}$  increased, as did the absorption at  $3478 \text{ cm}^{-1}$ . These changes are due to the water entering the coating substrate interfacial region and interacting with the evanescent wave. The bending mode of water at  $1640 \text{ cm}^{-1}$  was found to be insensitive to low concentrations of water and was not used for analysis.

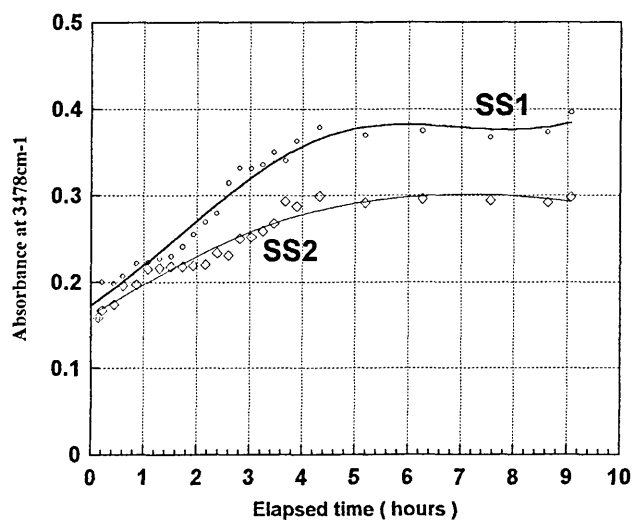


Figure 37 depicts the intensity change of the  $3478 \text{ cm}^{-1}$  band as a function of exposure time for lacquer systems SS1 and SS2.

The concentration of detected water increased rapidly at short exposure time but then increased rather more slowly at longer exposure times. The intensity at each exposure time taken from each curve of Figure 37 provided a value of  $A(t)$  in Equation 7.

The amount of water sorbed in the bulk coating within the probing depth of the evanescent wave,  $c_w$  was determined from the water uptake of free films; these results are given in

Figure 38. The maximum uptake was determined to be 2.2% for SS1 and 1.9% for SS2. The mass fraction of water sorbed in the coatings at a given exposure time was interpolated from the results of Figure 35 after multiplying the time scale by two. This was to provide a rough correlation between the water sorption process in the FT-MIR measurement and the water uptake in the free films.

Determination of the amount of water at the coating / substrate interface requires information on the penetration depths of the evanescent wave in the coating,  $d_{pc}$ , and in water,  $d_{pw}$ , at the wavelength of interest.

For the water in epoxy -acrylate coatings, the values were computed from equation (5) using an incidence angle of  $45^\circ$  and refractive index values of ;

KRS-5=2.4, water=1.30 and polymer=1.5.

At the OH stretching frequency ,the  $d_p$  values in the polymer film was  $0.50 \mu\text{m}$  and in water the value was found to be  $0.37 \mu\text{m}$ .

Since most (>85%) of the intensity of a band is from this depth, these results indicate that most of the water molecules detected were those from close to the coating / substrate interface. The thickness of the water layer at the coating / substrate interface as a function of time was calculated from equation (7) using  $A(t)$  and  $A_\infty$  values

The value of  $c_w(t)$  at a given exposure time was obtained from Figure 35

The amount of water at the interface at a given exposure time,  $Q_{wi}(t)$ , was then determined by equation (9) using a value of  $375 \text{ mm}^2$ , the surface area of the coated substrate within the water chamber and a density of the water at the coating / substrate interface of  $1 \text{ Kg /m}^3$ .

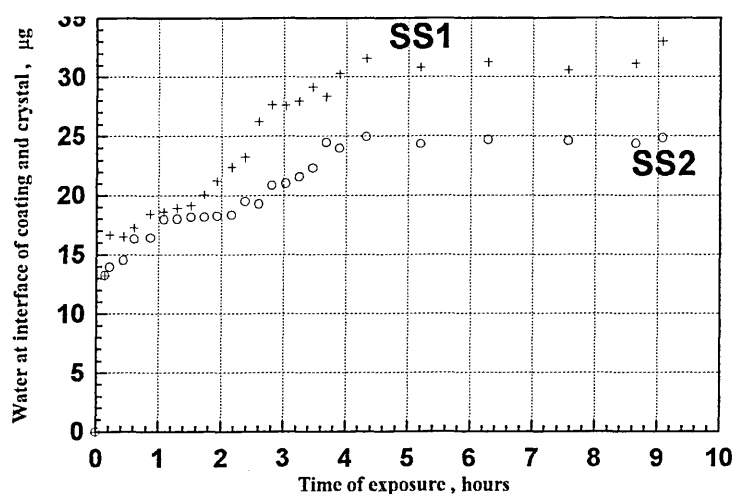


Figure 38: Amount of water at the coating /substrate interface for lacquers SS1 and SS2

### 6.6 Conclusions from observing water permeation by Infra-red spectroscopy

At short exposure times, the amount of water at the interface of SS1 was greater than that of SS2 . However at higher exposure times, the two epoxy-acrylates resins appear to hold approximately the same amount of interfacial water. It is evident from Figure 38 that at long exposure times, many monolayers of water have accumulated at the interface .Thus, the concept of the films having any substantial barrier resistance is unfounded as migration of water, a key precursor for the corrosion reactions , has been found to occur rapidly penetrating the films within 3-4 hours of exposure .

SS1 is formulated with 10% w/w phenol-formaldehyde cross-linking agent whereas SS2 is formulated to contain half that level. It is possible that the cured polymer film formed with SS2 is less densely cross-linked than SS1 and presents pathways for ion migration that are not present in SS1.

In order to test this hypothesis , a means of following ion migration across the cured polymer film needed to be devised.

Section 7

## **Ion Permeation Studies**

## ***7. Ion Permeation Studies***

The migration of water through films has been followed by FT-IR and the migration of iron from the metal surface into the pack solution demonstrated by both gravimetric and spectroscopic means. These techniques have been successful at showing corrosion to be occurring at the metal / polymer interface without contributing to an explanation of the mechanism by which the metal surface begins to corrode.

Uptake of ions into a polymer film will decrease the electrical resistance and allow corrosion currents to develop. Sodium ions within coatings permeate to cathodic corrosion sites to become the counter ion for any  $\text{OH}^-$  ion produced by the corrosion cell, and these may then diffuse as an ion-pair to the anodic sites completing the corrosion reaction and contributing to cathodic disbondment. The presence of chloride ions, in addition to decreasing the electrolytic resistance, may stimulate corrosion and thus the permeability of coatings to chloride ions will be detrimental. DC resistance is a direct measure of this electrolytic resistance although the technique is limited because it cannot show which particular ions are permeating the film and causing the lowering of the electrolytic resistance. Furthermore, DC measurements cannot give indications of the permeability of ions such as chloride that stimulate corrosion. Ionic permeability measurements can determine the specific ions involved. The technique can also provide mechanistic information e.g. whether ions permeate as ion pairs, whether the permeation follows a size exclusion principle or where there is selective permeation resulting from interactions with the polymer chains.

Ionic permeability was originally investigated by Glass and Smith<sup>[57]</sup> by radioactive tracer techniques. Due to safety reasons this is not a technique that could be used in the author's laboratory. The method used instead was a development of the method reported by Murray<sup>[25]</sup>. This uses ion-selective electrodes to detect the permeated ions. In this work, Murray



investigated the permeability of various surface coatings to chloride ions; he reported three types of behaviour:-

#### Type I

Concentration of permeated chloride ions increases linearly with time.

e.g. as in the case of cellulose acetate.

This type of behaviour is usually associated with a fast permeation of chloride ions. Murray concluded that there was no interaction between the organic polymer matrix and the chloride ions.

#### Type II

Non-linear permeation rate increases with time.

e.g. as in the case of Epoxy-polyamide (1:1) systems

The sample contained free amino groups due to the ratio of epoxy resin to polyamide resin used. Thus there is the likelihood of polymer-water interactions. Murray proposed that the aqueous ions are attracted to the polar groups of the epoxy-polyamide chain which results in a decrease in long range polymeric bonding and that in turn leads to an increased segmental motion of the polymer. Increased segmental motion not only facilitates ionic diffusion but also exposes further ionic groups which can also attract aqueous ions for further plasticisation. As a result, the permeation rate continues to increase with time.

#### Type III

Non-linear permeation rate decreases with time

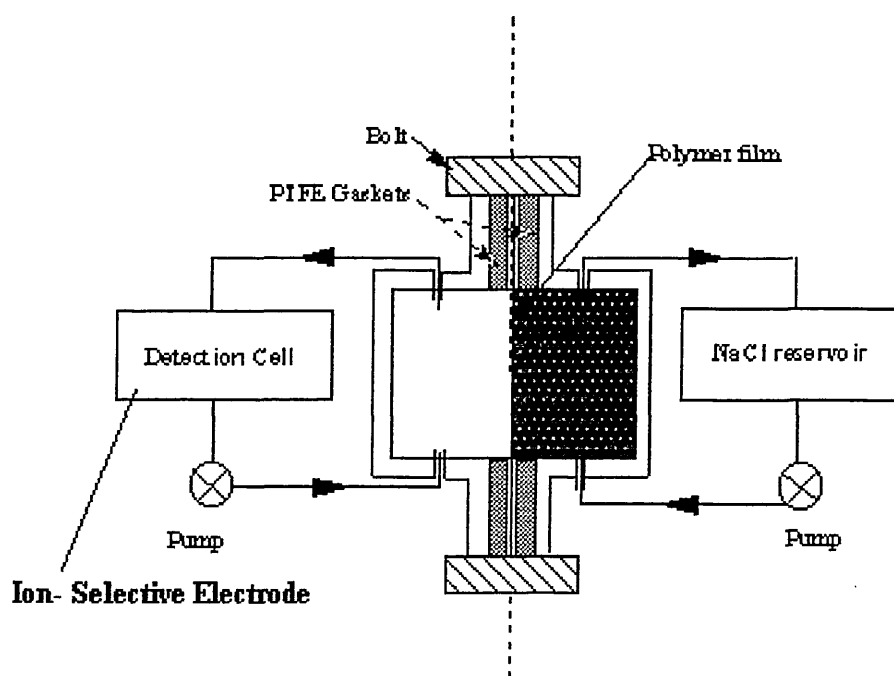
e.g. as in the case of epoxy-polyamide (2:1) systems

Epoxy-polyamide at a ratio of 2:1 produces a polymer that is very hydrophobic with few free amine groups. The change in epoxy-polyamide ratio also leads to a changed cross-linking

density and a reduction in the ionic permeability is expected. However, it is not only the rate of permeation that is affected but the mechanism also appears to change. Murray accounted for the slow permeation rate by proposing that the ions cluster within the hydrophobic matrix. These clusters eventually fill the free volume severely limiting ionic diffusion.

In the present study, it was therefore of interest to apply this approach to the lacquer films used in the can coating process.

### 7.1. Experimental method



*Dilute Aqueous Sodium chloride (<0.01M)      Concentrated Aqueous Sodium chloride (5M)*

Figure 39: Permeation cell schematic

The experiment measures the permeation of ions through a polymer film. One side of the film was exposed to a high concentration of sodium chloride ( $5 \text{ mol L}^{-1}$ ) the other exposed to initially, deionised water. This concentration gradient provides a driving force for the permeation of ions in an attempt to equilibrate the system.

The free standing film was sandwiched between the two halves of the permeation cell; PTFE gaskets were used to gain an effective seal; the body and the gaskets were greased with apiezon grease. Circulation of the liquid was effected by the use of peristaltic pumps ( 1 mL min<sup>-1</sup>). The sodium chloride solution was pumped across one face of the polymer film through the permeation cell; the deionised water was pumped across the face of the film from a detection cell. The volume in this side of the cell was minimal and accurately known with 50mL being the normal volume used.

### 7.1.2. Detection of ions

Ion-selective electrodes (ISE) were used to detect the presence of the permeating ions.

The chloride electrode is a solid state electrode , the sensing tip made of silver which has been electrolytically coated with silver chloride. The electrode can detect chloride ions down to a concentration of  $3 \times 10^{-6} \text{ mol l}^{-1}$  but only shows Nernstian behaviour to a concentration of  $1 \times 10^{-4} \text{ mol l}^{-1}$ . A calibration curve ( electrode potential versus chloride ion concentration ) is shown below;

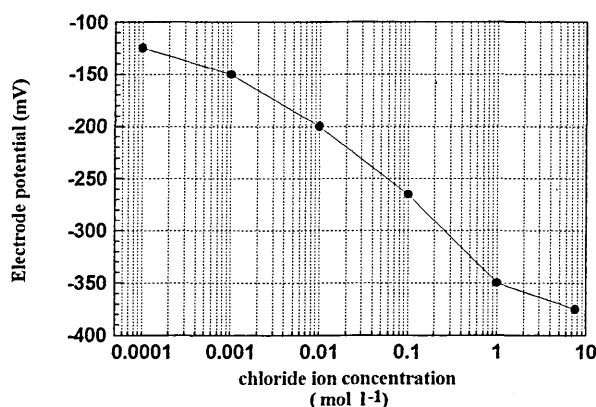


Figure 40: Calibration curve for chloride ISE

The sodium ion selective electrode is a membrane electrode. The electrode develops potential proportional to the activity of the sodium ions in the solution in which it is placed.

The sodium electrode has a Nernstian range of  $1 \text{ mol l}^{-1}$  to  $1 \times 10^{-5} \text{ mol l}^{-1} \text{ Na}^+$ .

The calibration curve for the sodium ion electrode is shown below;

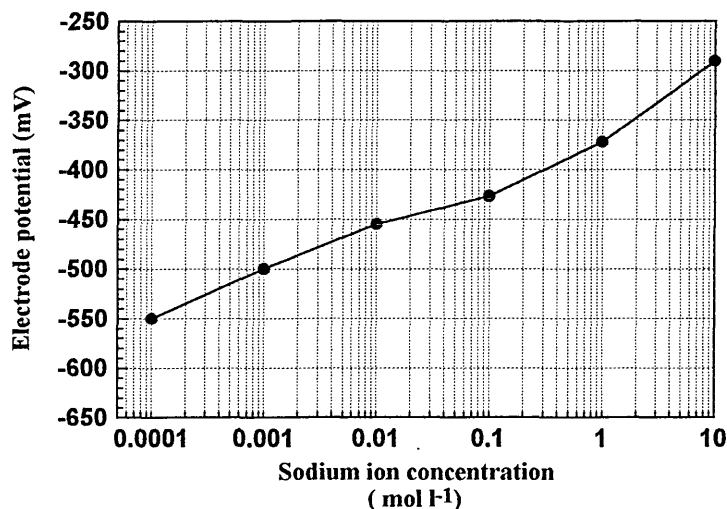


Figure 41: Calibration curve for  $\text{Na}^+$  ISE

The line of best fit for this curve is described by the expression:

$$E^{\theta} = -354.28 \times [\text{Na}^+]^{-0.0516} \dots\dots\dots(10)$$

Both ion selective electrodes were used with a mercury / mercury sulphate reference electrode. The standard saturated calomel electrode was not suitable for the experiment since chloride ions ( from the KCl filling solution) would have leaked into the detection cell.

The ion selective electrodes and electrodes were connected to a Dow Corning 350 pH / ion meter from which the electrode potential was obtained.

## ***7.2 Preparation of the Polymer films***

All the polymer films investigated were cast onto clean glass panels from solution using a draw down technique. A minimum film thickness of 10 $\mu$ m was found to be required to withstand the force of the pumps. An area of film ,detached from the glass panel, (approximately 4 cm x 4cm ) was cut from the film. The film was checked visually for defects. The film was then soaked in water for at least a week prior to the permeation experiment. This allowed complete water ingress into the film that helps to reduce induction effects. Furthermore , soaking allowed any leachable Cl<sup>-</sup> or Na<sup>+</sup> ions within the film to be removed so that true permeability measurements could be obtained.

## ***7.3. The Permeation Experiment***

The pre-soaked film was placed between the two PTFE gaskets (greased) and then placed between the two halves of the permeation cell. The cell was fastened tightly and the tubing of the circulation system was connected. The reservoir was filled with sodium chloride solution and 50mL deionised water was pipetted into the detection cell. The pumps were switched on allowing the permeation cell to fill. Readings of the electrode potential were taken at known time periods.

## ***7.4 Data analysis***

The raw data from the experiments were converted from electrode potential readings to ion concentration (molarity) using the appropriate calibration curve.

A plot of ion concentration versus time can indicate the permeability of the film to the ions. The permeability values were normalised to an area of 1 cm<sup>2</sup> of film. If a curve was obtained this was indicative of permeability not being constant and a quantitative estimate of the permeability is not given.

## 7.5.Epoxy-Acrylate Coatings Permeation studies

The following lacquers were investigated;

Lacquer	% phenolic
SS1	10
SS2	5
SS6	3

Table 18: Films used for Permeability studies

### 7.5.1. Sodium ion permeability

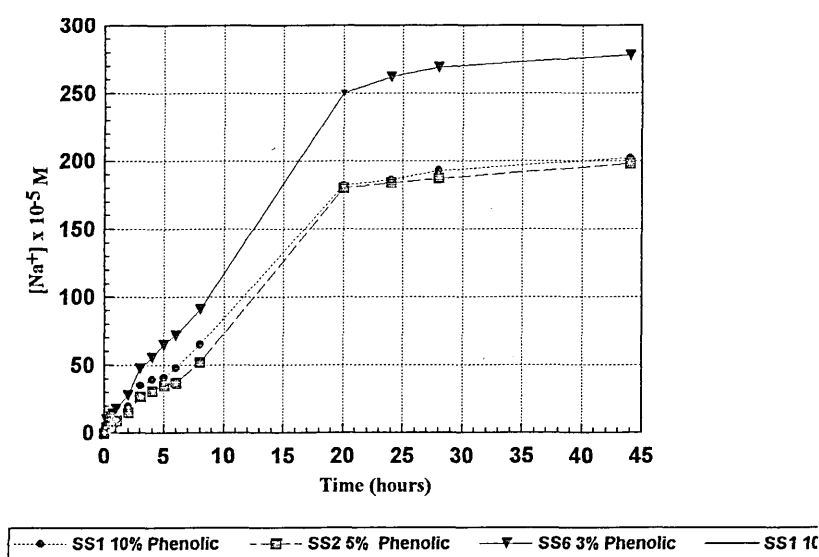


Figure 42 :  $Na^+$  permeability of films

The curves for the 10% and 5% phenolic variants may be described by the general equation;

where  $t$  is the time is the exposure time in hours and  $K$  is a constant.

$$[Na^+] = -0.15t^2 + 11t + K.....(11)$$

Thus the rate of change of sodium ion concentration with time is described by the first derivative;

$$\frac{d[Na^+]}{dt} = -0.30t + 11 \dots\dots\dots(12)$$

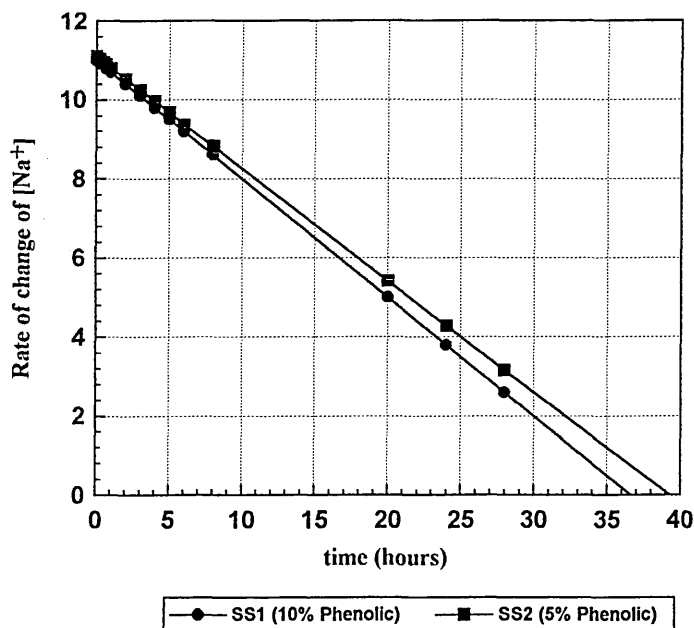


Figure 43: Rate of change of sodium ion concentration for lacquers SS1 and SS2

Thus for SS1 and SS2 epoxy acrylate films the rate of change of sodium migration through the film is at a minimum after 33 hours ( approximately 1.5 days) .This has implications for corrosion in that this time indicates when the films are liable to be saturated by cations which could then form an ion pair with any OH<sup>-</sup> ions generated by the cathodic corrosion reaction and lead to alkaline conditions being present under the film.

### 7.5.2. Chloride ion permeability

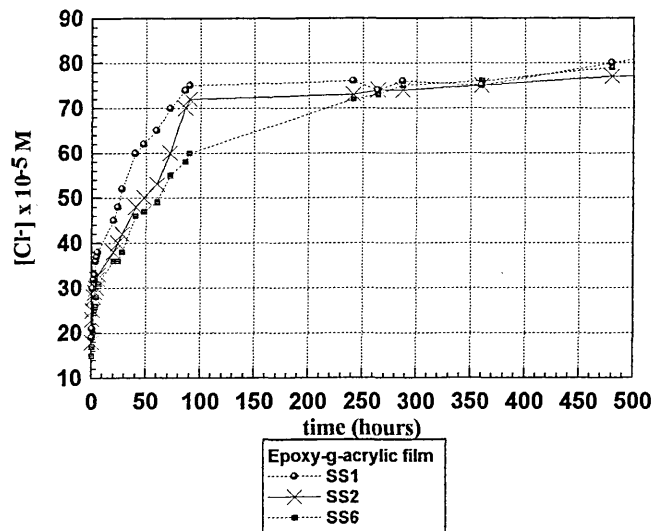


Figure 44 Chloride ion permeability of films

The chloride ion migration rate was found to be very low compared to the rate observed for sodium.

Furthermore, when the chloride migration rate is compared over the same time period as that of sodium, the migration rate for  $\text{Cl}^-$  appears to be linear.

It has been observed that rate of sodium ion migration slows down with time in agreement with work reported by Murray

However over the same time period, the chloride permeability is constant. The chloride permeation is represented by the best fit equation;

$$[\text{Cl}^-] = K_{\text{Cl}^-} \times t^{0.18} \dots\dots\dots(13)$$

with the rate of change of chloride ion concentration being

$$\frac{d[\text{Cl}^-]}{dt} = K' t \dots\dots\dots(14)$$



According to Murray, chloride transport would be of type I where the rate is linear with time. The ionic permeability data show that the epoxy-acrylate coatings studied are perm-selective, that is, sodium ions are transported through the films more easily than chloride ions.

If the perm-selectivity was purely due to size exclusion, then chloride would be expected to permeate more quickly as it is the larger ion. In the systems studied however, the sodium ion permeability is more than an order of magnitude greater than that for chloride.

Rudham and Sherwood<sup>[58]</sup> have shown that epoxy coatings carry a negative charge thus impeding the migration of the chloride ion and causing the perm selectivity.

The epoxy-graft-acrylic polymers may also be acting as ion-exchange resins

### 7.6. Formation of Idealised ion exchange resins

Generally, ion exchange resins are modified polystyrenes formed from either styrene (vinyl benzene) or divinyl benzene.

#### 7.6.1 Cation resins

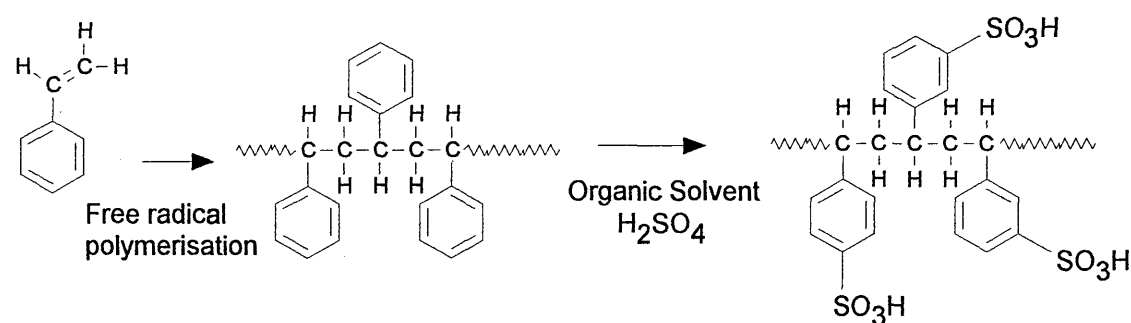


Figure 45: Cation exchanger resin formation

7.6.2. In anion exchange resins there is some variation between manufacturers but the following is typical of the route to both gel and porous anion resins;

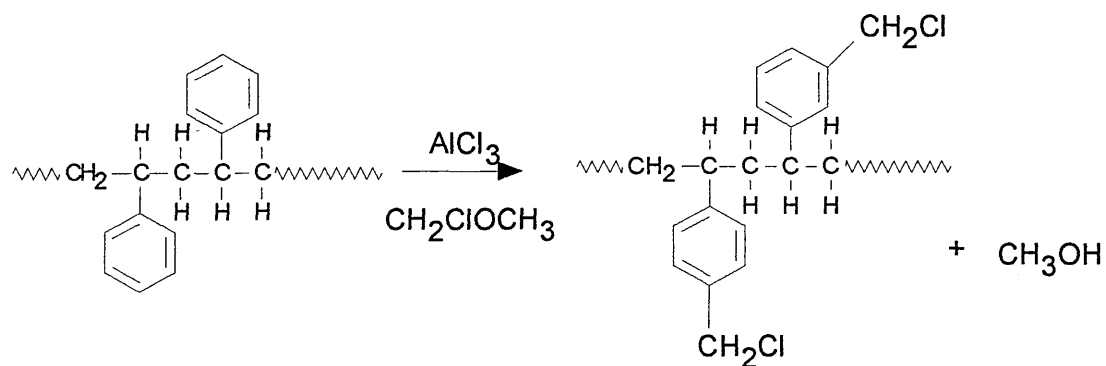


Figure 46: Anion exchanger resin formation

The chloromethylated polystyrene is then washed free of catalyst and excess reagent and then treated with an amine.

The type of amine determines the strength of the active group.

So called "Strong" anion exchange resins are made with trimethylamine;

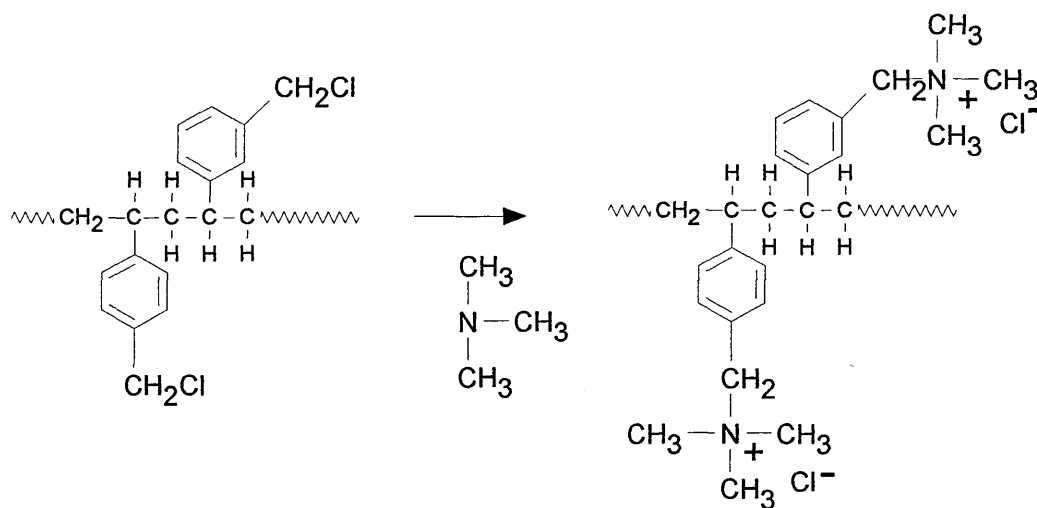


Figure 47: Formation of a "strong" anion exchange resin

### *7.7. Epoxy-graft-acrylic films as "ion exchange" resins*

If we now consider an idealised structure of a section of the epoxy-graft-acrylate, ignoring for a moment the phenol-formaldehyde cross-linker, structures within the polymer matrix are present that could conceivably account for the ability of the lacquer films to act as a potential cation exchange resin.

The ions present in a solution get to and from the sites of an ion exchange resin through the pore structure. The distribution of pores may be random across the formed film and the size of the pores is probably non-uniform.

Generally, the higher the valency of an ion, the tighter it is held by the exchanger ions. <sup>[59]</sup>

Ions such as  $\text{Fe}^{3+}$  and  $\text{PO}_4^{3-}$  are therefore removed from the resin only with difficulty.

This might give an explanation as to why the epoxy-acrylate films have the ability to "bind" iron into the polymer matrix. (see earlier work on rapid pack testing, optical emission glow discharge spectrometry and iron complexing studies) thus accounting for the extremely low iron contents found in solution after pack testing.

The transport of  $\text{Na}^+$  ions across the polymer membrane could be envisioned as an ion exchange process utilising the  $\text{H}^+$  and quaternary  $\text{N}^+$  ions found on the grafted acrylic portion of the epoxy-g-acrylate.

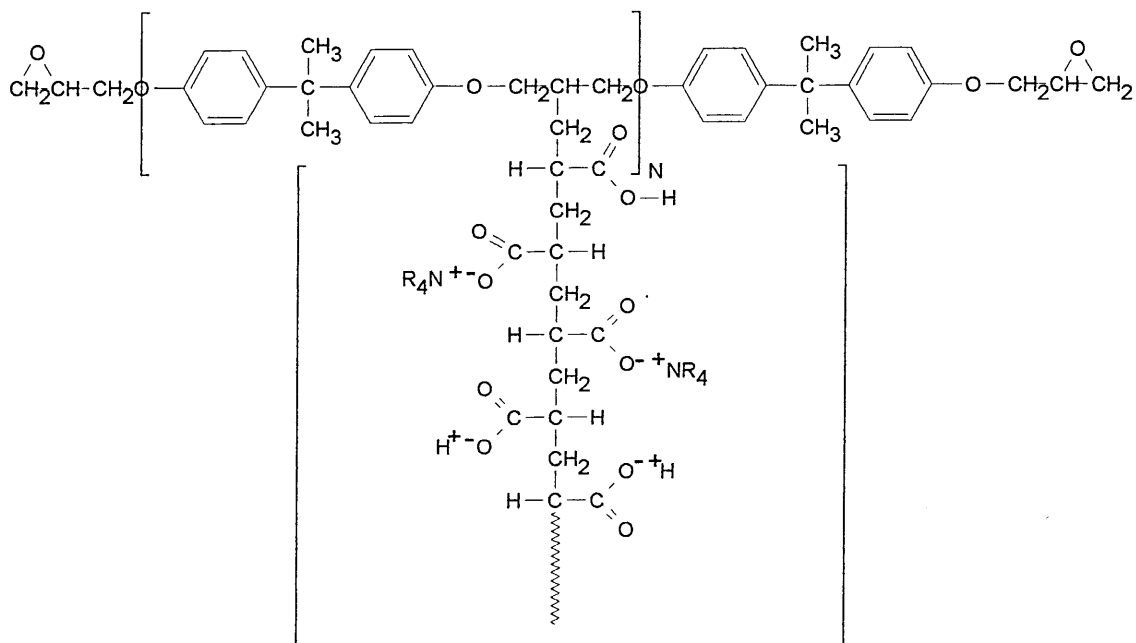


Figure 48: Transport of  $\text{Na}^+$  across membrane

Thus , the sodium ions could be exchanged slowly through the coating.

Chloride migration is impeded however by

- a) the overall negative charge on the epoxy resin backbone <sup>[58]</sup>, repelling the chloride ion cluster and
- (b) the lack of exchangeable anions through which anion exchange could occur.

Fick's first law of diffusion <sup>[60]</sup> states that the rate of flow through a membrane is;

$$\frac{dn}{dt} = DA \left( \frac{c_1 - c_2}{l} \right) \dots \dots \dots (15)$$

where D is the diffusion coefficient , A is the cross sectional area of the membrane, l is the thickness of the membrane ,and  $c_1$  and  $c_2$  represent the concentration of solute on either side of the membrane.

For sodium ions migrating through epoxy-g-acrylates, Fick's first law reduces to

$$\frac{dn}{dt} = DA \left( \frac{c_1 - c_2}{l} \right) = -0.3t + 11 \dots \dots \dots (16)$$

Thus the diffusion coefficient at different times during the experiment can be determined;

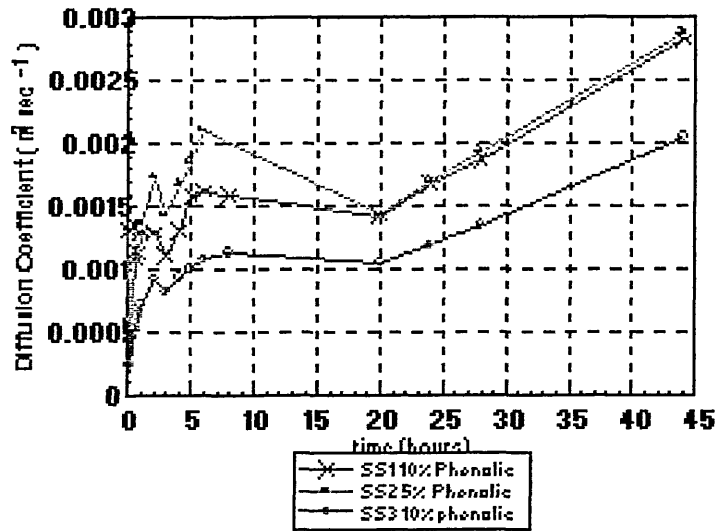


Figure 49: Diffusion Coefficient versus time for  $\text{Na}^+$

and for chloride ions diffusing through epoxy-graft acrylic films, Fick's Law reduces to;

$$\frac{dn}{dt} = DA \left( \frac{c_1 - c_2}{l} \right) = 0.18K't$$

where the constant  $K'$  takes values between 20 and 24 depending upon the lacquer variable under investigation

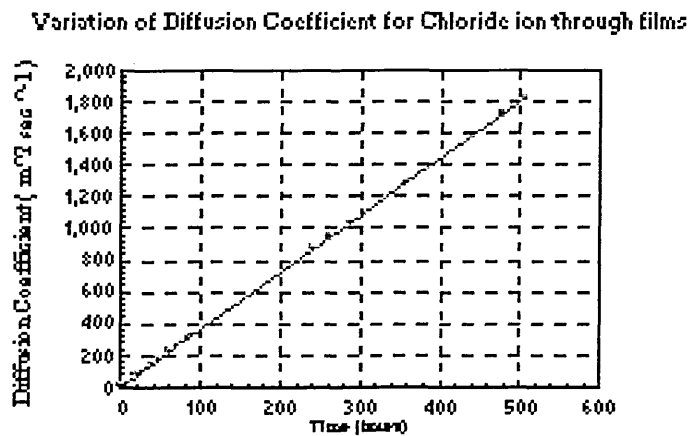


Figure 50: Diffusion constant for chloride through all epoxy-graft acrylic films

### ***7.8. Diffusion of sodium and chloride ions through epoxy-graft-acrylic films***

Thus the diffusion of sodium and chloride ions through epoxy-graft-acrylic films appears to occur by different mechanisms .

Sodium ions appear to have a diffusion coefficient which varies with time, with all the polymer films tested showing a similar profile.

The rate of diffusion of sodium ions across the films appears to increase until a critical time is reached ( typically 5-6 hours ) after this time the diffusion rate appears to slow until 20 hours of pumping electrolyte across the surface of the film. The rate then appears to increase until the end of the testing period.

This type of behaviour is postulated to be due to:

- a) initial diffusion of sodium ions across the film being osmotically driven and proceeding until the concentration of the sodium ions on each side of the film is approximately equal.
- b) the slow down in the diffusion coefficient of sodium after the first period of permeation is thought to be ion-exchange driven ; and
- c) the final increase in diffusion coefficient could be due to a swelling of the film pores by electrolyte (water ) allowing migration of sodium ions through enlarged pores and permitting the exposure of more ion exchange sites across which sodium ion exchange could occur.

The migration of chloride ion across the polymer films investigated appears to coincide with the Type III type of diffusion proposed by Murray<sup>[25]</sup> in which the diffusion rate increases linearly with time and there is no interaction between the ions and the polymer.

The migration in the case of chloride ions is slow and can only proceed via pores in the polymer. As time of exposure to electrolyte increases the polymer matrix is thought to swell slightly, thus opening up the pores and allowing the migration of more chloride ions.

The above studies have shown that ions migrate through the films at different rates and that although the composition of the cured film may change ( from 10% phenolic component loading down to 3% phenolic component ) the overall effect on the barrier performance of the cured films isolated from metal substrate, is only small.

The following studies, using Alternating Current Impedance spectroscopy were undertaken in an attempt to marry the information gathered from the studies of the film isolated from the metal substrate with the situation that occurs when the film is coated onto tin-plated steel.

Section 8

# **Alternating Current Impedance Spectroscopy Studies**



## ***8. Alternating Current Impedance Spectroscopy (AC Impedance)***

### ***8.1 Theory***

An electrochemical cell can be represented by a purely electronic model. For example, an electrode interface during an electrochemical reaction is analogous to an electronic circuit comprising an array of resistors and capacitors. It is this representation that allows an electrochemical cell to be described in terms of its “equivalent circuit” and enables interpretation of the elements comprising the circuit by reference to established ac circuit theory.

Of particular relevance is a branch of ac theory which concerns the response of a given circuit to an alternating current or voltage as a function of frequency. The mathematics of the theory are beyond the scope of this work but a rigorous theoretical treatment is given in references <sup>[61 - 65]</sup>

In direct current theory ( a special case of ac where the frequency equals 0Hz), a resistance is defined by Ohms Law;

$$R = \frac{E}{I} \quad (18)$$

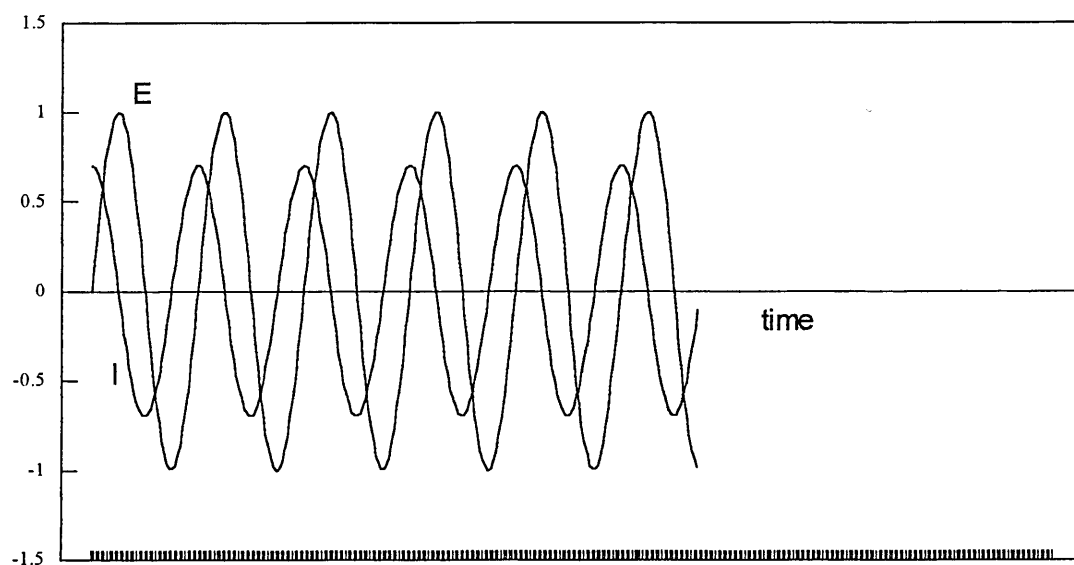
Thus it is possible to apply a dc voltage (E, volts) to a circuit, measure the current flowing ( I, amps ) and calculate the resistance (R, ohms ).

For an ac voltage, where the frequency is not equal to zero; the analogous equation is;

$$Z = \frac{E}{I} \quad (19)$$

In this equation, E and I are waveform amplitudes for the potential and the current respectively, and Z is defined as the “ac impedance”, the ac equivalent of resistance.

Figure 51 represents typical plots of a voltage sine wave (E) applied across a given circuit and the resultant ac current waveform (I). The two waveforms differ not only in amplitude but also in phase. In the case of a purely resistive circuit, the waveforms would differ only in amplitude but would be in-phase with each other.



*Figure 51: AC waveforms for an applied potential and a resultant current.*

The current sine wave can be described by the equation

$$I = A \sin(\omega t + \theta) \quad (20)$$

where I is the instantaneous current,  $\omega$  frequency in radians /sec =  $2\pi f$ , f is the frequency in hertz, A is the maximum amplitude and  $\theta$  is the phase shift in radians.

Vector analysis provides a convenient means of describing an ac waveform and it permits characterisation of a wave in terms of both its amplitude and its phase. A waveform can be described in terms of vectors in three ways;

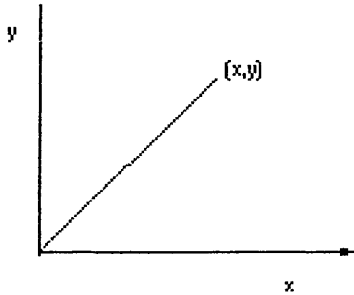


Figure 52a : x-y representation of Impedance

Figure 52a shows how the end point of the vector can be given in terms of an ( x,y) co-ordinate pair.

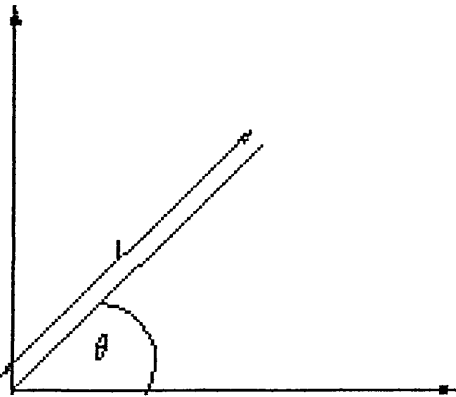


Figure 52b: Representation of vector in terms of an angle and its modulus

Figure 52b illustrates an equivalent description in which the vector is unambiguously described by an angle,  $\theta$  and a magnitude ,  $|I|$

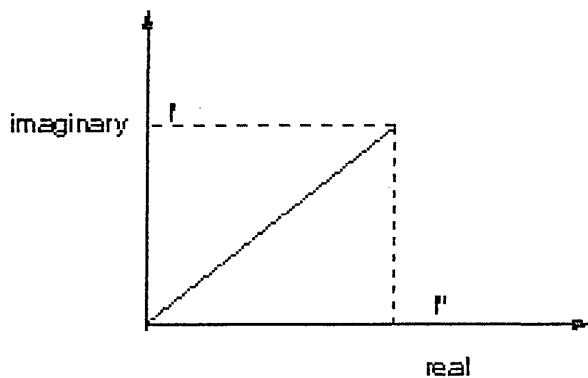


Figure 52c : Representation of Impedance in terms of real and imaginary components

A third approach to describing vectors is often used which is more convenient for numerical analysis; this approach is shown in Figure 52c. Here the axes are defined as *real*,  $I'$  and *imaginary* ,  $I''$ .

The mathematical convention for expressing quantities in this co-ordinate system is to multiply the “I” co-ordinate value by -1 , symbolised by “ i ” ( more commonly for electronics discussion , “ j ”)

Using this convention, any ac current vector can be defined as the sum of its real and imaginary components:

$$I_{\text{total}} = I' + I''j \quad j = \sqrt{-1} \quad (21)$$

Similarly , any ac voltage vector can be expressed as

$$E_{\text{total}} = E' + E''j \quad (22)$$

The real and imaginary components of an ac waveform are defined with respect to some reference waveform, and the imaginary component, also referred to as the ”quadrature component “ , is exactly 90° out of phase. The reference waveform allows expressions of the current and voltage waveforms as vectors with respect to the same co-ordinate axes, which facilitates the manipulation mathematically of the vector quantities.

The impedance of the circuit can thus be calculated as the quotient of the voltage and current vectors;

$$Z_{\text{total}} = \frac{E' + E''j}{I' + I''j} \quad (23)$$

The resulting vector expression for the ac impedance,  $Z_{\text{total}} = Z' + Z''j$  is defined in terms of the same co-ordinate axes as the current and voltage vectors.

From analytical geometry, the absolute magnitude of the impedance vector is given by;

$$|Z| = \sqrt{(Z')^2 + (Z'')^2} \quad (24)$$

whereby

$$\tan \theta = \frac{Z''}{Z'} \quad (25)$$

## 8.2 Circuit Elements and their AC Impedance Equations

Using the above theory expressions can be derived for simple electrical circuits


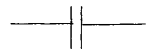
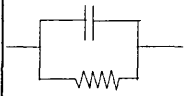
Circuit Element	AC Impedance Equation
	$Z = R + 0j$
	$Z = 0 - j$ $\frac{1}{\omega C}$ $\omega = 2\pi f$
	$Z = \frac{R}{1 + \omega^2 C^2 R^2} - \frac{j\omega C R^2}{1 + \omega^2 C^2 R^2}$

Table 19: Circuit elements and their impedance equations

The above table shows that the impedance of a resistor has no imaginary component and thus the phase shift is zero and the current is in phase with the voltage.

The ac impedance of a capacitor is, however, comprised of an imaginary component which is a function of the frequency and the capacitance, but no real component.

Similar expressions can be derived for other circuit elements and the impedance for any combination of circuit elements can be defined by a combination of expressions. The parallel resistor / capacitor network above is a typical example that shows both real and imaginary components.

### 8.3 Examination of Electrochemical systems in terms of their equivalent electrical circuits.

A simple system is represented by Figure 53, below;

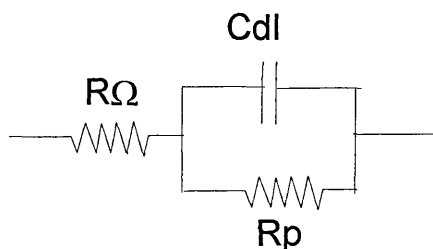


Figure 53: Equivalent Circuit 1 A non-porous conducting film

$R_{\Omega}$  is the uncompensated resistance between the working electrode and the reference electrode,  $R_p$  is the polarisation resistance at the electrode / solution interface and  $C_{dl}$  represents the double layer capacitance at the interface.

A knowledge of the value of  $R_p$  enables the calculation of corrosion rates.<sup>[66]</sup> Capacitance measurements can provide information on adsorption and desorption phenomena, film formation at the electrode and the integrity of coatings<sup>[67]</sup>.

Figure 54 , below illustrates a proposed equivalent circuit for a porous non-conducting film<sup>[67]</sup> where  $C_c$  is the coating capacitance and  $R'$  represents the pore resistance.

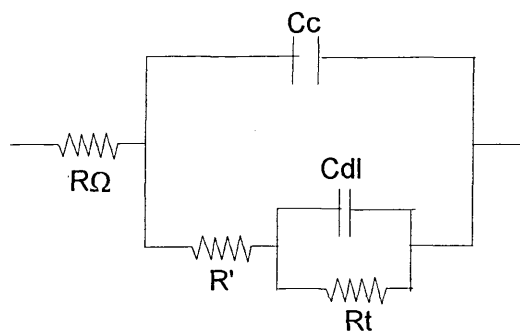


Figure 54: Equivalent Circuit 2- a porous conducting film

When a chemical reaction is occurring in conjunction with the processes within an electrochemical cell, further circuit elements can be built into the equivalent circuit; this is illustrated in Figure 55

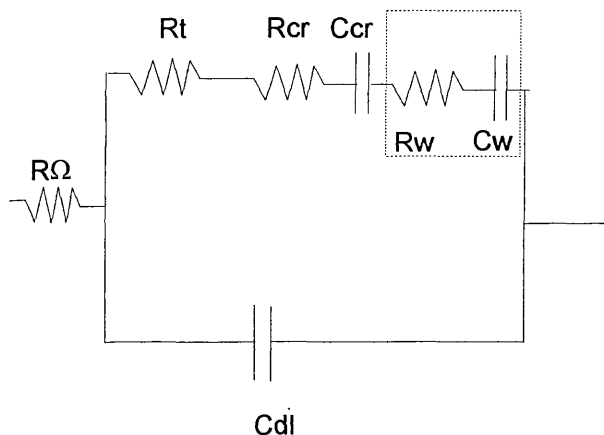


Figure 55: Equivalent Circuit showing a porous film exhibiting electrochemical reactions

where  $R_{cr}$  is the chemical reaction resistance,  $C_{cr}$  is the chemical reaction capacitance and  $R_w$  and  $C_w$  are Warburg impedance effects. The box enclosing  $R_w$  and  $C_w$  is a simplification of the circuit representing the Warburg impedance which rationalises mass transfer limitations due to diffusion processes adjacent to the electrode <sup>[68]</sup>

#### 8.4 Warburg Impedance and diffusion control

The rate of an electrochemical reaction can be strongly influenced by the diffusion of one or more reactants to the electrode surface. Often this is the case when solution species must diffuse through a surface layer on the electrode. If diffusion effects completely dominate the electrochemical reaction mechanism, the impedance to the reaction is known as a Warburg impedance.

For diffusion controlled electrochemical reactions, the current is out of phase by  $45^\circ$  with the exciting potential signal. This means that the real and imaginary components of the impedance vector ( $Z'$  and  $Z''$ ) are equal at all frequencies. As an equivalent circuit, the

diffusion process appears to be midway between a resistor ( $0^\circ$  phase shift) and a capacitor ( $90^\circ$  phase shift). The value of  $|Z|$  for a diffusion controlled system is proportional to  $\frac{1}{\sqrt{\omega}}$  where  $\omega$  is the frequency in radians.

### 8.5 AC Impedance Plots

Once an experiment is completed, the data generated consists of

- 1) the real component of the voltage,  $E'$
- 2) the imaginary component of the voltage,  $E''$
- 3) the real component of the current,  $I'$
- 4) the imaginary component of the current,  $I''$ .

From this data, it is possible to calculate the phase shift response,  $\theta$ , the real impedance,  $Z'$  the imaginary impedance,  $Z''j$  and the total impedance,  $|Z|$  for each applied frequency.

Various formats can be used to plot this data with each format having its own specific advantages for revealing certain characteristics of the system under test.

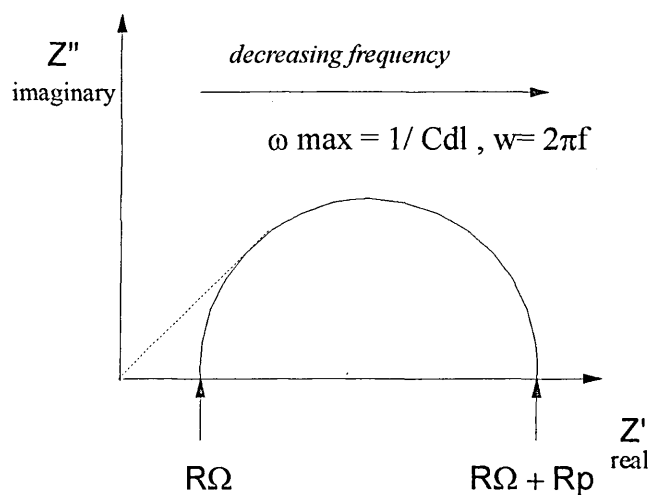


Figure 56: The Nyquist Plot (Cole-Cole plot)

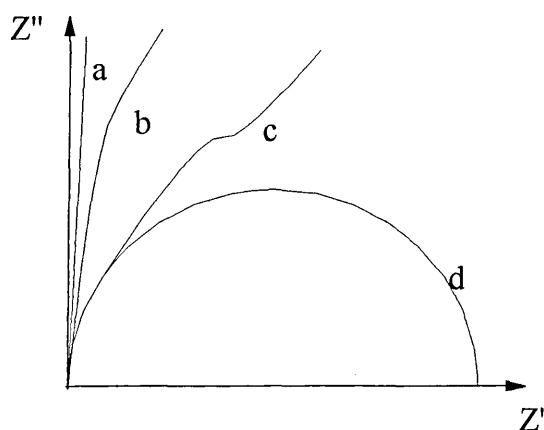


The imaginary component of the impedance ( $Z''$ ) is plotted against the real component of the impedance ( $Z'$ ) for each frequency of excitation.

This plot can be used to calculate the uncompensated resistance,  $R_{\Omega}$ , the polarisation resistance,  $R_p$  and the double layer capacitance,  $C_{dl}$ .

The shape of the Nyquist plot changes with the state of the electrochemical cell it is describing.

Upon initial immersion of the coating, the model circuit can be considered as the fraction of the coating unpenetrated by electrolyte and the resulting impedance spectrum is dependent upon the dielectric constant of the coating material. The Nyquist curve, indicative of an intact coating is close to the  $Z''$  axis and is linear ( Curve (a) Figure 57 )



*Figure 57 Changes in Nyquist Plots as electrolyte permeates through the coating*

As the electrolyte penetrates the coating, the impedance curve becomes more curved towards the  $Z'$  axis ( Curves (b) and (c) ) and at the extreme, representing a totally penetrated coating, the Nyquist plot is a semicircle (Curve (d) )

### 8.5.1 Bode Plots

The Bode plot, which plots the impedance of the system under investigation against the frequency of measurement, Figure 58, below, permits the examination of the absolute impedance,  $|Z|$  and the phase angle,  $\theta$ , of the resultant waveform, each as a function of frequency.

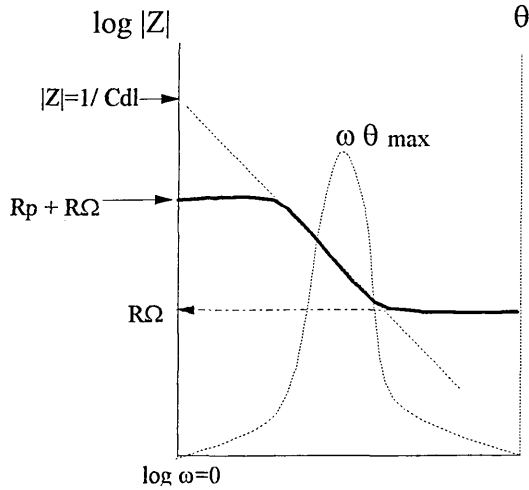


Figure 58 The Bode Plot

The  $\log |Z| \vee \log \omega$  curve can yield values of  $R_p$  and  $R_\Omega$ . At intermediate frequencies, the "break point" of the curve should lie on a straight line with a gradient of -1 <sup>[69]</sup>

Extrapolation of this line to the  $\log |Z|$  axis at  $\omega = 1$  ( $\log \omega = 0$ ) gives the value of Cdl from the relationship:

$$|Z| = \frac{1}{C_{dl}} \quad (26)$$

The  $\theta \vee \log \omega$  plot gives a peak at a frequency corresponding to  $\omega_{\theta \max}$ . Thus  $\omega_{\theta \max}$  is the frequency at which the phase shift of the response is at its maximum. From this frequency, the double layer capacitance, Cdl can be calculated <sup>[67]</sup>

$$\omega_{\theta \max} = \frac{1}{CR_p} \sqrt{1 + \frac{R_p}{R_\Omega}} \text{ where } \omega_{\theta \max} = 2\pi f_{\theta \max}$$

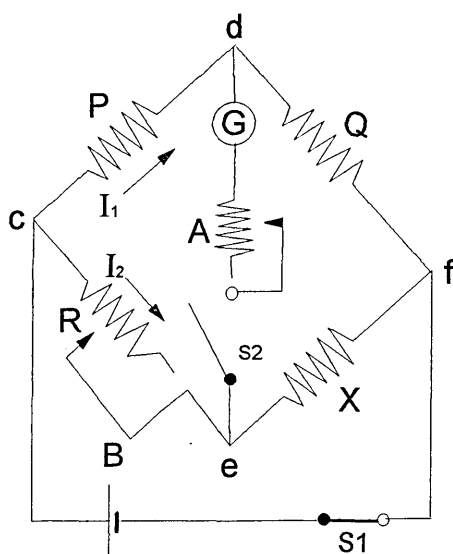
The Bode plot is a useful alternative to the Nyquist plot when scatter in experimental data makes an accurate fitting of the Nyquist semi-circle impractical. The Bode plot gives a clearer description of the electrochemical systems frequency dependent behaviour than does the Nyquist plot where the frequency values are implicit.

### ***8.6 Equipment used to carry out AC Impedance Studies***

There are two main designs of equipment with which AC impedance studies may be carried out

- 1) Traditional Wheatstone bridge analysers
- 2) Sine wave correlators

#### ***8.6.1 The Wheatstone bridge***



*Figure 59 The Wheatstone Bridge Circuit*

Historically, the A.C. Wheatstone bridge has been important in laying the foundations of A.C. electrochemical experiments. The four branches of the network, **cdfec**, have two resistances P and Q, a known variable resistance, R and unknown resistance, X. A battery,

resistances P and Q , a known variable resistance, R and unknown resistance, X. A battery, B, is connected through a switch , S1, to junctions **c** and **f**; and a galvanometer , G, a variable resistor, A, and a switch , S2, are in series across **d** and **e**

When the Wheatstone bridge is in “balance”, there is no current flow through the galvanometer ,G and the current flow through resistor P equals that through R with the current through Q being equal to that through the unknown X. It is therefore possible to calculate the unknown resistance X from  $X = R \cdot (Q/P)$

The typical electrochemical cell is not passive, i.e. it generates a potential difference ( by, for example, reactions or the absorption / desorption of species to and from electrode surfaces ).

The bridge therefore has both an a.c. and a d.c. detector with the d.c. detector serving also as a source of whatever steady current is taken by the cell. Balance of the bridge is indicated by an a.c. detector which may be a tuned amplifier / meter or an oscilloscope.

Both resistance and capacitance have to be balanced simultaneously, by iterative adjustment until the a.c. signal is at its minimum. This approach is slow which means that the Wheatstone bridge is suitable only for static or only very slowly changing systems. The main disadvantage of bridge circuits is that they do not easily lend themselves to dynamic measurements. They also have a restricted frequency range and cannot be used below approximately 10Hz.

### 8.6.2 Sine Wave Correlation

The process of sine wave correlation can be described as the multiplication of the measured signal with a reference sine wave derived from the exciting signal. The resulting signal is then integrated over a whole number of cycles of the reference wave to give a response that is unaffected by the harmonics of the reference frequency. The random noise components are thus reduced in proportion to the length of the integration period. In practice, two reference signals are used which are in-phase and in quadrature with the exciting signal. The correlator outputs are then proportional to the real and imaginary parts of the impedance.

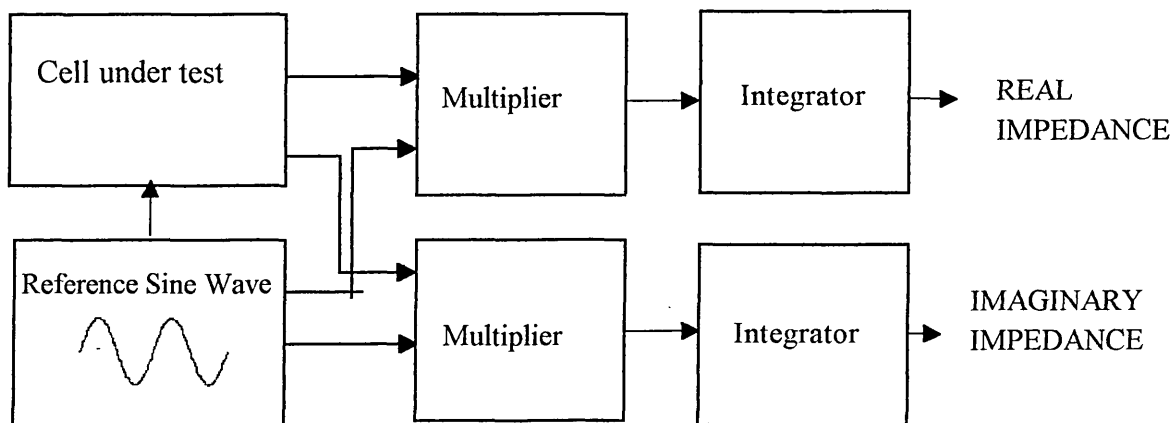


Figure 60: Sine Wave Correlation

### 8.6.3 Solatron 1250 Frequency Response Analyser (FRA)

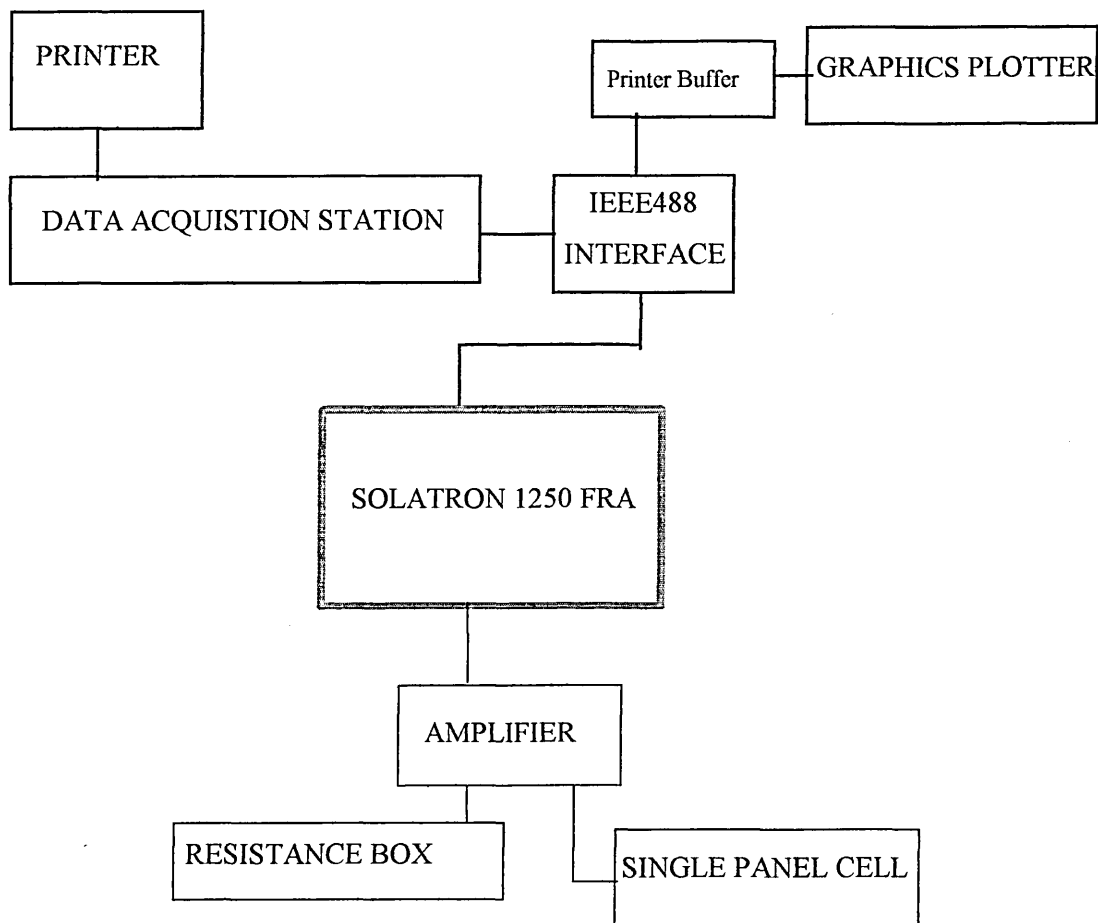


Figure 61: Schematic of AC Impedance Equipment used

This is an example of a Sine Wave correlator available from Solartron - Schlumberger. It is both a frequency generator and an analyser. It is capable of applying a constant signal at any frequency from 10mHz to 65.5kHz and scanning a range of frequencies in either rising or falling linear or logarithmic steps. It may be programmed via the key board on the instrument facia or from a remote computer using an IEEE488 interface. It is possible to pre-program the FRA using up to nine different types of experiment. These programs are described separately in Appendix 1.

## ***8.7.AC Impedance Studies Experimental Detail***

### ***8.7.1 Running an A/C impedance experiment***

The crocodile clips were attached to an exposed metal area of the can body and to the counter electrode suspended in the electrolyte. The method of analysis was selected via the computer, the manual resistance box adjusted to account for solution resistance, the resistance due to the wires in the circuitry, and the Solatron FRA was set up and started. The FRA scanned the frequency range selected and collected the real and imaginary parts of the cell impedance response. The data was stored on the computer hard disk for data processing.

### ***8.7.2 Data processing***

The data obtained from the Solatron were of the following form;

FREQUENCY;

REAL PHASOR;

IMAGINARY PHASOR;

PHASE ANGLE,  $\phi$

## 8.8. AC Impedance Spectroscopy of epoxy-acrylate films on tin-plated steel

### 8.8.1. Experimental Details

All films studied were prepared by spray coating the lacquer onto pre-cleaned ( washed in 2-butanone followed by 1 minute drying at 150°C in a box oven ) can bodies. The spray coated lacquer was then stoved for 3 minutes at 188°C to cure the polymer.

The counter electrode was a panel of uncoated tin-plated steel .

As a preliminary study, the epoxy-g- acrylate films were studied in simple electrolyte systems. The electrolytes chosen were;

Electrolyte	pH nature	Expected corrosion phenomenon
0.01M NaCl	neutral	Corrosion occurring by neutral blistering mechanisms
0.1 M NaCl	neutral	Corrosion occurring by neutral blistering mechanisms
1M NaCl	neutral	Corrosion occurring by neutral blistering mechanisms
0.01M H <sub>3</sub> PO <sub>4</sub>	acidic	Should cause underfilm corrosion
0.1M H <sub>3</sub> PO <sub>4</sub>	acidic	Should cause underfilm corrosion
1M H <sub>3</sub> PO <sub>4</sub>	acidic	Should cause underfilm corrosion

Table 20: Preliminary electrolytes used in AC Impedance Studies



### 8.8.2 0.01M NaCl solution

Cans spray coated with SS1 ( 10% phenolic ) were analysed by AC Impedance spectroscopy over the frequency range 0.01 Hz to 65000 Hz using a frequency response analyser set to give 5 steps per decade. The perturbing voltage used was 10mV at 63096 Hz.

The impedance response across the frequency range was monitored over 50 days with data collected in terms of frequency, real and imaginary components of the impedance, total impedance and phase angle ( theta ).

The data for 1 to 49 days exposure are plotted below as a Bode plot.

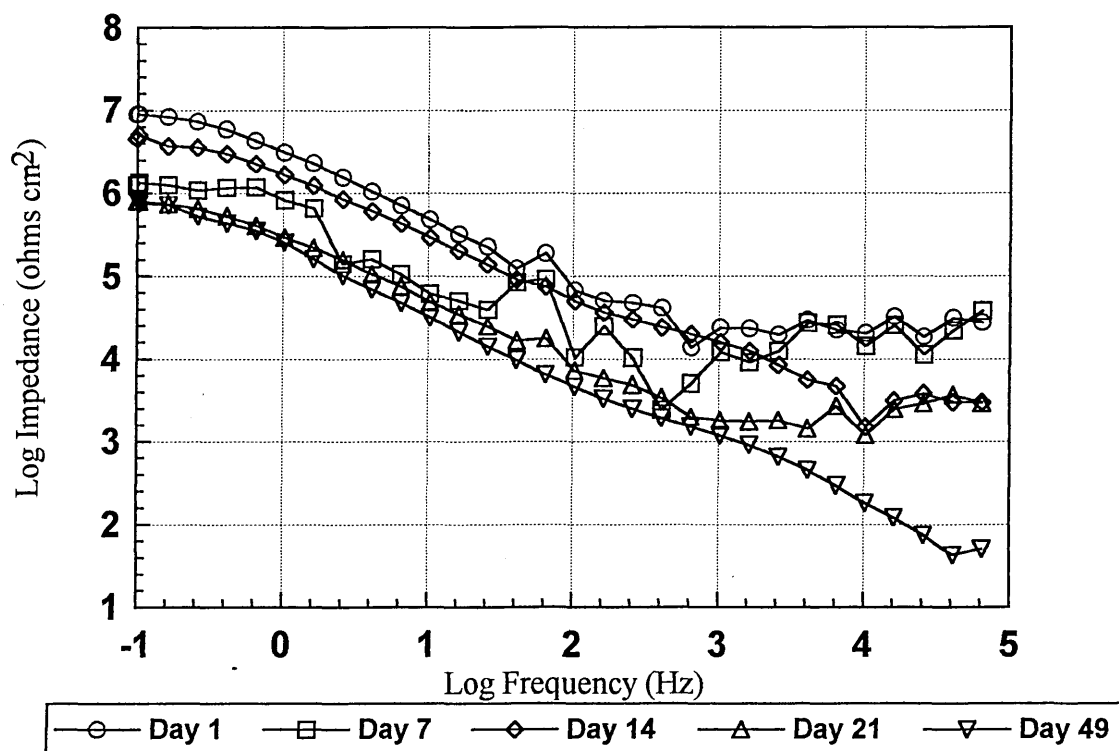


Figure 62: Bode plot for SS1 film exposed to 0.01M NaCl up to 49 days

Analysis of the Bode plots yield the following information;

Day	$R_p$ ( ohms cm <sup>-2</sup> )	$R_\Omega$ ( ohms cm <sup>-2</sup> )	Cdl ( Farads cm <sup>-2</sup> )
1	$3.097 \times 10^6$	$37.6 \times 10^3$	$6.34 \times 10^{-8}$
7	$1.663 \times 10^6$	$27.4 \times 10^3$	$6.12 \times 10^{-8}$
14	$0.822 \times 10^6$	$2.99 \times 10^3$	$6.37 \times 10^{-8}$
21	$0.292 \times 10^6$	$2.942 \times 10^3$	$8.52 \times 10^{-8}$
49	$0.256 \times 10^6$	$0.050 \times 10^3$	$6.15 \times 10^{-8}$

*Table 21 Analysis of Bode Data for SS1 exposed to 0.01M NaCl solution*

The data suggest that over the 49 day period of investigation there is

- 1) A decrease in the polarisation resistance of the polymer , implying that the electrolyte permeates the polymer to the metal surface.
- 2) The double layer capacitance, Cdl, remains relatively stable over the period of testing SS1 epoxy-g-acrylate film within 0.01M sodium chloride solution.

This suggests that the film allows the penetration of electrolyte to the metal surface , but since the concentration of  $Cl^-$  ions within the electrolyte is not sufficient to stimulate the corrosion process and the concentration of  $Na^+$  is low so as not to become the counter ion for any  $OH^-$  produced by the corrosion cell , significant cathodic disbondment of the coating from the metal does not occur. Thus, the polymer coating affords protection to the steel substrate over the period of the test.

### 8.8.3 0.1M NaCl solution

A series of cans coated with SS1 (10% phenolic ) was analysed by AC Impedance spectroscopy using a perturbation voltage of 10mV at 63096Hz and the frequency response was measured over the range 0.01 Hz to 65000 Hz using the frequency response analyser set to give 5 steps per decade ( i.e. 30 data points ) (Program 6 see Appendix I )

The frequency response v impedance was monitored over 60 days with the data obtained in terms of frequency, real and imaginary components of the impedance , and phase angle.

For each set of data, the response of the coating / electrolyte was plotted in both the Nyquist and Bode data representations . Modelling the coating response was undertaken using the Boukamp <sup>[71]</sup> impedance fitting software.

#### 8.8.3.1 Nyquist Plots

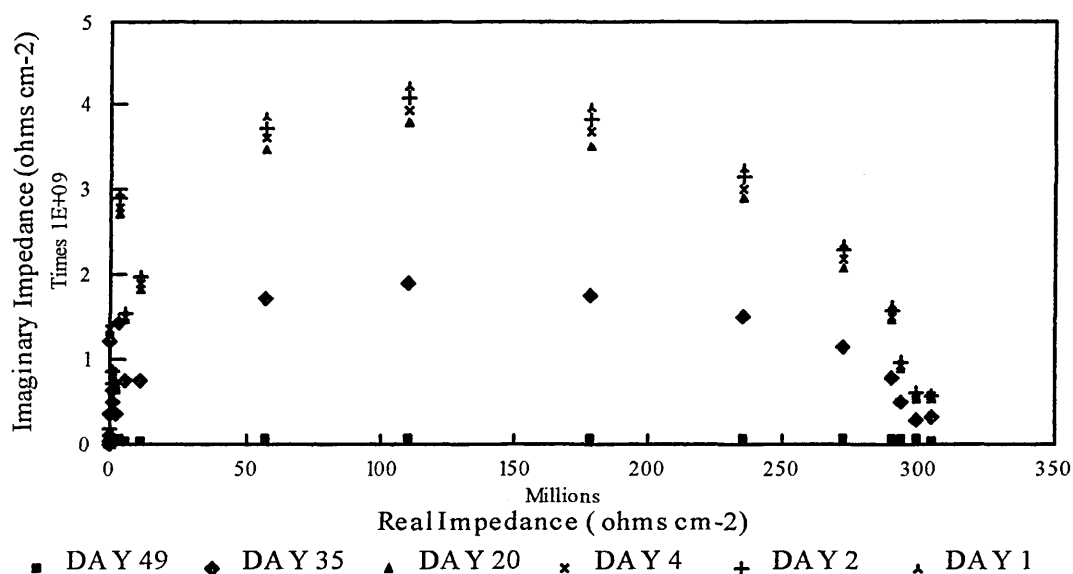


Figure 63 Nyquist Plot : SS1 film exposed to 0.1M sodium chloride solution

The data for day 49 are shown below with the plot expanded so as to aid investigation

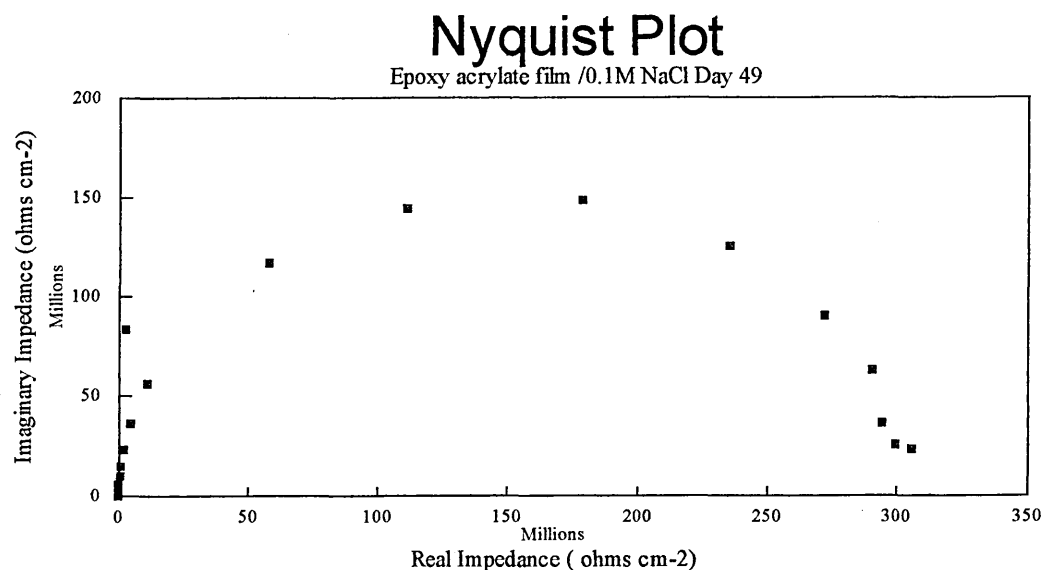


Figure 64: Nyquist plot 0.1M NaCl / SS1 film Day 49 Expanded

### 8.8.3.2 Bode Plots

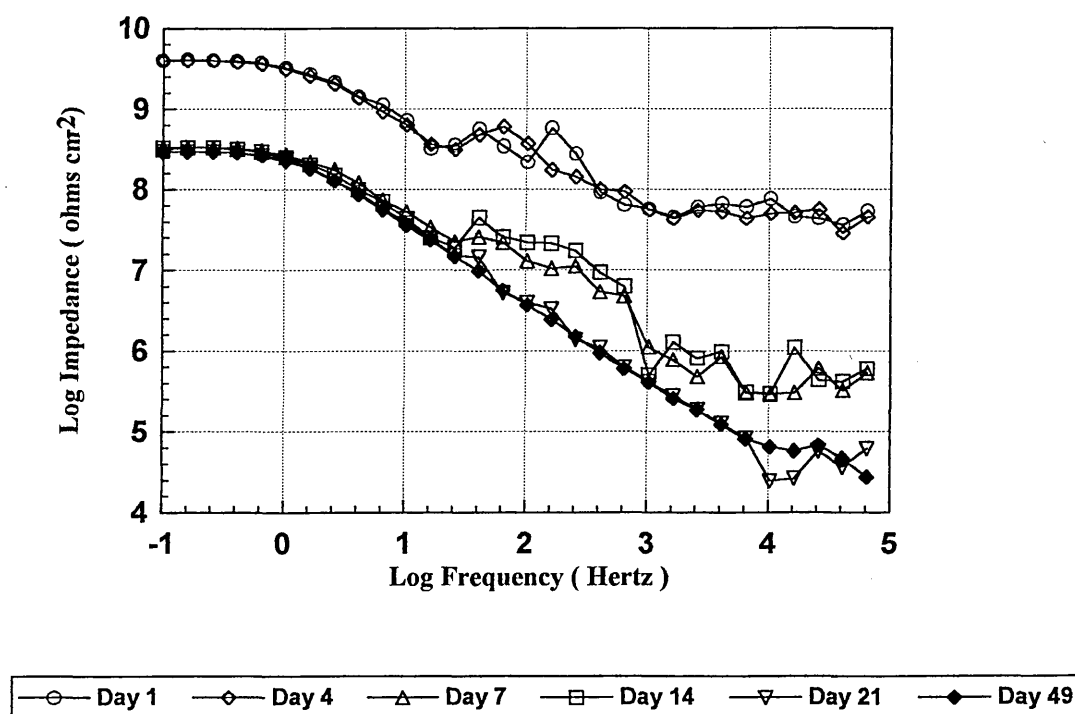


Figure 65 Bode Plots 0.1M NaCl / SS1 polymer film

The film polarisation resistance was calculated from the Bode plot at each day of exposure .

The results are plotted below in Figure 66

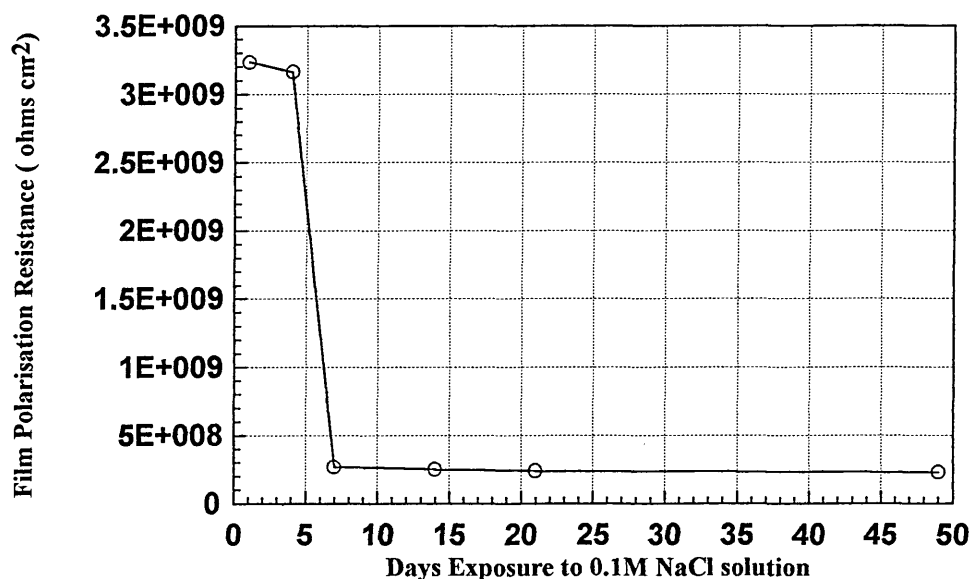


Figure 66: Polarisation resistance v exposure time for SS1/ 0.1 M NaCl

The Nyquist and Bode plots show evidence of the reduction in coating resistance as exposure time increases . The double layer capacitance is stable for 10 days and then the film appears to fail catastrophically in the period between 10 and 14 days suggesting a change in electrochemical mechanisms from one of neutral blistering to a rupturing of the film blisters and the onset of film blistering at secondary sites. The lack of a secondary semicircle in the Nyquist plots until day 49 suggests that corrosion is not occurring .

Boukamp modelling suggests that the equivalent circuit for epoxy-acrylate film in the presence of 0.1M NaCl can be represented by a circuit in which only the polarisation resistance of the film changes.

#### 8.8.4 1M NaCl solution

When a more concentrated electrolyte is in contact with the film, the development of the corrosion processes is more pronounced. The Bode plots show a rapid change from a system absorbing electrolyte to a system undergoing corrosion relatively rapidly. The changes are shown below (Figure 67):

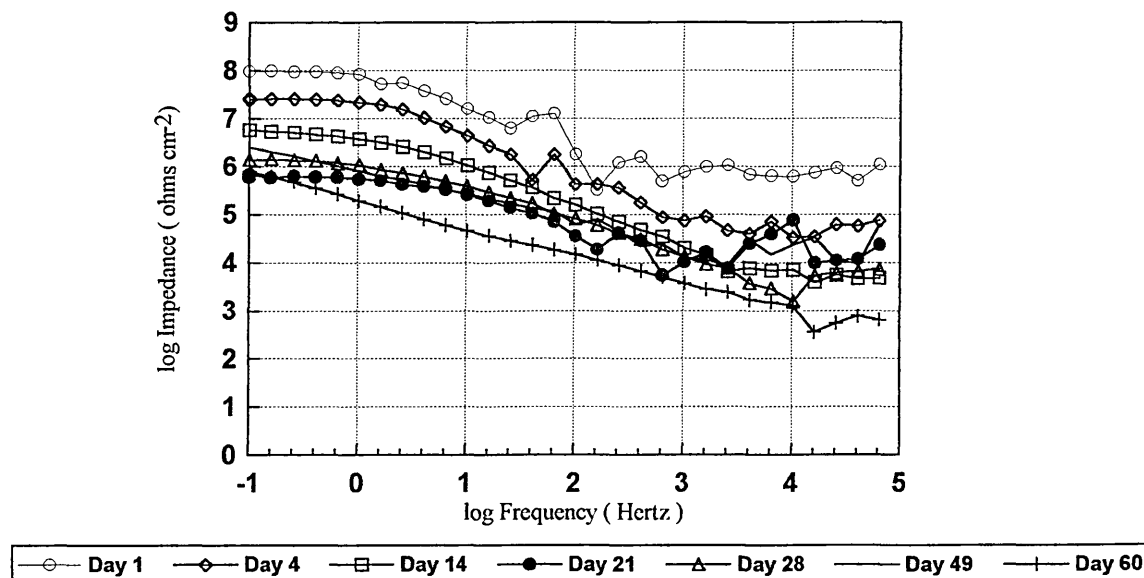


Figure 67: Bode plot SS1 film in 1M NaCl solution v exposure time

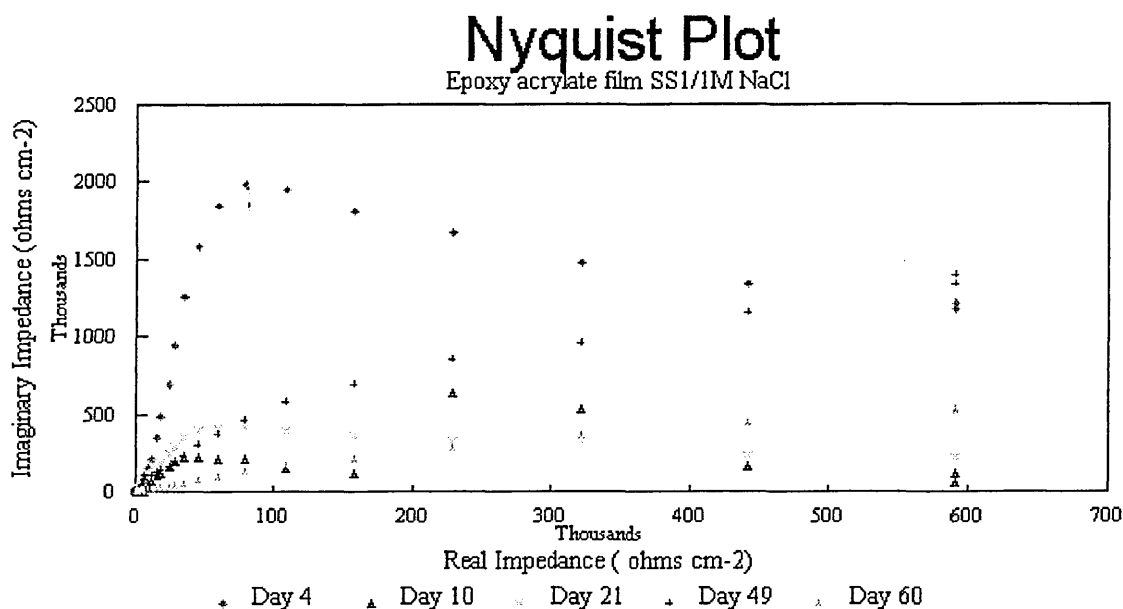


Figure 68: Nyquist plots for SS1 film in 1M NaCl solution v exposure time

#### 8.8.5 Interpretation of Bode and Nyquist plots for SS1/ 1M NaCl

On day 4, the Nyquist semicircle is completed, indicative of complete penetration of the electrolyte across the film to the metal surface. The semicircle has a large diameter showing the coating to still be intact with a high polarisation resistance. On Day 10 of exposure, the semicircle of the Nyquist plot is still complete but is much reduced in radius. This illustrates the fact that ions are migrating through the coating, causing a reduction in the coating resistance although the coating still holds back the onset of corrosion of the underlying metal, since no evidence is present in the Nyquist plot for a second semi-circle which would indicate that a secondary process ( such as charge transfer ) is occurring.

After 21 days of exposure to 1M sodium chloride solution, the Nyquist plot of the film begins to show evidence of deviation away from purely resistive behaviour. The high frequency response of the coating departs from the semi-circular response. This frequency

dependent behaviour is a sign that the film is beginning to become a less effective barrier against corrosion and that some secondary processes are occurring at the film / metal interface.

The polarisation resistance ( calculated from the corresponding Bode plots ) of the coating changes rapidly with time.

Analysis of the Bode plots gives the following data

Day	$R_p$ (ohms/cm <sup>2</sup> )	$R \Omega$ (ohms cm <sup>-2</sup> )	$C_{dl}$ Faradscm <sup>-2</sup> )
1	$8.318 \times 10^7$	$0.708 \times 10^6$	$8.32 \times 10^{-8}$
4	$2.188 \times 10^7$	79,432	$7.522 \times 10^{-8}$
7	$3.715 \times 10^6$	63,095	$6.511 \times 10^{-8}$
14	$0.549 \times 10^6$	10,000	$4.680 \times 10^{-8}$
21	$1.07 \times 10^6$	8,912	$4.125 \times 10^{-8}$
49	$0.812 \times 10^6$	23,451	$3.16 \times 10^{-8}$

Table 22: Analysis of Bode data SS1 film /1M NaCl solution

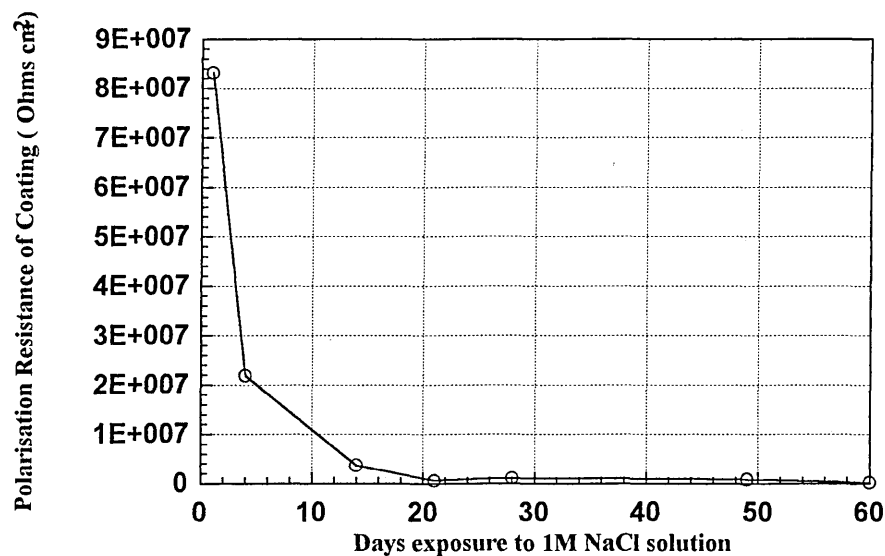


Figure 69: Change in polarisation resistance of SS1 film in 1M NaCl solution



### 8.9. Investigation of SS1 in aqueous phosphoric acid solutions.

AC Impedance spectroscopy was used to analyse a series of cans coated with SS1 film

(10% phenolic ) using a perturbation voltage of 10mV at 63096Hz ,with frequency response measurement of the system impedance over the range 0.01 Hz to 65000 Hz (Program 6 see Appendix I )

Data were collected over 60 days, with the data obtained in terms of frequency, real and imaginary components of the impedance and phase angle, in order to characterise the system under test.

For each set of data, the response of the coating / electrolyte was plotted in the Bode data representation as the measurements produced data that was unsuitable for Nyquist fitting .

Modelling the coating response was undertaken using the Boukamp impedance fitting software.

#### 8.9.1. SS1 film exposed to 0.01M Phosphoric Acid

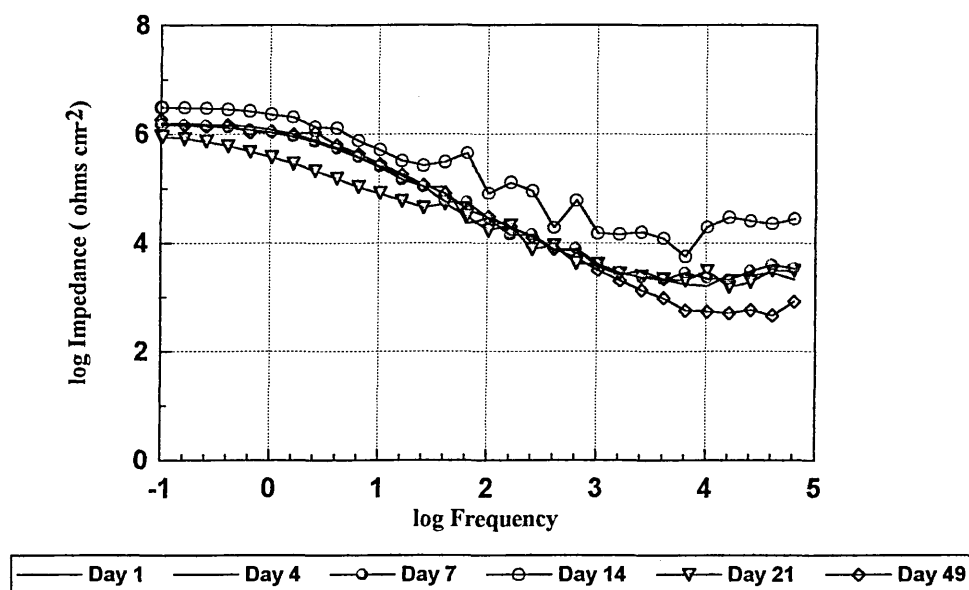


Figure 70 : Bode Plots SS1 film in 0.01M Phosphoric acid solution

Analysis of the Bode plots yields the following data

Day	$R_p$ (ohms/cm <sup>2</sup> )	$R_{\Omega}$ (ohms cm <sup>-2</sup> )	$C_{dl}$ Faradcm <sup>-2</sup> )
1	$3.099 \times 10^6$	22,233	$8.32 \times 10^{-8}$
21	$1.462 \times 10^6$	3,030	$2.77 \times 10^{-8}$
49	$0.896 \times 10^6$	2,118	$3.16 \times 10^{-8}$

Table 23: Analysis of Bode data 0.01M phosphoric acid / SS1 polymer film

The data suggests that:

- i) Over the time period assessed , there is a decrease in the polarisation resistance of the polymer. This implies that the polymer is being permeated by electrolyte.
- ii) The double layer capacitance remains relatively stable over the time period of testing the epoxy-acrylate SS1 within 0.01M phosphoric acid.

#### 8.9.2 SS1 Epoxy-acrylate in the presence of 0.1M Phosphoric Acid.

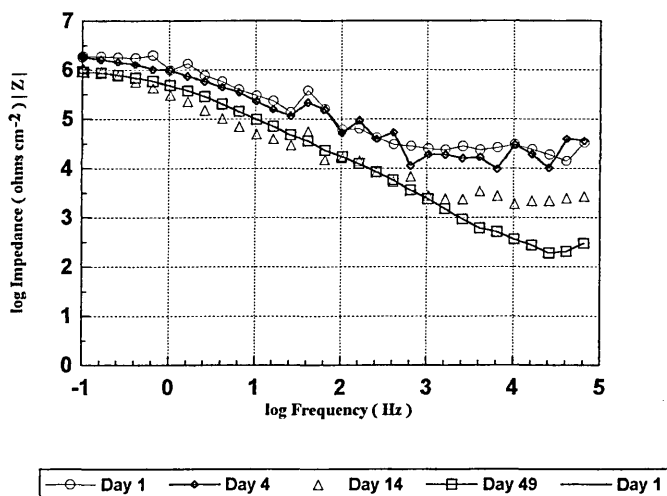


Figure 71: Bode plot SS1 film exposed to 0.1M phosphoric acid

The Bode plots yield the following data

Day	$R_p$ (ohmscm <sup>-2</sup> )	$R_\Omega$ (ohmscm <sup>-2</sup> )	$C_{dl}$ Farads cm <sup>-2</sup> )
1	$0.977 \times 10^6$	39,810	$4.03 \times 10^{-12}$
4	$0.978 \times 10^6$	38,100	$3.296 \times 10^{-12}$
8	$0.478 \times 10^6$	3,162	$4.228 \times 10^{-10}$
49	$0.301 \times 10^6$	320	$1.419 \times 10^{-8}$

*Table 24 Analysis of Bode data for SS1 in 0.1M Phosphoric acid*

The Bode plots show that for SS1 in 0.1M Phosphoric acid solution, over the testing period, the polarisation resistance of the polymer is of the order of  $10^6$  ohms cm<sup>-2</sup>. It was observed however in the later stages of the corrosion test, the  $C_{dl}$  value of the coating began to fall. This could indicate the onset of corrosion in the system.

Since 0.01M H<sub>3</sub>PO<sub>4</sub> (aq) had little effect upon the impedance response of SS1 coating and only small differences were observed when the coating was exposed to 0.1M H<sub>3</sub>PO<sub>4</sub> solution it was decided to investigate the impedance response of an the coating system to exposure to 1M phosphoric acid solution.

### 8.9.3. SS1 in the presence of 1M Phosphoric acid solution

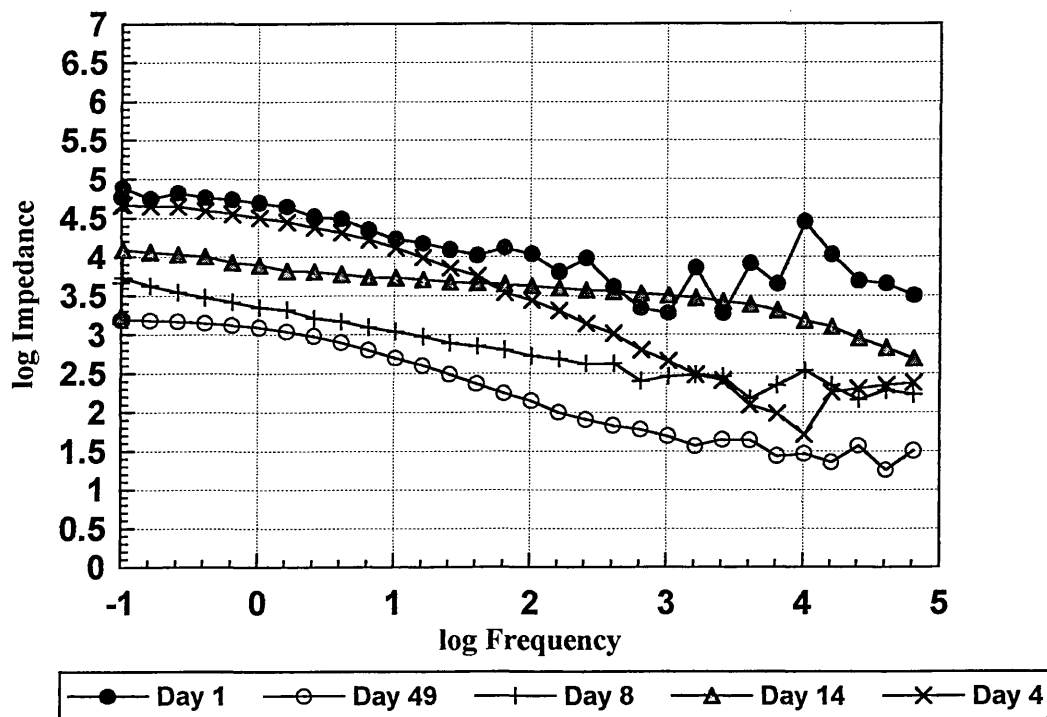


Figure 72: SS1 film exposed to 1M phosphoric acid solution

Analysis of the Bode plots generated from SS1 exposed to 1M phosphoric acid solution gives the following table ( Table 25 ):

Day	$R_p$ (ohms $\text{cm}^2$ )	$R_o$ (ohms $\text{cm}^2$ )	$C_{dl}$ Farads $\text{cm}^2$ )
1	67,000	10,000	-
4	46,000	450	$2.23 \times 10^{-7}$
8	5,000	215	-
49	1,000	22	$1.00 \times 10^{-5}$

Table 25 Analysis of Bode data for SS1 in 1M phosphoric acid

The polarisation resistance of the coating is very low after only one day of exposure to 1M  $H_3PO_4$ . This is strong evidence for the complete and rapid penetration of the electrolyte quickly through the polymer to the metal surface. The capacitance observed after 4 days exposure in the 1M phosphoric acid is equivalent to 49 days exposure in 0.1M phosphoric acid.

After 49 days exposure to the higher acid concentration, the film resistance is negligible whilst the low  $C_{dl}$  value confirms that the corrosion of the base metal is well established.

The fall in polarisation resistance of SS1 polymer film in 1M phosphoric acid solution with increasing time of exposure is shown below;

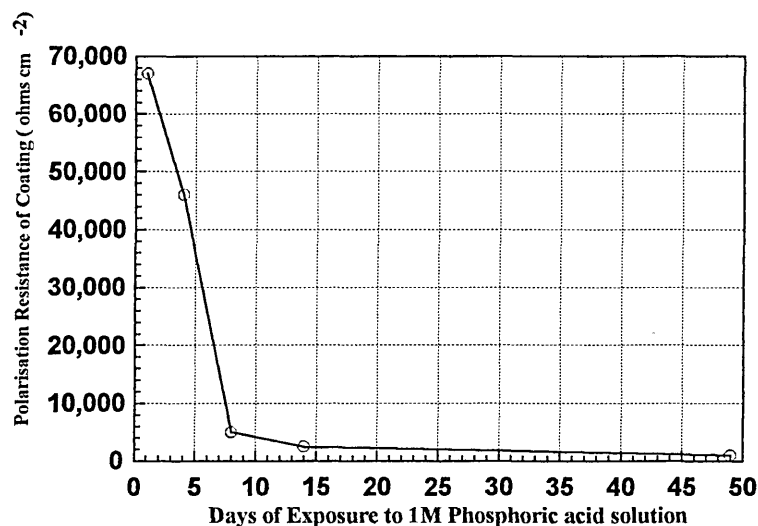


Figure 73: Variation in  $R_p$  of SS1 film with exposure time to 1M  $H_3PO_4$  solution

#### ***8.10 AC Impedance analysis of SS2 Polymer film ( 5 % phenolic )***

Previous work had shown for SS1 ( 10% phenolic cross-linking agents ) that only solutions containing relatively high concentrations of electrolyte had any significant effect upon the impedance response of the coating. It was therefore decided to proceed using 1M NaCl (aq) as a solution likely to cause alkaline deblistering and 1M phosphoric acid solution as a true corrosive medium, using SS2 polymer film ( 5 % phenolic cross-linking agent )

33cL cans coated with SS2 were investigated by AC Impedance spectroscopy using a perturbation voltage of 10mV at 63096Hz , the frequency response was measured over the range 0.01 Hz to 65000 Hz using the frequency response analyser set to give 6 steps per decade ( i.e. 30 data points )

Monitoring of the frequency response v impedance was carried out over 60 days .

For each set of data, the response of the coating / electrolyte was plotted in the Bode data representation .

### 8.10.2 SS2 Polymer films exposed to 1M Sodium Chloride solution

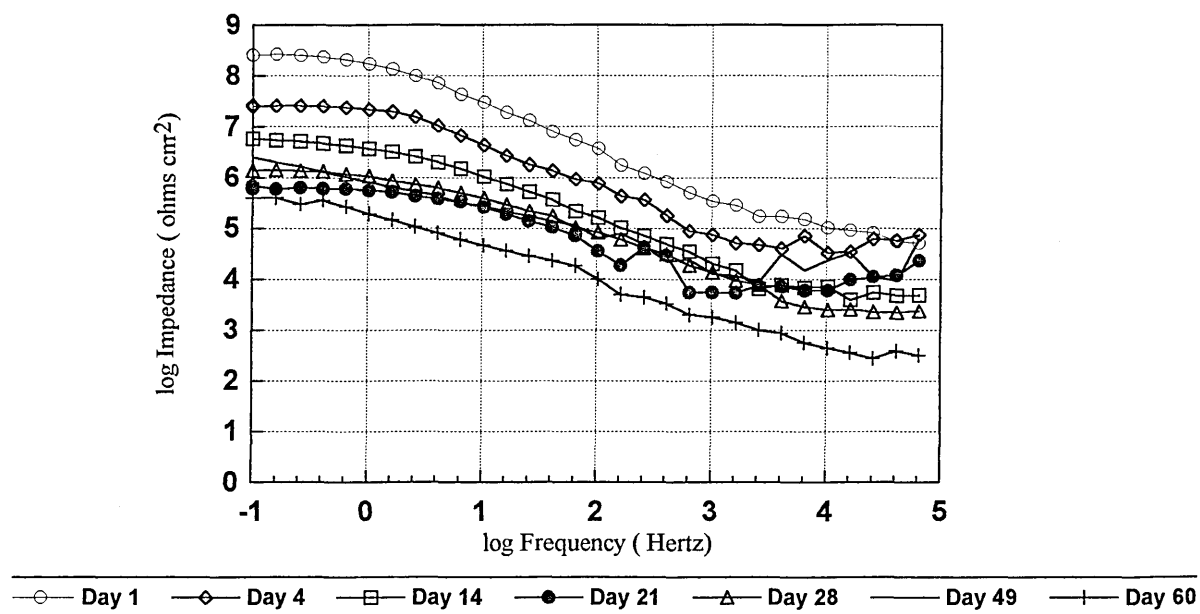
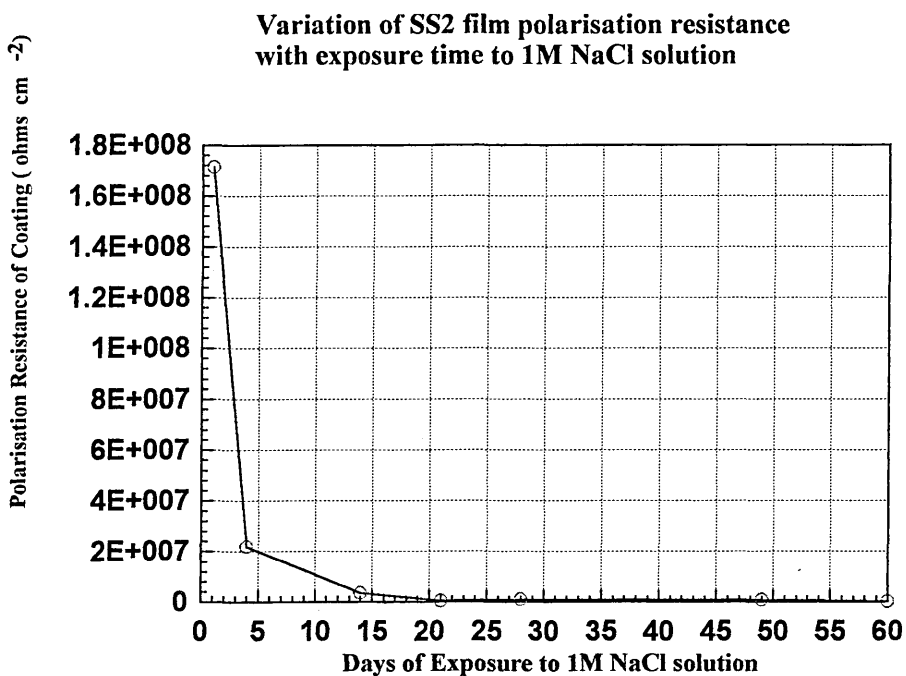


Figure 74 Bode Plot SS2 film exposed to 1M NaCl solution

Analysis of the Bode data yields the following information

Day	$R_p$ (ohms cm <sup>2</sup> )	$R_\Omega$ (ohms cm <sup>2</sup> )	$C_{dl}$ (Farads cm <sup>2</sup> )
1	$171.3 \times 10^6$	51,050	$2.54 \times 10^{-12}$
4	$21.82 \times 10^6$	61,659	$2.23 \times 10^{-11}$
14	$3.709 \times 10^6$	5,495	$1.47 \times 10^{-9}$
21	$538.5 \times 10^3$	10,965	$1.37 \times 10^{-9}$
28	$1.070 \times 10^6$	2,239	$0.87 \times 10^{-9}$
49	$801.8 \times 10^3$	10,965	$1.00 \times 10^{-8}$
60	$190.2 \times 10^3$	269	$0.98 \times 10^{-8}$

Table 26: Analysis of Bode data for SS2 in 1M NaCl



*Figure 75: Change in Polarisation resistance of SS2 with exposure to 1M NaCl*

#### **8.10.3 A summary of the information for SS2 film exposed to 1M NaCl solution**

- i) Over the time period assessed , there is a decrease in the polarisation resistance of the polymer. This implies permeation of the coating by the sodium chloride solution.
- ii) The double layer capacitance increases over the period of testing the SS2 polymer immersed in 1M NaCl .

This implies that within four days of exposure to 1M sodium chloride solution , charge transfer is occurring and that the SS2 coating changes from one exhibiting purely capacitive behaviour to a system that exhibits both capacitive and resistive elements .



### 8.11 SS2 film in the presence of 1M phosphoric acid

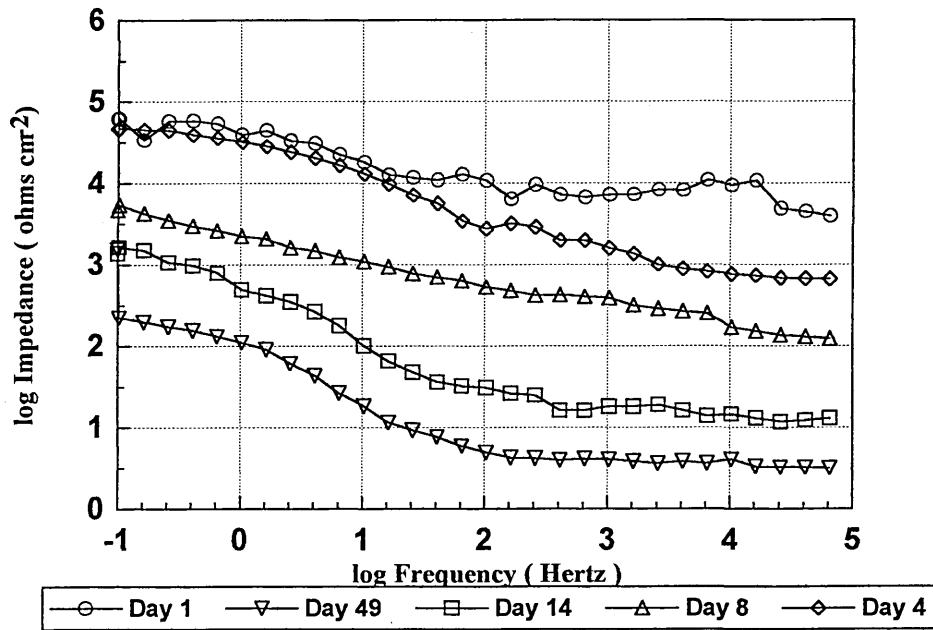


Figure 76: Bode plots of SS2 film at days exposure to 1M phosphoric acid solution

Analysis of the Bode data gives the following

Day	$R_p$ (ohms $\text{cm}^2$ )	$R_\Omega$ (ohms $\text{cm}^2$ )	$C_{dl}$ (Farads $\text{cm}^2$ )
1	$39.1 \times 10^3$	4,467	$5.21 \times 10^{-8}$
4	$31.7 \times 10^3$	672	$2.27 \times 10^{-7}$
8	2,226	131	$1.75 \times 10^{-6}$
14	490.9	12.3	$4.92 \times 10^{-6}$
49	300	9,998	$0.89 \times 10^{-5}$

Table 27: Analysis of Bode data SS2 in the presence of 1M phosphoric acid

As observed for the SS1 film, the polarisation resistance of SS2 film after 1 day exposure is very low compared with the value obtained in 1M NaCl. This suggests SS2 to be completely and rapidly penetrated by the acid solution.

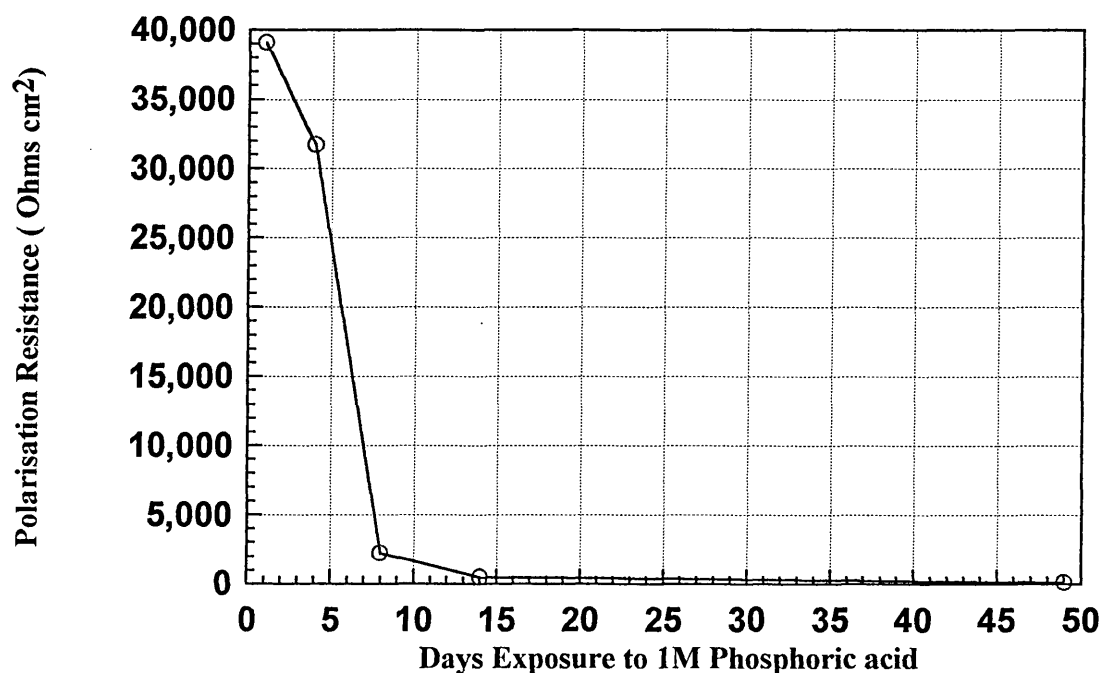


Figure 77: Variation in  $R_p$  for SS2 film exposed to 1M phosphoric acid solution

From Table 27, the increase in  $C_{dl}$ , the double layer capacitance, suggests corrosion ( i.e. charge transfer reactions ) to be occurring at the metal / SS2 polymer interface after four to eight days exposure to 1M phosphoric acid solution

## ***8.12 Discussion of AC Impedance Analysis Data of SS1 and SS2 polymer films***

### ***8.12.1 Sodium chloride solutions***

Changing the level of phenolic resin formulated into the spray liner technology does not appear to affect the barrier performance of the epoxy-graft-acrylic films to aqueous solutions of sodium chloride.

The similar values obtained for the film polarisation resistance of SS1 and SS2 films ( see sections 8.8.4 and 8.10.2 respectively ) in 1M sodium chloride suggests that there is little influence of the film phenolic content on polarisation resistance of the coating. The increase in double layer capacitance observed (  $C_{dl}$  ) over the exposure time for SS2 film is due to electrolyte permeation into the surface of SS2 polymer film during days 1 - 21 of exposure followed by a prolonged period ( days 21-60 ) where the  $C_{dl}$  value was relatively stable and comparable to the value obtained for SS1 film . The  $C_{dl}$  value for SS1 film was observed to be stable throughout the period of testing.

### ***8.12.2 Phosphoric acid solutions***

The barrier properties of the spray liner technology are, however, affected when solutions of phosphoric acid are used as electrolyte.

It appears that the SS2 formulation, containing 5% w/w phenol-formaldehyde cross-linker , allows the migration of phosphoric acid solutions through the coating more easily than does the SS1 formulation, containing 10% w/w phenolic resin.

### 8.13 Variation of Impedance Performance of a Coating system with Composition

In order to determine which components of the epoxy-g-acrylic film have a contribution to the impedance of the coating system, it was decided to turn to computerised experimental design procedures. The computer program utilised was Domain RS1 V3 <sup>[52]</sup>.

#### 8.13.1 Experimental Design Matrix

To investigate the effect of epoxy: acrylic ratio , acrylic monomer ratio within the acrylic portion of the polymer and the effect of acrylation temperature upon the impedance response of the coating a nineteen coating Response Surface Methodology (RSM) design was undertaken. The coatings manufactured were;

Lacquer No.	Epoxy:Acrylic Ratio	% Monomer in Acrylic portion			Acrylation Temp (°C)
		Methacrylic acid	Ethyl acrylate	Styrene	
SS7	75:25	65	1	34	125
SS8	85:15	43	1	56	125
SS9	80:20	65	17.5	17.5	115
SS10	85:15	54	1	45	115
SS11	75:25	65	34	1	115
SS12	85:15	65	34	1	115
SS13	85:15	43	34	23	115
SS14	75:25	54	17.5	28.5	115
SS15	75:25	43	1	56	125
SS16	85:15	65	34	1	125
SS17	85:15	43	17.5	39.5	125
SS18	80:20	43	1	56	115
SS19	75:25	65	1	34	115
SS20	75:25	43	34	23	115
SS21	85:15	65	1	34	125
SS22	75:25	43	1	56	115
SS23	75:25	43	34	23	125
SS24	80:20	54	34	12	125

Table 28 : Composition of Coatings for Impedance measurements

### ***8.13.2 Specimen Can preparation***

All of the polymer films were spray coated onto tinplated steel can bodies at film weights of 150-160mg /330mL can body and stoved at 188°C peak metal temperature for 60 seconds to achieve polymer curing.

### ***8.13.3 Impedance Measurements***

A three electrode impedance apparatus was used with the can body as working electrode, a Saturated Calomel electrode (0.241V v Standard Hydrogen Electrode ) as reference and a platinum mesh electrode as counter.

Impedance measurements were made using a 10mV perturbing ac signal, with the frequency response being measured by the Solartron1250 controlled by computer as detailed earlier.

The electrolyte used was 1M sodium chloride solution

Since a qualitative comparison of the polymer films was required, the impedance at a constant frequency ( 1000 Hz ) was recorded . This frequency was chosen as being above the frequency range usually associated with corrosion cells and within the range associated with the impedance response of the coatings.

The computerised chemometrics package was utilised to aid in data interpretation by a process of modelling the data, fitting the data to the computer generated model, refining the accuracy the fitted data by calculating the errors and performing any transformation of the model to produce a model more closely matching the raw data.

The fitted model of the impedance characteristics of lacquers SS7 to SS24 was able to analyse the effects of epoxy level, acrylic composition and acrylation temperature on the impedance response of the epoxy-g-acrylate film .

The contour plots, Figures 78 and 79, overleaf, graphically illustrate the domains within which, the experimental design matrix generated data of similar coating impedance.

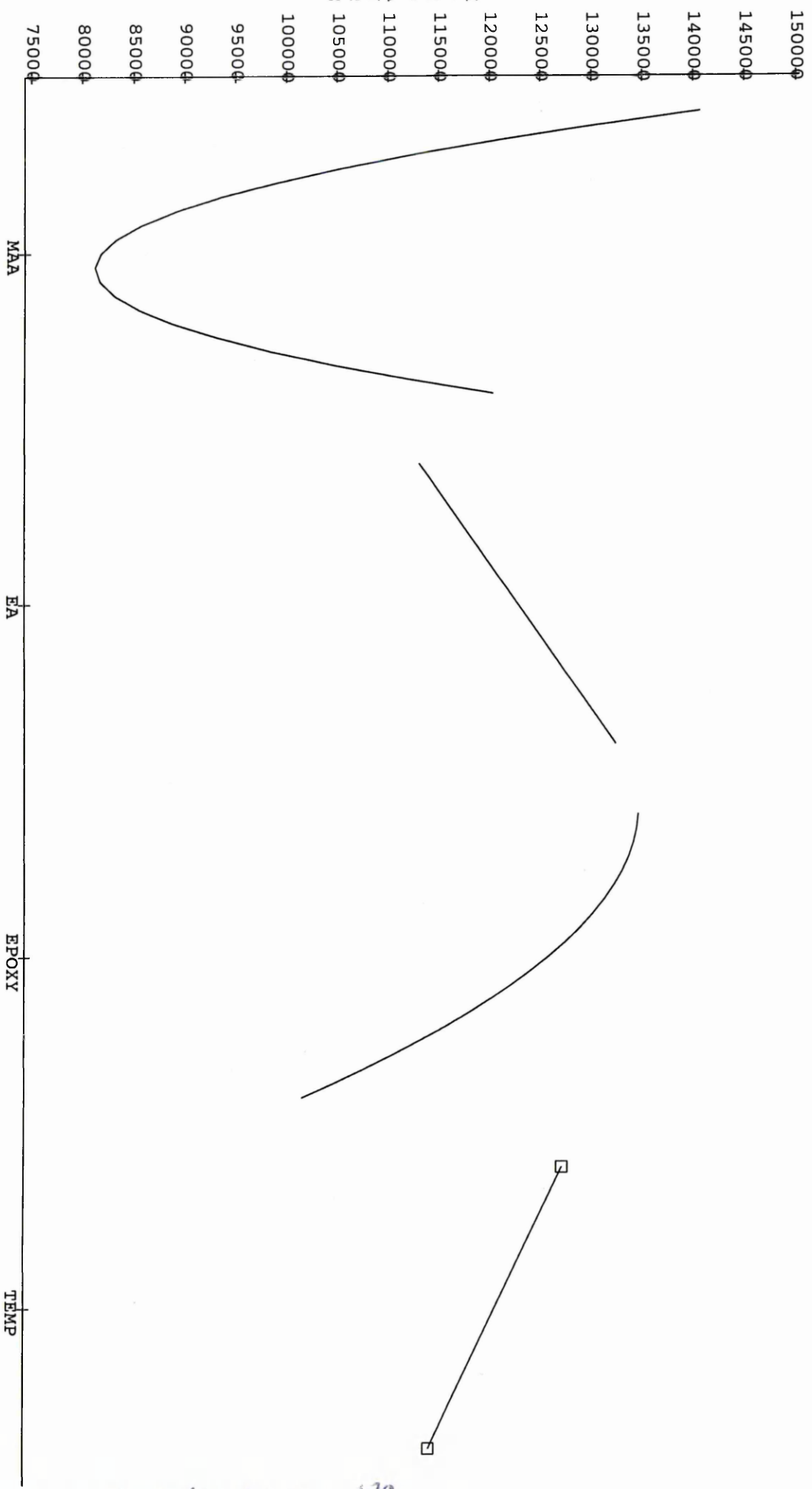
The major effect on the impedance response of the applied films appears to be the level of methacrylic acid in the acrylic portion of the polymer.

Low and high levels of methacrylic acid in the acrylic portion of the polymer, give impedance values at 1000Hz, for the cured polymer film, that are higher than for intermediate levels of methacrylic acid suggesting there is a critical range of acid functionality, with which the coating must be formulated to ensure the optimum barrier protection properties are achieved..

A secondary influence upon the impedance of the polymer coated metal system is the epoxy content in the epoxy-g-acrylate film. Increasing the epoxy:acrylic ratio from 75:25 to 85:15 appears to have a severe detrimental effect upon the impedance of the coating.

It can be seen, that the region 50 -62% methacrylic acid, in conjunction with 1-25% ethyl acrylate, gives rise to polymer systems with a relatively low impedance ( although the impedance values are  $200 \text{ to } 250 \times 10^6 \text{ Ohms cm}^{-2}$  ). In contrast, formulating at low ( 40 - 47 % ) or high ( 60 - 65% ) methacrylic acid contents, together with preferentially high ethyl acrylate contents, produces coatings with high impedance and which are potentially less susceptible to permeation by an aqueous corrosive medium, thus providing a better barrier coating for the metal substrate.

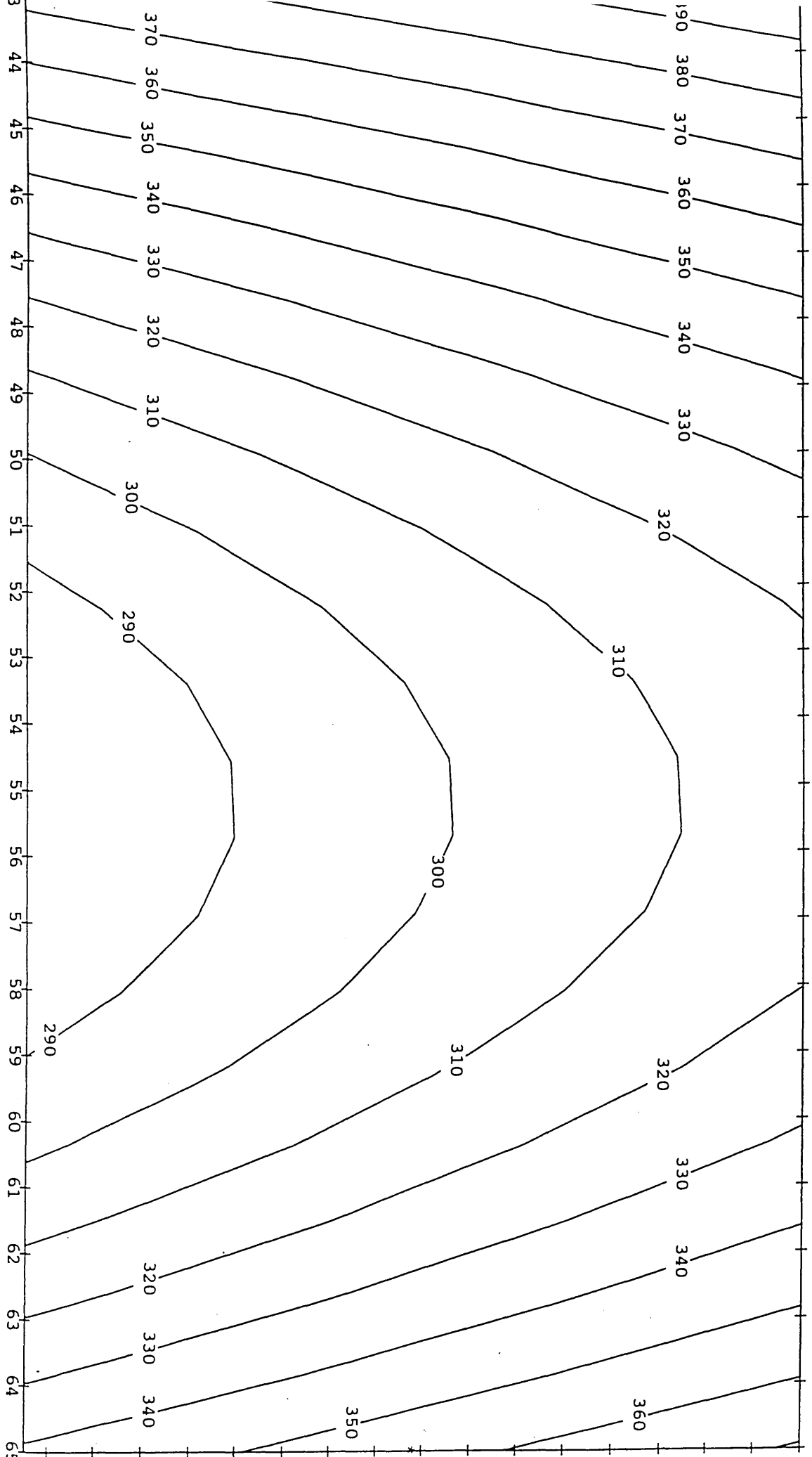
Adjusted Response Curves for IMPEDANCE  
Using Mulreg FIST2@MULREG, Model Z



MAA: 43 to 65  
EA: 1 to 34

Figure 77: Adjusted  $\gamma$  Plots for Impedance<sup>120</sup>

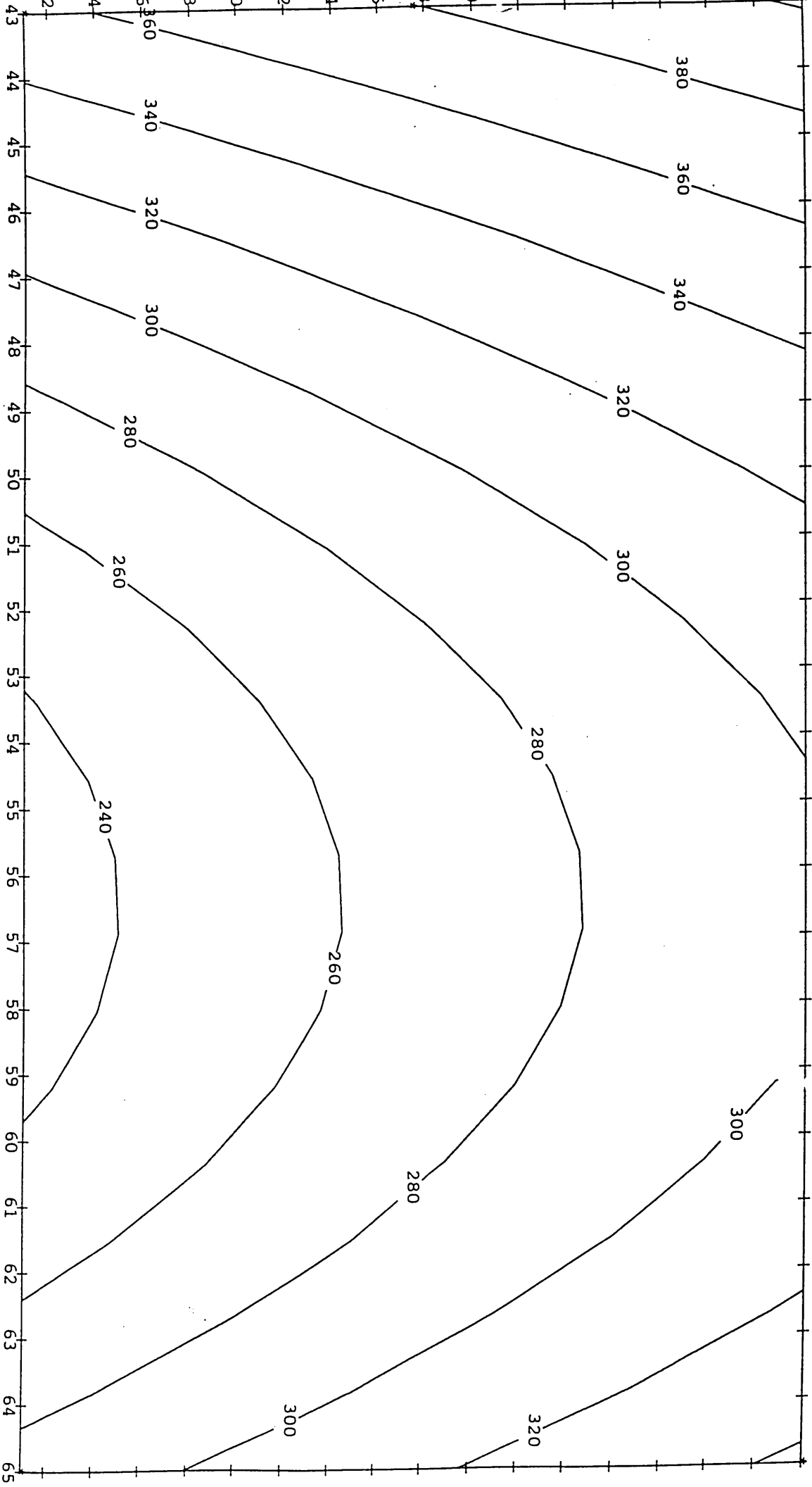
IMPEDANCE  
EPOXY = 80, TEMP = 118



7:00 pm, 11/18/80



IMPEDANCE  
EPOXY = 85, TEMP = 128



## Section 9

# **Overall Conclusions and Suggestions for Further Work**

## *9 Overall Conclusions and suggestions for further work*

### *9.1 Barrier properties of Spray-Coated Epoxy-graft-acrylic films on Tin-Plate in Corrosive*

#### *Environments.*

Very thin ( 3- 10  $\mu$  m thick ) water borne epoxy-acrylate polymer systems are coated onto the interior surfaces of tin-plated steel two piece beer and beverage drinks cans as a protective layer to guard the metal from the corrosive nature of the contents . Such films are much thinner than those in other surface protection applications, where films of approximately 20  $\mu$  m are commonly used.

This thesis describes an investigation of the corrosion processes that occur under such thin polymeric layers and suggests ways by which such films suppress the onset of corrosion of the bulk metal in corrosive aqueous environments.

A series of synthetic corrosive solutions has been developed which replicate the conditions , in terms of pH and conductivity, likely to be found in beverage cans and these solutions have been used to conduct corrosion studies of lacquer systems in commercial use .

The studies included metal egress into the solution , through the polymer, over varying time periods, and electron microscopy / X-ray energy dispersive analysis of the metal surface, observing changes in elemental composition with time of exposure.

The polymer films are considered to be microporous permeable membranes across which electrolyte and metal ions can readily migrate. The ability of the film to retard the corrosion of the metal is thought to be a complex combination of many different features.

Studies carried out highlight the following points:

i) The degree and nature of the film cross-linking has a role in the anti-corrosive action of the films i.e. films containing high levels of phenolic component in the epoxy-acrylic polymer show pronounced anti-corrosive nature c.f. films containing lower levels of phenolic component

ii) The amount of iron released into the beverage is much lower than expected when the corrosivity of the solution and the relative thinness of the films are considered. This may be explained by the “ion trapping” ability of the film, both physically in the film pore and chemically by the interaction of the ions with a component of the film.

Studies indicate a possible means by which the iron might be complexed by the phenolic cross-linker component of the film, with evidence having been obtained which shows the ease with which phenolic cross-linker / iron complexes can be formed.

iii) The amount of iron trapped by cured films has been assessed and the amount trapped has been related to the amount of cross-linking agent present in the film. Higher levels of phenolic cross-linker make the film more able to trap metallic ions within the matrix.

iv) Studies carried out using Optical Emission Glow discharge spectrometry provided evidence that the iron migrating from the bulk metal substrate after the onset of corrosion is trapped within the polymer matrix- this is a significant finding since for many years the films have been thought to trap metallic ions but there has been no documentary evidence to support this. The work has also led to the development of a means of accurately determining the film thickness.

v) Water permeation across the cured films has been followed using infra-red spectroscopy with different films being able to “absorb” different amounts of water into their cured polymeric structures. A diffusion coefficient has been calculated for the permeation of water across cured films of different cross-linking densities.

vi) The use of ion selective electrodes has enabled a study of the permeation of ions across cured epoxy-g-acrylic films to be carried out. The studies showed that films containing lower levels of phenolic cross-linking agents allow a greater degree of permeation of cations through the membrane than films formulated with higher levels of cross-linking agents.

The films have also been shown to be perm-selective towards the diffusion of sodium ions in preference to chloride ions, in aqueous sodium chloride solutions, thus exhibiting a duality in the nature of the coatings towards the constituents of corrosive environments.

vi) Alternating Current Impedance spectroscopy, which passes a low voltage sinusoidal wave of variable frequency across the polymer and then measures the response of the coating system in terms of impedance, has been used to observe the electrolyte penetration and corrosion initiation processes, *in situ*. The studies have included work on model systems using simple electrolytes, of varying molarities and pH ranges, and have utilised the previously developed corrosion test solutions for assessing accelerated corrosion under conditions similar to those observed for commercial drinks. A knowledge of the electrochemical processes occurring for these water-based epoxy-acrylate films during electrolyte penetration, saturation of the film and development of corrosion underneath the film has been obtained.

Using AC theory, the equivalent circuit, for the film at the various stages of the corrosion process, has been obtained and this has used to procure data relating to the changes in the film resistance and capacitance with exposure time. Thus a model has been constructed which proposes the corrosion process for the films under investigation.

## ***9.2 Suggestions for further work***

The areas highlighted in the current research for further investigation are :

9.2.1 The iron complexing ability of the phenolic component of the lacquers warrants further investigation with regard to both the mechanism by which this occurs and an investigation into the effects of changing the composition of either the whole coating system, or the phenolic component in isolation to assess the barrier effectiveness of the cured film.

9.2.2 The ion permeation work shows interesting promise and, with the availability of more ion-selective electrodes, it might be possible to investigate the diffusion of different complexing agents ( for example citrates, oxalates and tartrates) which have been shown to have major effect upon the corrosion of mild steel.

9.2.3 The most significant area for further research is in the application of AC Impedance to the investigation of epoxy-g-acrylic film barrier properties. The author considers the following areas to be of importance in the study of the barrier properties of polymeric metal coating films by Impedance spectroscopy:

#### 9.2.3.1 The effect of retained solvent in the cured film

Retained solvents in the cured film arise from either insufficient cure during the coating application or from reactions occurring during the cure.

Work previously reported <sup>[41]</sup> investigated the impedance spectra changes for a thermoplastic phenoxy ( polyhydroxy ether ) system with retained solvents content. The system investigated demonstrated the problems of retained solvents on the corrosion performance characteristics of thermoplastic coatings when the coating was dried at various temperatures. Studies have shown that the physical and mechanical properties of polymer films are greatly affected by the amount of retained solvent. Large amounts of retained solvents in a coating tend to create less protective films against corrosion, because these films have a large free volume and are thus porous in nature. <sup>[4]</sup> The higher the porosity of a polymer film, the easier it is for corrosive agents like water, oxygen and ions to penetrate. Therefore it is desirable to protect metallic substrates against corrosion with a coating that contains the smallest amount of retained solvent.

The chemistry of the lacquer system studied in the present work suggests that methanol may be generated upon polymer curing , with n-butanol and 2-butoxyethanol being present from the waterborne polymer dispersion.

The following should be studied:

- i) The effect of retained solvents in an epoxy-co-grafted acrylic polymer which has been dried at various temperatures ( room temperature , 50°C , 100 °C, 150 °C and 250°C ), and the subsequent changes that are observed in the AC Impedance Spectra.
- ii) The changes that are observed in the free volume ( pore size ) of the above films.

- iii) The variation with time of exposure to a corrosive environment in film capacitance and resistance of the above films.
- iv) The rate of electrolyte transport across the polymer membrane to the metal surface and the time at which corrosion of the metallic substrate is initiated.

#### 9.2.4 The effect of varying cured film composition on the AC Impedance response

In the present study, little attention has been focused on varying the composition of the lacquer system in order to assess both the barrier properties and the anti-corrosive nature of the films produced. Variation is possible in the epoxy : acrylic ratio on the polymer backbone, the composition of the acrylic in the backbone , the phenolic component loading and composition of the phenolic component.

All of these changes in composition could have a dramatic effect upon the barrier properties of the film and should be investigated.



Section 10

## **Appendices**

## ***10 Appendix 1***

The frequency response analyser is capable of holding several programs within its memory

Listed below are the programs set up for this series of experimental work.

### **PROGRAM 1**

65KHz - 10mHz, 2 steps per decade, 11 data points

<b>19</b>	NUMBER OF LINES IN PROGRAM
<b>00 OP 02,00</b>	DATA OUTPUT GPIB OFF
<b>00 FR +6.5000E+04</b>	GENERATOR FREQUENCY 65000Hz
<b>00 AM +1.0000E-02</b>	GENERATOR AMPLITUDE 0.01V
<b>00 FC</b>	CLEAR FILE
<b>00 AU 00</b>	AUTOINTEGRATION OFF
<b>00 RG</b>	START GENERATOR
<b>00 OP 03,01</b>	DATA OUPUT FILE ALL
<b>00 C0 00</b>	DISPLAY COORDINATES a,b
<b>00 BP 01</b>	ERROR BEEP OFF
<b>00 MI +1.0000E+00</b>	SWEEP FREQUENCY MINIMUM 1Hz
<b>00 MA +6.5000E+04</b>	SWEEP FREQUENCY MAXIMUM 65000Hz
<b>00 GD +2.0000E+00</b>	SWEEP LOG INCREMENT 2 STEPS PER DECADE
<b>00 SC 02</b>	START SWEEP LOG DOWN
<b>00 RE</b>	RECYCLE
<b>00 PP 06</b>	GPIB PARALLEL POLL CONFIGURE ON DATA LINE 6
<b>99 *Q</b>	EXIT FROM LEARN/EDIT MODE

## PROGRAM 2

65KHz-650.3Hz, 20 steps per decade, 650Hz-1Hz, 8 steps per decade

<b>26</b>	NUMBER OF LINES IN PROGRAM
<b>00 OP 02,00</b>	DATA OUTPUT GPIB OFF
<b>00 PP 00</b>	GPIB PARALLEL POLL UNCONFIGURE
<b>00 FR +6.5000E+04</b>	GENERATOR FREQUENCY 65000Hz
<b>00 AM +1.0000E-02</b>	GENERATOR AMPLITUDE 0.01V
<b>00 FC</b>	CLEAR FILE
<b>00 AU 02</b>	AUTOINTEGRATION LONG ON CHANNEL 2
<b>00 RG</b>	START GENERATOR
<b>00 OP 03,01</b>	DATA OUPUT FILE ALL
<b>00 FS 0065</b>	FILE SIZE 65 BLOCKS
<b>00 SO 0201</b>	DISPLAY SOURCE CHANNEL 2 / CHANNEL 1
<b>00 C0 00</b>	DISPLAY COORDINATES a,b
<b>00 BP 01</b>	ERROR BEEP OFF
<b>00 MI +6.5030E+2</b>	SWEEP FREQUENCY MINIMUM 650.3Hz
<b>00 MA +6.5000E+04</b>	SWEEP FREQUENCY MAXIMUM 65000Hz
<b>00 GD +2.0000E+01</b>	SWEEP LOG INCREMENT 20 STEPS PER DECADE
<b>00 SC 02</b>	START SWEEP LOG DOWN
<b>00 RE</b>	RECYCLE
<b>00 AU 04</b>	AUTOINTEGRATION SHORT ON CHANNEL 2
<b>00 MI +1.0000E+00</b>	SWEEP FREQUENCY MINIMUM 1Hz
<b>00 MA +6.5000E+02</b>	SWEEP FREQUENCY MAXIMUM 650Hz
<b>00 GD +8.0000E+00</b>	SWEEP LOG INCREMENT 8 STEPS PER DECADE

00 SC 02	START SWEEP LOG DOWN
00 RE	RECYCLE
00 SA	STOP ANALYSERS
00 PP 06	GPIB PARALLEL POLL CONFIGURE ON DATA LINE 6
99 *Q	EXIT FROM LEARN/EDIT MODE

### PROGRAM 3

65KHz-650.3HZ, 20 steps per decade, 650Hz-10mHz, 8 steps per decade, 73 data points

26	NUMBER OF LINES IN PROGRAM
00 OP 02,00	DATA OUTPUT GPIB OFF
00 PP 00	GPIB PARALLEL POLL UNCONFIGURE
00 FR +6.5000E+04	GENERATOR FREQUENCY 65000Hz
00 AM +1.0000E-02	GENERATOR AMPLITUDE 0.01V
00 FC	CLEAR FILE
00 AU 02	AUTOINTEGRATION LONG ON CHANNEL 2
00 RG	START GENERATOR
00 OP 03,01	DATA OUTPUT FILE ALL
00 FS 0073	FILE SIZE 73 BLOCKS
00 SO 0201	DISPLAY SOURCE CHANNEL 2 / CHANNEL 1
00 CO 00	DISPLAY COORDINATES a,b
00 BP 01	ERROR BEEP OFF

<b>00 MI +6.5030E+2</b>	SWEEP FREQUENCY MINIMUM 650.3Hz
<b>00 MA +6.5000E+04</b>	SWEEP FREQUENCY MAXIMUM 650000Hz
<b>00 GD +2.0000E+01</b>	SWEEP LOG INCREMENT 20 STEPS PER DECADE
<b>00 SC 02</b>	START SWEEP LOG DOWN
<b>00 RE</b>	RECYCLE
<b>00 AU 04</b>	AUTOINTEGRATION SHORT ON CHANNEL 2
<b>00 MI +1.0000E+00</b>	SWEEP FREQUENCY MINIMUM 1Hz
<b>00 MA +6.5000E+02</b>	SWEEP FREQUENCY MAXIMUM 650Hz
<b>00 GD +8.0000E+00</b>	SWEEP LOG INCREMENT 8 STEPS PER DECADE
<b>00 SC 02</b>	START SWEEP LOG DOWN
<b>00 RE</b>	RECYCLE
<b>00 SA</b>	STOP ANALYSERS
<b>00 PP 06</b>	GPIB PARALLEL POLL CONFIGURE ON DATA LINE 6
<b>99 *Q</b>	EXIT FROM LEARN/EDIT MODE

## PROGRAM 4

65KHz -100mHz, 5 steps per decade, 31 data points

20	NUMBER OF LINES IN PROGRAM
00 OP 02,00	DATA OUTPUT GPIB OFF
00 PP 00	GPIB PARALLEL POLL UNCONFIGURE
00 FR +6.5000E+04	GENERATOR FREQUENCY 65000Hz
00 AM +1.0000E-02	GENERATOR AMPLITUDE 0.01V
00 FC	CLEAR FILE
00 AU 00	AUTOINTEGRATION OFF
00 RG	START GENERATOR
00 OP 03,01	DATA OUPUT FILE ALL
00 FS 0031	FILE SIZE 73 BLOCKS
00 SO 0201	DISPLAY SOURCE CHANNEL 2 / CHANNEL 1
00 CO 00	DISPLAY COORDINATES a,b
00 BP 01	ERROR BEEP OFF
00 MI +1.0000E-01	SWEEP FREQUENCY MINIMUM 0.1Hz
00 MA +6.5000E+04	SWEEP FREQUENCY MAXIMUM 650000Hz
00 GD +5.0000E+01	SWEEP LOG INCREMENT 5 STEPS PER DECADE
00 SC 02	START SWEEP LOG DOWN
00 RE	RECYCLE
00 PP 06	GPIB PARALLEL POLL CONFIGURE ON DATA LINE 6
99 *Q	EXIT FROM LEARN/EDIT MODE

## 11 References

- 1 Uhlig,H. Tridas, D and Stern,N      *J.Electrochem Soc.*,**102** (1955) pp 41-44
- 2 Evans, U.R.      *An Introduction to Metallic Corrosion*, 3rd  
Ed, Arnold 1981
- 3 Gabe, D.R.      *Principles of Metal Surface Treatment and  
Protection*, Vol 28,Pergamon Press,Oxford  
1978
- 4 Kamm, C.C.      *Corrosion*,**17**, (1961) pp 98 -100
- 5 Willey, A.R.      *Brit Corros.J.*,**7**, (1972) pp 29 -31
- 6 Britton, S.C.      *Tin versus Corrosion*, International Tin  
Research Institute, 1977
- 7 Scully, J.C.      *The Fundamentals of Corrosion*, Pergamon  
Press, Oxford, 1979
- 8 Patrick, G.W.      *Anti-Corrosion*, **6**, (1976) , pp 10 -14
- 9 Kohman,E.F and Sanborn,N.H.      *Ind. Eng. Chem.*,**20**, (1928) pp 76 -79
- 10 Jeffereys,L.H.      *Trans. Farad. Soc.*,**20** , (1924), pp 392 -395
- 11 Food and Agriculture Organisation      *Guidelines for can maunfactuers and food  
of the United Nations      canners*, Rome, 1986
- 12 Hoare, W.E, Hedges,E.S and      *The Technology of Tinsplate*, Arnold Press,  
Barry,B.T.K      London (1965)
- 13 Daly, J.J.      *Can Corrosion Problems*, Corrosion  
(NACE), Vol **15**,11,Nov 1959

- 14 Beese,R.E.,Willey,A.R and Kamm,G.G. *Canned Soft drinks: a study of Corrosion mechanism, 8th Annual meeting Proceedings of Soft Drinks Technologists, USA,1993*
- 15 Buller,M., Mayne,J.E.O.and Mills,J.D. *J.Oil Colour Chem. Assn., 59 (1976) pp 351 -356*
- 16 Funke.W and Haagen,H. *J.Oil Colour Chem. Assn., 58 (1975) pp 359 -362*
- 17 Perea, D.Y and Heerjtes, P.M. *J.Oil Colour Chem. Assn., 54 (1977) pp774 -777*
- 18 Kinsella,E.M.,Mayne,J.E.O. and Scantlebury,J.D. *Br.Polym. J. 3 (1971) pp 41 - 42*
- 19 McBane,B. *J.Paint Technol., 49 (1970) pp 62 - 65*
- 20 Haagen, H and Funke,W. *J.Oil Colour Chem. Assn., 58 (1975) pp 359 - 362*
- 21 Bullett, T.R. *J.Oil Colour Chem. Assn., 44 (1961) pp 807 -809*
- 22 Meyer, W and Schwenck, W *W. Farbe and Lack, 85 (1979) pp 179- 182*
- 23 Evans, U.R. *Metallic Corrosion Passitivity and Protection, E. Arnold,London 1945, 268*
- 24 Ruggeri, R.T and Beck T.R. *Corrosion (NACE) ( Houston ), 39,( 1983 ), pp 452 - 455*



- 25 Murray, J.D. *J.Oil Colour Chem. Assn.*, **56** (1973) pp210 - 213
- 26 Couves, L.D. *I.C.I. Paint Report PA00676* , (1990)
- 27 Mills, D.J. and Mayne, J.E.O. *J.Oil Colour Chem. Assn.*, **58** (1975) pp 155 -157
- 28 Funke.W. *Ind. Eng. Chem.,Prod. Res. Dev.*, **24** (1985) pp343 -347
- 29 Yarwood,J. *Analytical Proceedings*, **30**, (1993), pp 13 -17
- 30 Bellucci,F. and Nicodemo,L. *Corrosion*,**49** , (1993) pp 235 - 237
- 31 Leidheiser,H. *J.Ctgs Technol.*, **63** (1991) pp 22- 30
- 32 Bacon,R.C.,Smith,J.J. and Rugg,F.M. *IInd. Eng. Chem.*,**40** ( 1948) pp 161-165
- 33 Leidheiser,H., Mills,D.J. and Bilder,W. *Electrochem Soc.Proc.*, **87-2**( 1987) pp 23 -27
- 34 Kendig, M.W. and Leidheiser,H. *Electrochem Soc.Proc.*, **87-2**( 1987) pp 46 -50
- 35 Walden, N. *J.Paint Technol.*, **40** (1968) pp 174 - 176
- 36 Cole, C.L. *Poly.Paint Colour J.*, **177**( 1987) pp 250 -257
- 37 Mansfeld,F. and Tsai,C.H. *Corrosion* , **47** (1991) pp 958 - 962

- 38 Hollaender, Ludwig and Hillebrand     *International Tin-Plate Conf.*, London (1993)  
Paper 26
- 39 Thompson, I. and Campbell, D.     *Corrosion Sci.* **36**, (1994) pp 187 - 193
- 40 Leidheiser, H and Kendig, M.W.     *Corrosion Sci.*, **32**, (1967) pp 145 - 151
- 41 Geenen, F.M., van Westing, E.P.M.     *Proc. 11th Int. Corrosion Congress, Florence*  
and de Wit, J.H.W.     *Italy*, April (1993), pp 231 - 241
- 42 Tait, Handrich and Maier     *J. Ctgs Technol.* **62** (1990), pp 781 - 786
- 43 Ramnelt, R.H and Reinhard H.     *Prog. Org Coatings*, **21** (1992) pp 205 - 209
- 44 Al-Hashenn, A.H. and Habib, K.J.     *J. Ctgs Technol.* **64** (1992) pp 813 - 815
- 45 Tsurumaru, M.,     *Proc. Int. Tinplate Conf.*, London (1993),  
Masuda, K., Yamamoto, Y.     Paper 19
- 46 Junges, P., Pennera, G., Billen, L., Darre     *Proc. Int. Tinplate Conf.*, London (1993),  
, J.M. and Birck, J.C.     Paper 37
- 47 Monanari, A., Milanese, G., Cassara, A.     *Proc. Int. Tinplate Conf.*, London, (1993),  
Tomasicchio, M. et al     Paper 18
- 48 Kim, C.D. and Helwig, E.J.     *Proc. Int. Tinplate Conf.*, London (1993),  
Paper 20
- 49 Nekvasil, J. and Pitter, J.     *Proc. Int. Tinplate Conf.*, London (1993),  
Paper 17
- 50 Servais, J.P, Bastin, p. Lamberigitis, M     *Proc. Int. Tinplate Conf.*, London (1993),  
et al     Paper 26

- 51 James, D.J. *ICI Internal Report 10038*
- 52 Domain RS/1 Experimental Design BBN Limited (1996)
- 53 Harrick,N.J. *J.Opt.Soc. Am.*,**55** (1965), pp 851 -854
- 54 Mirabella,F.M. *Spectrosc.*,**20** (1990) , pp 5 -9
- 55 Iwamoto,R. and Ohta,K. *Appl.Spectrosc.*,**38** (1984), pp 359 -364
- 56 Nguyen,T., Bentz, D and Byrd,W.E. *J.Ctgs Technol.***66** (1994) pp 103 -104
- 57 Glass, A.L. and Smith,J. *J. Paint Tech.* **38**(1966), pp 35 -35
- 58 Rudham, A.T.S and Sherwood,A.F. *Paint Tech.* **30** (1966) pp 15 -17
- 59 Holt,G.S. The Structure of Ion exchange resins  
*Dewplan Techical Bulletin* (1994)
- 60 Fick , A.E. *Pogg. Ann*,**94**,59 (1855)
- 61 Armington,R.E and Voltz,C *An Introduction to Electric circuit analysis*,  
Prentice-Hall (1967)
- 62 Hughes,E *Electrical Technology*, Longman,(1985)
- 63 Branson,L.K. *Electronics for Scientists and Engineers*,  
Oxford, ( 1982)
- 64 Malmstadt,H. V.,Enke,C.G and Toren,E.C. *Electronics for Scientists*,  
W.A. Benjamin , ( 1963)
- 65 Issacs,H.S., Davenport,A.J. *Corrosion Science*,**33**,(1992) pp 147 -152  
,Hawkins,J. and Thompson,G.E.

- 66 Mansfeld,F.,Kendig,W. and Tsai,S. *Corrosion*,**38** (1982), pp 9- 13
- 67 MacDonald,D.D. *Transient effects in Electrochemistry*,  
Plenum Press (1977)
- 68 Szauer,T. *Prog. Org Coatings*,**10** (1982), pp 171 - 175
- 69 Colombo,A.,  
Rocchini,G.,Scolari,P.V. and  
Spinelli,P. *Corrosion Prevention and Control*,**4**,(1992)  
pp 45 -47
- 70 Mansfeld,F. *Corrosion*, **36** (1981) , pp 301 - 304
- 71 Boukamp, B.A. *Proc. 9th European Congress on Corrosion*,  
Utrecht(NL)( 1989) FU252

## ***11.2 Other Useful References (Uncited in thesis )***

### ***Corrosion/ Electrochemisty***

- Colombo,A., Rocchini,G.and  
Spinelli,P. *Proc. 11th International Corrosion Congress*  
,Florence Italy pp 2.191 -2.199
- Al-Hashenn,A.H. and Habib,K.J. *J.Ctgs Tech.*,**64**, (1992) pp 813 -820
- Rocchini,G *Corrosion Science*,**33**,(1992) 1347- 1361
- Nasrazadori,S and Raman,A. *Corrosion Science*,**34**,(1993) pp 1355 - 1365
- Steinsmo,U and Bardal,E. *Corrosion*,**48**,(1992) pp 11 - 13
- Callow,L.M. and Scantelbury,J.D. *J.Oil Col. Chem. Assoc.*, **64**,(1981)
- Callow,L.M. and Scantelbury,J.D *J.Oil Col. Chem. Assoc.***64** (1981)pp 119-123

Part II

- Callow,L.M. and Scantelbury,J.D      *J.Oil Col. Chem. Assoc.***64** (1981) pp 140  
-143 Part III
- Woodhouse,J.      *Industrial Corrosion*, (1996) pp 6 -9
- Tait, S.W      *J. Ctgs. Techn.* **61**, (1989) pp768 - 772
- Quarishie,R.L.      *Industrial Corrosion*, (1996) pp 5
- Marshall ,K. and Valensi,D.      *Materials World*,**3**(1995) pp 471 -473
- Vogt,O.      *Pitture e Vernici Europe*,**16** (1995) pp 9-11
- Monnetta, T.,Bellucci,F.      *Prog. Org Coatings*,**21**(1993) pp 353 -369  
,Nicodemo,L and Nicolais,L.
- Bonora,P.L.      *Pitture e Vernici Europe* ,**6**, (1992) pp 13-15
- Roberge,P.R.,Hallop,E. and      *Corrosion*,**48**, (1992) pp 125 -129  
Sastri,V.S.
- Seri,G.,Furaya,S. and Noga,S      *Proc 11th Int Corrosion Congress Florence*  
Italy 1990
- Tait,S. and Maier,M.      *J. Ctgs Techn.*,**62** (1990)pp 781 -783
- Westing,E.P.M, Ferrari,G. and de      *Corrosion Science*,**34** (1993) pp 9 -11  
Witt,J.H.W
- Fedrizzi,L.,Deflorian,F.,Boni,G.,Bon      *Proceeding of Eurocoat Conference*,1995  
era,P.L. and Pasini,E.      pp 171 - 187
- Chen,J.F. and Bogarets,W.F      *Corrosion*,**52**,(1996) pp 753 - 759

- Gabrelli,C. and Keddah,M      *Corrosion*,**48**, (1992) pp 794 -811
- Baustista,A      *Prog. in Org Ctgs* ,**28** (1996) pp 49-58
- Grandle,J.A. and Taylor,S.R.      *Corrosion*,**50**, (1994) pp 792 -802
- Liedheiser.H.      *J.Ctgs Tech.* **63**, (1991) pp 802 - 810
- Rocchini,G      *Corrosion Science*,**36**,(1994)pp 8 - 10
- Al-Hashem,A.H.      *Proc 11th Int Corrosion Congress Florence*  
Italy (1990)
- Souchet,R.,Dalard,F.,Rameau,J.J.      *Anti-Corrosive Method and*  
and Rebaul,M      *Materials*,**42**,(1995) pp 3 -9
- Steward, P.A.,Heorn,J. and      *Polymer Int.*,**38**,(1995) pp 110 -112  
Wilkinson,M.C.

*Polymer/Metal Interface analysis and adhesion*

- Adadurov,A.F      *J. Adhesion Sci. Tech*,**9** (1995) pp 1279-1289
- Ooij,W.J. and Sabata,A      *Surface and Interface Analysis*,**19**,(1992) pp  
10 - 15
- Chiontone,O. and Guaita,M      *J.Applied Polym. Sci,Applied Polymer*  
*Physics Symp.*,**52**,(1993) pp 21 -23
- Sakellariou,P. and Kapadia,K.      *European Polymer Journal* ,**32**,(1996) pp 1-7
- Yanabe,H.      *Prog Org Ctgs*,**28** (1996) pp 123 - 127
- Edwards,D.A      *J.Poly. Sci,PartB,Polymer Physics*  
**34**,(1996) pp 981 -997

- Austin,J. *Paper 15,Paint Research Assn.,2nd Asia Pacific Conference* *del?*
- Sherlock,J.C. *7th Int. Tin-plate Conference Proceedings, London ( 1993)*
- Ahem.A.H., Schwartz,P.R. and Shaffer, L.A. *Applied Spectroscopy,46,(1992) pp 1412 - 1419*
- Argent,C.J. and Gray, D. *International Gas Research Conference 1989*
- Huttinger,K.J., Hohmann,W. and Kernkel,G. *J. Adhesion Sci. Techn.,6,(1992) pp 10-14*
- Peng-Keong,T and Hajais,J. *Paper 21,Paint Research Assn.,2nd Asia Pacific Conference* *del?*
- Sugerman,G. and Monte,S.J. *Proc. 15th Waterborne Ctgs Symp, New Orleans (1988)*
- Fondeur,F. and Koenig,J. *Applied Spectroscopy,47, (1993) pp 51 - 55*

*Permeation across polymers*

- Lin,M.,Nguyen,T. and McKnight,M. *Prog. in Org Ctgs ,20,(1992) pp 47-52*
- Feliu,S. and Marcillo,M *Prog. in Org Ctgs ,25,(1995) pp 25 - 27*
- Chi-Lan,W, Zhou,X-J and Young-jun,T *Prog. in Org Ctgs ,25,(1995) pp 30 - 33*
- Bastidas,J.M. , Cabanes,J.M. and Catala,R *J.Ctgs Tech, 69,(1997) pp 871- 875*
- Feliu,S Jr,Morcillo,M. and Feliu,S. *J.Ctgs Tech,68,(1996) pp 365-367*

- Feliu,S Jr,Morcillo,M. and Feliu,S. *J.Ctgs Tech*,**68**,(1996) pp 365-367
- Cohen,S.M. *J.Ctgs Tech.*,**68**,(1996) pp 73 -81
- Reinhard,G., Simon,P. and Rammelt,U. *Prog.in Org, Ctgs.*,**20**,(1992) pp 383 - 392
- DesLauriers,P.J. *Proc. 14th WaterBorne Ctgs Symp.* 1987  
pp 58 -75
- Monetta,T., Bellucci,F., Nicodemo,L and Nicolais,L. *Prog.in Org, Ctgs*,**21**,(1993) pp 353- 369
- Takahagi,T. *Int. Poly. Sci and Tech.* **20**, (1993) pp 60-66
- Changjian,L., Nguyen,T. and McKnight,M.E *Prog. Org Coatings*, **20**, (1992) pp 169-185
- Nguyen,T.,Byrd,E. and Bentz,D *J. Adhesion Sc. Tech.*,**38**,(1996) pp 45 -49

#### *Beverages*

- Daly,J.D. *Packaging Enginnering* ,**10**,10 (1965)
- Alderson,M.G. *Food Manufacturer*, August 1970
- Anderson,D.G *Anal. Chem.* **65** (1993) pp 32 -34